THESIS FOR THE DEGREE OF DOCTOR OF PHILOSOPHY

Prediction of Traffic Noise Shielding by City Street Canyons

Mikael Ögren

CHALMERS

Department of Applied Acoustics
School of Civil Engineering
CHALMERS UNIVERSITY OF TECHNOLOGY
Göteborg, SWEDEN, 2004

Prediction of Traffic Noise Shielding by City Canyons
Mikael Ögren

ISBN 91-7291-438-6

Doktorsavhandlingar vid Chalmers tekniska högskola
Ny serie nr 2120

ISSN 0346-718X

Department of Applied Acoustics
Chalmers University of Technology
SE-412 96 Göteborg
Sweden
Tel. +46 31 772 2200
Fax +46 31 772 2212

Cover: Sound field at a frequency of 40 Hz in a two canyon situation. The source is in the left canyon, which is 11 m wide and 18 m high. The right canyon is 20 m wide and 18 m high.

Reproservice
Göteborg, Sweden, 2004

Prediction of Traffic Noise Shielding by City Canyons

Mikael Ögren
Department of Applied Acoustics
Chalmers University of Technology
Report F04–01

Abstract

Reducing the sound level on the exposed building facades due to traffic noise in cities is difficult and expensive. Creating access for the inhabitants to a quiet side can be an alternative method for reducing the annoyance. Therefore it is of interest to predict the level on shielded positions such as courtyards. This is however difficult using traditional methods. Distant sources contribute to the level, and multiple reflections can be very important. The equivalent sources method is used here to make predictions for canyon-like geometries. This method is extended to include effects of diffusion, absorption and atmospheric turbulence in order to improve the predictions. Substantial decreases on quiet side sound levels have been shown when introducing absorption and diffusion, and small increases have been shown due to turbulence.

Measurements indicate that the level is relatively constant for courtyards throughout a city area, and a very simple model called the flat city model is proposed to explain this effect. This model assumes that all sources and receivers are located on a flat rigid plane. The effect of shielding by buildings is introduced as a correction term determined from measurements, and this term is within a relatively small range (6–10 dB) for all the areas studied.

Keywords: outdoor sound propagation, traffic noise, city street canyons, turbulence, diffusion, equivalent sources method.

List of papers

Paper I "Thick barrier noise-reduction in the presence of atmospheric turbulence: Measurements and numerical modelling"
Published in Applied Acoustics 63, 2002
Jens Forssén and Mikael Ögren

Paper II "Road traffic noise propagation between two dimensional city canyons using an equivalent sources approach"
To be published in Acustica – Acta acustica 90, 2004
Mikael Ögren and Wolfgang Kropp

Paper III "Modelling of a city canyon problem in a turbulent atmosphere using an equivalent sources approach"
Published in Applied Acoustics 65, 2004
Mikael Ögren and Jens Forssén

Paper IV "Including absorption and diffusion effects in city street canyon calculations using the equivalent sources method"
Submitted to Applied Acoustics
Mikael Ögren and Wolfgang Kropp

Paper V "Noise levels on the shielded side in cities using a flat city model"
Published in Applied Acoustics 65, 2004
Pontus Thorsson, Mikael Ögren and Wolfgang Kropp

Paper VI "Macroscopic modeling of urban traffic noise – influence of absorption and vehicle flow distribution"
Submitted to Applied Acoustics
Pontus Thorsson and Mikael Ögren

The author of this thesis contributed with 50% of the work for all papers except for Paper V where the contribution was 33%.

Acknowledgments

In the year 2000 approximately 900.000 scientific papers were published[1]. If the growth rate has been constant since then, that number should be doubled for the current year, 2004. My contribution is in your hand right now.

The work behind this thesis was funded by the Swedish Foundation for Strategic Environmental Research (MISTRA), the Swedish Agency for Innovation Systems (Vinnova), the Swedish National Road Administration (VV) and Formas (the Swedish Research Council for Environment, Agricultural Sciences and Spatial Planning).

While writing it I have received help and support from many persons. First of all I would like to thank Gunilla Skog and Börje Wijk for helping me with the administrative and technical routines at the department. A warm thanks to Wolfgang Kropp for being a good supervisor. To my other brave colleagues in the outdoor acoustics group, Jens Forssén and Pontus Thorsson: thank you for helping out, for listening and for sharing your ideas.

Most of the scientific work has been made using free software, licensed under GPL (the GNU Public License). I would like to thank all developers of free software for sharing it with me.

Finally a warm thanks to my family, Stephan, Lena, Andreas, Jenny, Felicia and Karin. “Without you, I’m not OK.”

[1] According to “The Universe in a Nutshell” by Stephen Hawkins.

Contents

CHAPTER 1

Introduction

1.1 The quiet side

The concept of access to a "quiet side" as an alternative to decreasing the sound levels on the exposed façade is discussed by Tor Kihlman in [1]. The idea is to try to compensate for a noisy façade of the building by having access to a quiet area such as a courtyard, either via a window or as a space that can be used as a recreational area, see Figure 1.1.

To lower the sound pressure level on the exposed façade is difficult and expensive [2]. The traffic volume flowing trough a part of the city cannot simply be decreased without affecting the mobility and accessibility of the inhabitants. Building high noise barriers or moving traffic into tunnels are possible but expensive solutions. To seal gaps between buildings, and make apartments having access to both an exposed and a shielded side might be more feasible.

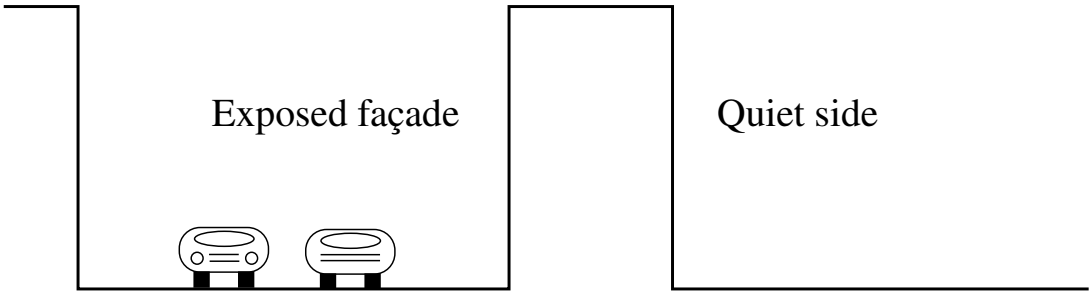

Figure 1.1: Illustration of an exposed façade and the quiet side.

Table 1.1: Table from [4] describing the number of residents that report that they are very or extremely annoyed by road traffic noise."Noise/Noise" means that the subjects apartment is exposed to high levels on all sides, "Noise/Quiet" means that at least one side of the apartment is exposed to lower levels.

	City		Suburb	
	Noise/Noise	Noise/Quiet	Noise/Noise	Noise/Quiet
Number of respondents	81	164	47	115
Very + extremely annoyed	7%	1%	21%	11%

Is there a positive effect of having access to a quiet side? This question has been investigated within the Swedish research programme "Soundscape support to health" [3], which has also financed parts of the research behind this thesis. Although much work is still ongoing, the results so far show that the annoyance reported in questionnaires is reduced when the residents have access to a quiet side [4, 5]. The questionnaire data presented in Table 1.1 are from two different locations, one in a city centre and one from a suburb. It shows that the number of residents that report that they are very annoyed or extremely annoyed is substantially reduced if they have access to a quiet side.

Most of the the regulations for road traffic noise levels are based on the level on the exposed façade. Therefore the standardized calculation models are developed with this in mind, and are aimed at determining the level on the exposed façade. The experience from this research programme is that the accuracy of prediction methods such as the Nordic method [6] decreases as the sound level at the receiving position is decreased. This makes perfect sense since the method is aimed at verifying if the level at an exposed façade is lower than the limit value given by the regulations. This also makes sense since close to a strong source the level is determined by the sound power of the source and the propagation along a few direct and reflected paths. Further away many other sources and transfer paths might have an influence.

For predictions on the quiet side, other approaches than those used for the exposed façade are needed. Transmission paths that can safely be ignored at exposed positions might become important at shielded ones, and sources that normally can be ignored might have an influence. This does not necessarily mean that a model

for engineering purposes must be very complex though, since many measurements at shielded positions in cities give very similar equivalent levels, usually around 47–52 dB. That the equivalent level is relatively constant at shielded positions throughout a city district does not mean that the all aspects of the sound field are fully understood however. The sound field is far from completely described by the A-weighted equivalent level. Temporal and spectral differences that do not change the A-weighted level may be clearly audible, and could be perceived rather differently. However, this is beyond the scope of this thesis, which is aimed at developing prediction methods relevant for the quiet side.

1.2 Requirements for predictions on the quiet side

What are the requirements of a prediction method for the quiet side? The short answer is that it must include all relevant sources and be able to capture multiple reflections accurately.

During a short measurement series at the beginning of the research programme it was noted that the level when no cars were close to the microphone on the exposed side was very similar to the level at the shielded side of a nearby building. This might be thought of as the city background level, a level that reaches all over the city like mist. This level is drowned by the direct sound at exposed positions, but at shielded positions or when no sources happen to be in the vicinity, it dominates.

The concept of a city background is a simple concept, but where does the background come from? Sound does not fill the city landscape like mist, or does it? It is demonstrated in [7] that solving the wave equation of sound propagation in a medium with many randomly spaced reflecting and absorbing objects gives the same answer as using a linear transport approach where sound is seen as small energy packets propagation in a scattering and absorbing medium.

Another approach that gives interesting results is if we use a very simple model of a city as in Paper V where all sources are lifted up out of their street canyons to the rooftop level and we calculate the sound pressure at the flat landscape above the rooftops. The level at the center of the city blocks is relatively constant as can be seen in the example given in Fig. 1.2.

Both the above mentioned approaches points in the direction of a very simple model, where the level at shielded positions is limited by a minimum level, the background level. This level is perhaps only dependent on the number of vehicles per unit area of the city, or in a slightly improved model, on the average grid spacing and traffic load for a city, as explained in [2]. Such a simple model may be very useful, but it is a blunt instrument. No details are given for specific positions, and

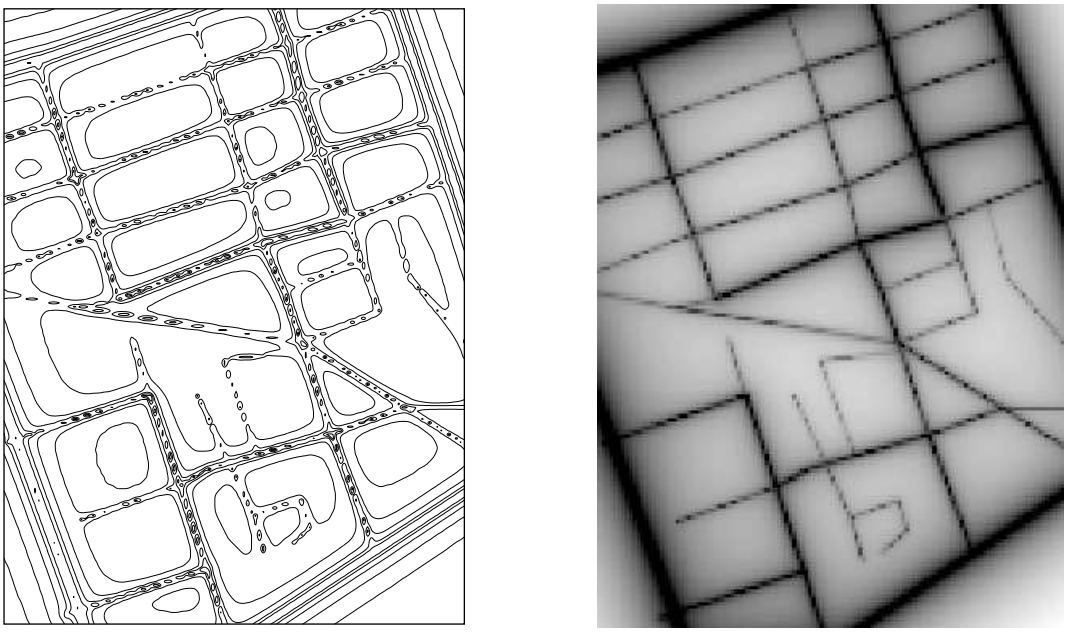

Figure 1.2: Contour curves (2.5 dB steps) and a grayscale colormap of the sound levels using the flat city method at Söder, Stockholm. The level at the center of the city blocks is relatively constant throughout the area ($\pm$1.5 dB).

there is little room for calculating the effect of different measures for improvement apart from changing the source characteristics.

A more detailed model of what goes on inside a shielded courtyard must describe how the sound waves are diffracted (or otherwise transported) into it, and how they interact with the inner façades and ground surface. The absorption of the inner façades is important, as well as effects of diffuse reflections, as has been shown by many authors [8, 9, 10]. Absorbing surfaces reduce the reverberation time, which will lower the levels. Surprisingly the qualitative effect off diffusion is the same, since the sound field is better mixed in the courtyard if there are diffusing objects present [11].

In Paper II a first attempt at modelling these effects using the equivalent sources method (ESM) for a simple two dimensional situation is presented. Prediction methods used for room acoustics presents one possible three dimensional approach, but then some work on the source modeling is needed, since the source is normally assumed to be located within the room itself in such methods.

1.3 Reducing the level at the quiet side

What can be done to improve the situation at the quiet side? Reducing the traffic flows would of course be efficient, but assuming that we would like to preserve the mobility of the residents this is not a way forward (unless other means of transport that are quieter are taken into account). Redistributing the traffic flows between different streets is acceptable up to a certain extent, and a theoretical evaluation of such an approach is given in Paper VI. The results show that concentrating the traffic gives lower levels at shielded positions, but we can only reduce the traffic down to a certain level before we make the district effectively unaccessible. This amount of traffic might be sufficient to make traffic redistribution inefficient. Another drawback is the very high levels on the exposed façades of the streets holding the concentrated traffic flows.

One important aspect that is evident from the calculations is that if we want to achieve an effect at shielded positions, we have to have a global approach. Reducing the traffic on a single street close to the quiet side in question will have little or no effect, since the level is determined by the traffic of all streets in the vicinity. This forms a sharp contrast to what is true on an exposed façade, where the level is determined by the closest street only, unless it has a very low traffic flow.

So is there nothing we can do locally on the shielded courtyard itself? To see the potential for improvements locally we have to abandon the simple idea of a background level, and realize that we can lower the level locally by adding absorption, and to some extent diffusion. A courtyard with absorbing inner façades and a soft ground will give a lower sound pressure level than if the surfaces are acoustically hard. The reverberation time will decrease, and any sound energy being diffracted into the canyon will decay faster in the soft case, leading to lower levels. Assuming that the background level above the rooftops is the same, the level down in the courtyard is reduced due to absorption.

Absorption can of course be used also in the street canyons where the traffic is located, and would give similar effects. However, to reduce the level at a certain shielded position, all contributing streets would have to be treated with absorbers. Perhaps the first thing that springs to the mind is to use an absorbing road surface where the traffic flow is high. Hence, in order to reduce the level in one single shielded area it is more cost effective to apply the absorbers there. On the other hand, treating the street side will give benefits at many shielded positions simultaneously.

The following chapter will discuss the two dimensional city canyon, which is a simple for a courtyard as a quiet side. In chapter 3 the equivalent sources solution method is presented in detail, and it is explained how absorption, diffusion and tur-

bulence can be included into the solution. Chapter 4 discusses the simple flat city method. Results are given in 5.1, and finally the conclusions are given in chapter 5. The appendices include a short discussion on free field correction in courtyards and the effects off calculating the level at the quiet side with buildings seen as traditional noise barriers.

CHAPTER 2

The City Canyon

2.1 The 2-D canyon

In an urban environment where rows of connected houses line the streets, a city canyon is formed. In Fig. 2.1 an aerial photograph from Söder, Stockholm, shows a typical configuration, with straight streets and 5–7 floor buildings surrounding the streets. Here the houses form closed backyards. The backyards vary a lot in size and shape, but the street side is more regular, only the widths of the streets are changing.

Figure 2.1: Aerial photograph over Söder, Stockholm. © Lantmäteriet.

A first approximation of the city street environment is to visualise it as a straight and infinitely long canyons sunken into an infinite and flat plane, see Fig. 2.2. This approach has the advantage of being two dimensional, at least if the source is a line source in parallel canyons. In this thesis not only the streets are seen as canyons, but also the courtyards. Real courtyards are sometimes similar to the street side, but often they are not infinite canyons since buildings shield them from the side streets. In this case the two dimensional canyon geometry is used as an analogue of a courtyard, since the numerical models used here are computationally too heavy for three dimensional calculations.

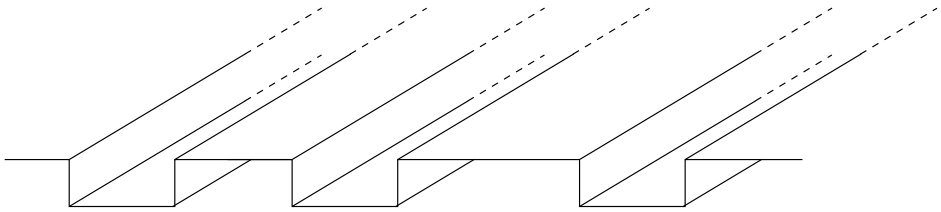

Figure 2.2: Sketch of a simplified series of street canyons and courtyards.

The sound field inside the canyon can be excited by either a line source, which is the purely two dimensional situation, or by a point source. A point source is relevant for a single vehicle, and is suitable for predictions where the time variations of the sound pressure are in focus. If only the equivalent level over a time period is interesting, a line source representing a vehicle flow is sufficient. Note that using a point source makes the situation three dimensional again. In many situations two dimensional calculation methods can still be used though, and the results translated to three dimensions using a transformation, see [12]. And although there is no strict proof, there is evidence that the level relative to free field in a two dimensional and the corresponding three dimensional case are similar [13], at least for simple screening cases and probably also for more complex cases. More accurate prediction methods aiming at describing more detailed effects of the sound field at courtyards should of course be three dimensional.

2.2 Damping in the canyon

If the canyon has high side walls, standing waves will be formed between them. This can be seen as the effect of many reflections interfering constructively with each other at the resonance frequencies, and the sound level becomes very high at

these frequencies. Therefore taking into account the effect of damping inside the canyon is very important.

In Paper II the effect of changing the height of the side walls in a canyon with very little damping is studied using the equivalent sources method. The canyon is 20 m wide, and the height of the side walls is changed from 2 m up to 30 m. The figure is included here also, but as a 3D plot of waterfall type of the frequency response. The source is located 0.5 m from one corner of the canyon, and the receiver 0.5 m from the opposite corner. Already when the height is around 10 m, half of the width of the canyon, the resonance peaks are rather sharp.

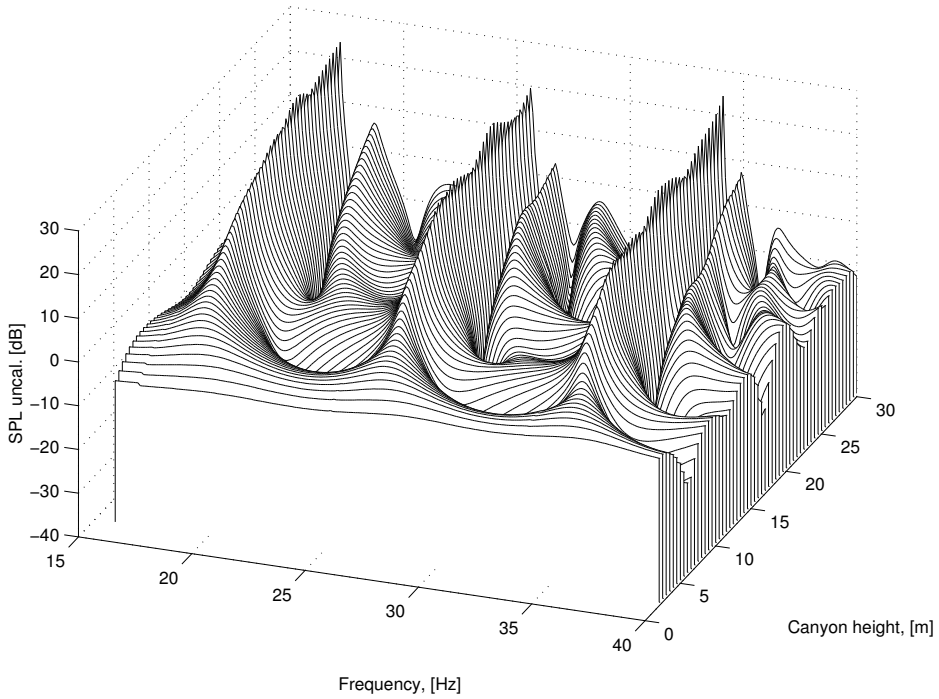

Figure 2.3: Frequency response in a canyon of width 20 m for side wall heights of 2–30 m.

The damping in the canyon comes both from the absorption of the air itself, and from absorption by the canyon surfaces. The façade materials are usually rather hard, but since many reflections are involved they can still be important. On the floor surface of the canyon the absorption can be substantial, either if it is partly grass covered, or covered by a porous asphalt. The importance of the floor surface can be studied using the method presented in [14], where the floor can have arbitrary impedance and the canyon side walls are seen as infinitely high.

Another approach is to apply methods from room acoustics, and use the concept

of reverberation time [15, 16, 17], where a diffuse field is assumed in the canyon, and the opening is considered as a perfect absorber. One problem with this approach is that the standard models assume a uniform distribution of damping throughout the whole canyon. The opening of the canyon must be included as an absorber, since the room acoustic methods require a closed space. If the other walls are relatively hard, the damping is not evenly distributed.

Using Sabine's formula underestimates the reverberation time when the damping is not uniformly distributed, since it assumes that all modes are damped similarly. When the absorption is concentrated to the ceiling (the opening of the canyon), the absorption strongly affects modes in the up-down direction but hardly at all modes in the horizontal direction. Mixed modes are affected depending on how much they interact with the absorbing ceiling. The reverberation time will be determined by those modes that are weakly damped, therefore it will be underestimated if a uniform absorption distribution is assumed. This effect is more pronounced for low courtyards, where the area of the opening is large in comparison to the area of the side walls.

An example from a measurement in a courtyard is given in Fig. 2.4. The courtyard has a height of 4 m, width of 23 m and length of 26 m. The façades are 50% brick and 50% glass and the floor is concrete and wood. Assuming an absorption coefficient of 1 for the opening and a uniform distribution of damping gives a reverberation time of about 0.6 s with Sabine's formula, and the measured value is 1.2 s (based on nine different source and receiver positions). Changing the absorption on the other surfaces have only a small influence on the result. There are however better methods for modelling the reverberation time when the damping is unevenly distributed. One such method is presented in [18][1], where the calculation is separated into two terms; one for ceiling-to-floor absorption and one for wall-to-wall absorption. Using this method instead and assuming an absorption coefficient of 0.1 for the side walls gives a reverberation time of 1.0 s.

Note that for a three dimensional backyard the decay curve can be well described by two straight lines. The slope is steeper right after the source is turned off, when the modes that radiate out of the canyon quickly decays. Then the modes mostly in the horizontal direction decay slower. Finally we reach the background level. This means that the reverberation time measured over a small drop in level will be shorter than if it is measured over a larger drop (e.g. $T_{10} < T_{30}$). For more canyon-like (two dimensional) situations the decay curve is more concave [16].

Using numerical models that discretize the canyon geometry such as the boundary element method (BEM) or the equivalent sources method (ESM), the damping

[1] There is a misprint in the formula for T_{60} in [18], the last numerator should be lw.

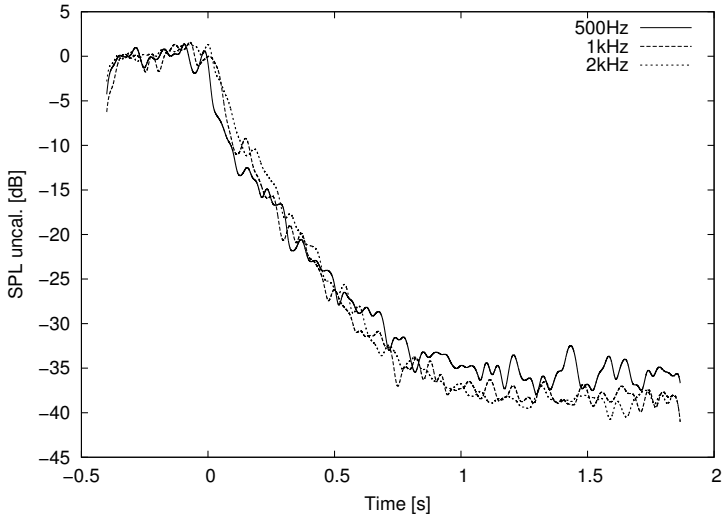

Figure 2.4: Decay curves for a courtyard ($4 \times 23 \times 26\,\mathrm{m}^3$) for the octave bands 500, 1000 and 2000 Hz.

in the canyon can be treated using impedance boundary conditions on the surfaces. These boundary conditions are included when solving the system of equations constructed by the respective method, and influence the pressure at the receiver position. This approach is more realistic than using a diffuse field approximation and the reverberation time concept. It also makes it possible to investigate the effect of introducing absorbers in the canyon, and determine which positions give the largest influence, as has been done in Paper IV using the ESM.

The results from this paper show that an absorber is more efficient if placed inside the city canyon, than outside. This is not surprising; imagine a plane wave travelling along the hard plane above the canyon, see Fig. 2.5. If an absorber is located here, the wave will only be slightly affected as it only passes once. Once the plane wave reaches the canyon, the energy that enters the canyon via diffraction bounces back and forth between the walls. If an absorber is located on one of the side walls, it will interact several times with the sound wave, thus having a higher influence on the total level compared to placing the absorber outside the canyon.

Almost the same argument can be used to understand that an absorbing patch on the canyon floor will have less effect than if it is placed on one side wall, since waves in the up-down direction will radiate out of the canyon. Waves that reflect back and forth between the side walls will interact with the absorber on the floor at gracing incidence, which in these cases leads to less efficient absorption of the sound energy. This effect is also visible in the extensive model measurements presented in

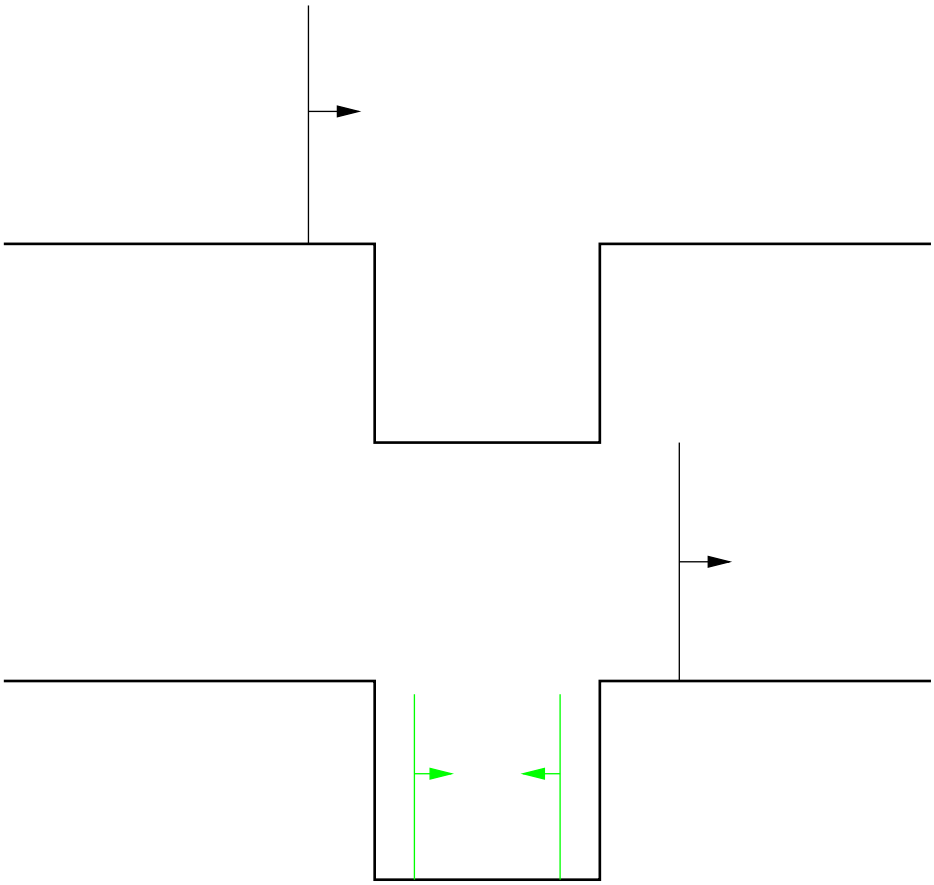

Figure 2.5: Sketch of a plane wave passing the canyon, giving multiple waves in the canyon via diffraction.

[19], where an absorber over the whole floor surface gives approximately the same effect as absorption on a small part of the side walls. The results are however a bit difficult to compare, since the absorbers used on the floor and on the side walls are of different types.

2.3 Diffusion in the canyon

A real city street does not have perfectly flat surfaces. Irregularities are present on different scales, from roughness on a façade surface in the order of millimetres up to gates and bay windows in the order of meters. These irregularities influence the reflection of sound waves by the surfaces, causing energy to be spread over all angles instead of only in the specular direction.

Introducing diffusion into a canyon leads to shorter reverberation times and

lower sound pressure levels [10, 20]. This can be explained by studying the standing waves between the canyon side walls. Each time the sound wave is reflected against the diffusively reflecting surface, some of the energy in the wave is directed upward, and will propagate out of the canyon. The same effect is known from room acoustics, where diffuse reflection leads to a shorter reverberation time if the absorption is non-uniformly distributed in the room [21, 11, 22].

When predicting noise levels in city canyons using ray based methods, diffusion is often included as a separate process, as for instance in [9, 23, 24]. The surfaces are seen as flat, giving only specular reflections, and then a roughness value for the surface feeds energy from the specular sound field to the diffuse sound field. At the receiver the pressure is determined by adding up the contribution from whats left of the specular field with the diffuse field under the assumption that these contributions are uncorrelated.

This approach demands two separate models, one for the propagation of the specular field, which will be the same as a model without diffusion, and one for the propagation of the diffuse field. Also a way to transfer energy from the specular field into the diffuse one is needed. Unfortunately this approach might lead to the misunderstanding that there are two separate processes in the canyon, which are difficult to combine. There are no two processes; diffusion is described by the wave equation. Solving it in a canyon with all irregularities and impedances correctly modeled would give an answer including diffusion effects.

When solving the city canyon problem with numerical methods such as ESM or BEM there are two different approaches for the inclusion of diffusion. Either including the diffracting elements in the description of the boundary, as has been done in Paper IV, or by modifying the numerical method in some way to allow for diffusion as a separate process. Using the first approach the solution will give a single realization for exactly the condition that is modeled. Changing the geometry slightly will require the whole problem to be solved numerically again. The second approach might lead to a more usable result. Instead of solving for a situation with a large number of scattering elements at different positions, and shapes, a solution for an average number and size of elements would be obtained. On the other hand there is no reason to suspect that the sound level change in a city canyon due to minor changes will change dramatically, so a single realization might serve as a good estimate of the average effect.

2.4 City canyon meteorology

For traffic noise propagation over medium and long ranges, the effects of meteorology are very important [25, 26, 27]. The refraction from temperature and wind gradients have a large influence, the humidity determines the intrinsic damping of the air (which is very important for long ranges), and turbulence in the atmosphere causes decorrelation and scattering into shadow regions. In this thesis only the effects of turbulence are treated in, but for future improvements it is very important to include other weather effects as well.

The meteorological situation in and above a street canyon has been studied extensively, both using field measurements and numerical simulations [28, 29, 30, 31]. The focus is often on the spreading of pollutants in urban environments. In [30] the basic air flow structure in the canyon is explained: if the wind direction is perpendicular to the canyon there will be recirculation in the canyon, and a turbulent shear layer at the opening. These effects are illustrated schematically in Fig. 2.6. The recirculation is not a stationary process, it is intermittent. If the angle between the wind direction and the canyon is neither parallel or perpendicular, there will be a spiraling recirculation, and if the wind direction is parallel to the canyon, there will be a channeling effect. Other types of flow can occur in extreme cases, i.e. for a very deep and narrow or very wide and shallow canyon.

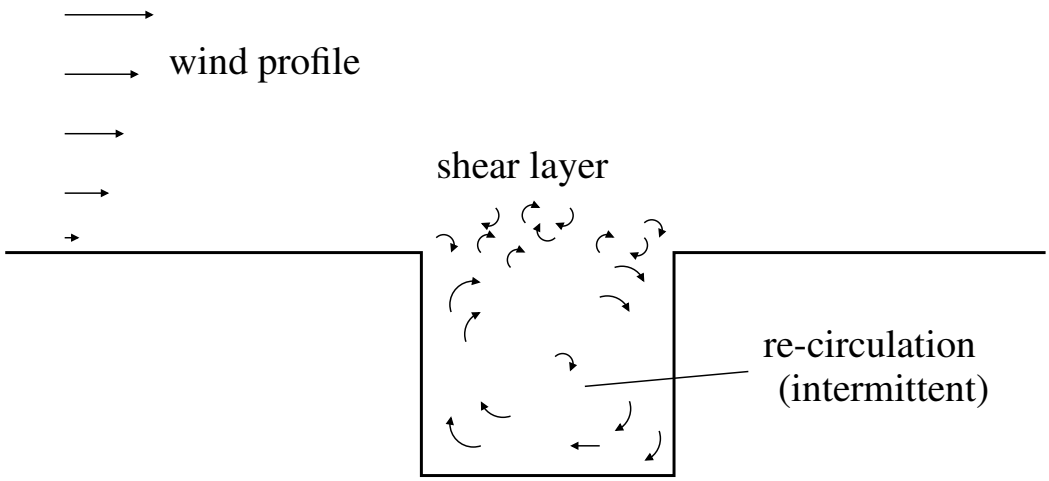

Figure 2.6: Sketch of flow within and above the street canyon.

The measurements in [29] show that the air in the canyon is well mixed with respect to temperature, and that the air in the canyon is slightly warmer that the air above it. The strength of the turbulence in the canyon is not dependent on the wind

direction relative to the canyon, but the average wind profile is. This indicates that a sound propagation model for the effect of turbulence can ignore the wind direction, but if refraction is to be included, wind direction must be taken into account.

In Paper I and Paper III the turbulence is described by the von Kármán spectrum. The strength of the velocity and temperature turbulence is determined by the outer scale and the structure parameters. The outer scale describes the large eddies that are created in the source region, which then decays into smaller eddies in a cascade process in the inertial region. There is also a dissipation region, where the energy of the eddies is lost into heat, but that region corresponds to eddies so small (in the order of millimeters) that it has little or no effect on sound propagation.

The refraction due to meteorological effects is not studied in this thesis, but could be included in the equivalent sources method if the Green functions used are updated to reflect this. One way of doing it would be to calculate the Green function above the canyons using the fast field program method (FFP, see [32]), using the effective sound speed profile. Another approach would be to use more advanced methods where both the flow velocity field of the atmosphere as well as the acoustic sound propagation are solved numerically, see [33, 34]. These methods are however computationally heavy, and would be most valuable if they could include the disturbance on the wind field that the presence of the canyon causes. Such effects are important for sound barriers, see [35].

CHAPTER 3

Numerical Modelling

3.1 The equivalent sources method

The basic idea of the equivalent sources method (ESM) as it is used here is very simple. Choose a simple geometry for your problem, and where the situation is not so simple, put sources. The problem is then reduced to finding out the strengths of these sources, and then adding up the contributions from the sources, both the original ones and those added to avoid the difficulties.

The name of the method is not universally accepted as is the case with for instance the finite element method (FEM). Alternative names for the same or closely related methods are source simulation and substitute sources. There are also variations regarding if it is to be called a method, model, technique or something else.[1]

A very thorough investigation of the properties and limitations of the ESM in general can be found in [36] and [37]. Here the ESM is presented as an interior or exterior problem, where the field is described in one domain by sources located outside this domain. The method described here uses the same approach, but the sources are located between two domains and ensures that the boundary conditions between those domains are fulfilled. The first use of the ESM to couple two fields in this manner in acoustics is reported in [38], and a good explanation of the background is given in [39].

The ESM was chosen since it provides a computationally more efficient method than other applicable numerical methods such as the boundary element method

[1] A discussion on the slight differences between these words would be pointless, since there is almost no potential for misinterpretation. If all researchers would agree on a single name, it would certainly lead to similar and perhaps less informative titles on future papers on the subject.

(BEM) or the finite difference time domain method (FDTD). These methods discretize the entire domain (FDTD) or the entire boundary (BEM), whereas the ESM only discretizes the opening of the canyon. The Green functions used in the ESM negates some of this advantage, since they are relatively time consuming to evaluate. In special cases such as very high damping or very wide canyons the other methods might still be faster, and if the results are needed in the time domain the FDTD is of course a better alternative.

Since the basics of the ESM used in this thesis is described in both paper Paper II and Paper III, the text here is instead aimed at explaining in more detail how to interpret the mathematics of the method, and how to implement it as a computer program.

The starting point is the wave equation for the pressure, p, in two dimensions for a harmonic time dependence of $\exp(\mathrm{j}\omega t)$, also known as the Helmholtz equation

$$\nabla^2 p(x,y) + k^2 p(x,y) = -\mathrm{j}\omega\rho_0 q(x,y). \tag{3.1}$$

A derivation of the Helmholtz equation can be found in [32]. Here $p(x,y)$ denotes the pressure, k the wave number, ρ_0 the density of air, $\omega = 2\pi f$ the angular frequency and $q(x,y)$ the source strength density, which is a volume velocity in the three dimensional case. Perhaps it is more logical to still call it a volume velocity, but in two dimensions it becomes velocity times length instead of velocity times surface, whereby surface velocity is an alternative description. To avoid confusion the names familiar from three dimensional analysis, is used throughout this thesis. The factor $\mathrm{j}\omega$ is a derivative with respect to time, making the right side of the equation of type "density times acceleration".

The aim is to solve the equation for a two dimensional city canyon of width l_x and height l_y, see Fig. 3.1. The domain D_2 is the half-space above $y = l_y$ and D_1 is the domain inside the canyon, $0 \leq x \leq l_x$ and $0 \leq y \leq l_y$. Γ is the boundary between the two domains D_1 and D_2. A boundary condition is also needed, and of course some kind of excitation, either via sources inside the domain $D_1 \cup D_2$ or a radiating condition on the boundary $\partial(D_1 \cup D_2)$.

To start with, the boundary condition is that the velocity in the normal direction to the boundary is zero, which corresponds to an infinitely rigid surface. The effect of an impedance on the boundary (Robin condition) can be modeled by placing a source density on the rigid boundary as will be explained in section 3.5. For the infinite half-space the boundary at infinity must fulfill the Sommerfeldt radiation condition. Now we have an equation valid inside our domain, and boundary conditions all around it, which is a minimum requirement for solving the equation.

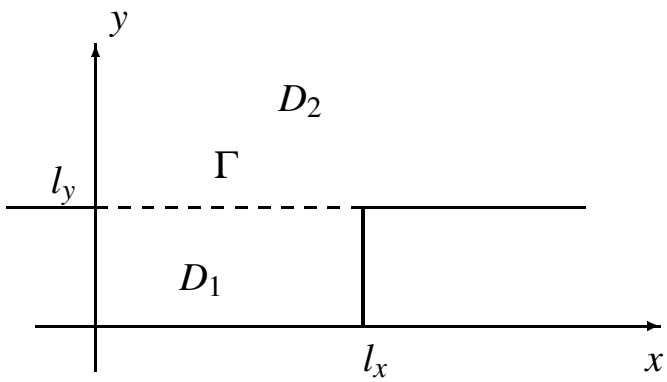

Figure 3.1: Geometry and coordinate system of the two dimensional city canyon.

The starting point for the ESM in this case is to divide our problem into two separate domains, D_1 and D_2, see Fig. 3.2. The boundary Γ is replaced by an infinitely thin rigid barrier. Then D_1 will be a closed rectangular cavity, and D_2 a simple two dimensional half-space. In each of these simple domains we can find a Green function, a function that describes the pressure in the whole domain if it is excited by a point source (a point source in two dimensions could also be called a line source). The corresponding Green functions are

$$G_1(x_s, y_s | x_r, y_r) = \mathrm{j}\omega\rho \frac{c^2}{l_x l_y} \sum_n \sum_m \frac{\Psi_{n,m}(x_s, y_s)\Psi_{n,m}(x_r, y_r)}{\Lambda_{n,m}(\omega_{n,m}^2(1+\mathrm{j}\eta) - \omega^2)} \tag{3.2}$$

and

$$G_2(x_s, y_s | x_r, y_r) = \mathrm{j}\omega\rho \frac{-\mathrm{j}}{2} H_0^{(2)}(kr), \tag{3.3}$$

where (x_s, y_s) is the position of the source and (x_r, y_r) the position of the receiver. The notation and properties of the modal summation in Eq. (3.2) is discussed in section 3.2, note however that it is an approximation for low loss factors η. The sound speed is denoted c, $\Lambda_{n,m}$ are the modal weights and $\Psi_{n,m}$ the modal shape functions.

The Green function for the half-space G_2 contains the Hankel function of the second kind, and describes a source on a rigid surface. If the source is not at the rigid surface, but somewhere in the domain D_2, the Green function will be exactly half of G_2, and an image source will contribute to the pressure. The distance between the source and the receiver is denoted $r = \sqrt{(x_s - x_r)^2 + (y_s - y_r)^2}$.

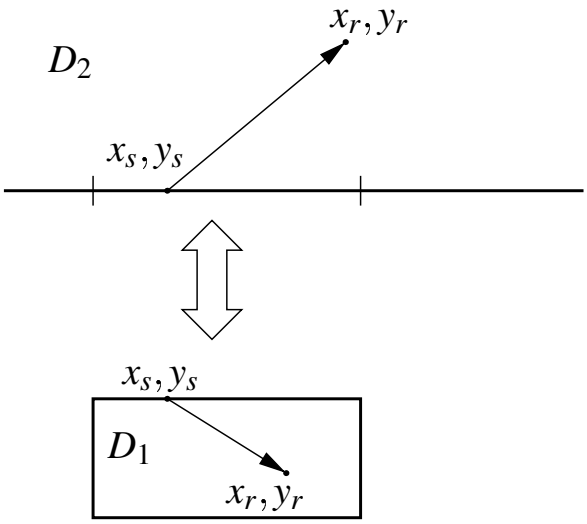

Figure 3.2: Separation of the domains D_1 and D_2 with a ridgid boundary.

To compensate for the fact that the half-space is not rigid where the canyon is located, we add a source density $q_u(x)$ from $x = 0$ to $x = l_x$ along Γ. Using the same reasoning we add a source density $q_l(x)$ on the underside of Γ to compensate for the fact that there is no ceiling. The normal direction for the source densities q_l and q_u is into their respective domains. The pressure can be determined by

$$p_l(x_r, y_r) = \int_\Gamma q_l(x) G_1(x, l_y | x_r, y_r)\, \mathrm{d}x + p_{ol} \tag{3.4}$$

inside the canyon $(x_r, y_r \in D_1)$ and

$$p_u(x_r, y_r) = \int_\Gamma q_u(x) G_2(x, l_y | x_r, y_r)\, \mathrm{d}x + p_{ou} \tag{3.5}$$

above the canyon $(x_r, y_r \in D_2)$. The contribution from the original sources is included as p_{ol} and p_{ou}. If for example only one source is present inside the canyon $p_{ou} = 0$ and p_{ol} would be the contribution from that source to a receiver located within the canyon $(\in D_1)$.

Now we have two fields which are the solution to the Helmholtz equation in the respective domains, but not a solution to the whole domain. To obtain that we must ensure that both the particle velocity and the pressure are continuous across the boundary Γ. Pressure continuity gives

$$p_l(x, y) = p_u(x, y) \quad (x, y) \in \Gamma \tag{3.6}$$

and velocity continuity gives

$$q_l(x,y) = -q_u(x,y) \quad (x,y) \in \Gamma. \tag{3.7}$$

Note the minus sign for the volume velocity. Moving air from one domain into the other gives a positive contribution on one side of the boundary and a negative contribution on the other. This is what makes the assumed source density a coupling between the two fields instead of an ordinary source, which would give a positive contribution on both sides if placed on the boundary Γ.

The pressure right at the boundary can be calculated both with equation (3.4) and (3.5) from the boundary source density $q(x)$ $(= q_l(x,l_y) = -q_u(x,l_y))$ and the contributions from the original sources. The resulting equation can in principle be used to obtain the unknown density $q(x)$. Unfortunately no analytical solution is available, and therefore one must rely on numerical methods, where the density $q(x)$ is divided into a finite number of elements. The solution approach used here divides the boundary into N equally sized elements $\Gamma_1, \Gamma_2, \ldots, \Gamma_N$ with center points $(x_1,y_1),(x_2,y_2),\ldots,(x_N,y_N)$. The density $q(x)$ can now be discretized using these elements, and the problem can be written as a matrix equation, which is described in more detail in section 3.3.

3.2 Modal summation

The Green function G_1 is a modal summation where the eigen-frequencies $\omega_{n,m}$, modal shapes $\Psi_{n,m}$ and modal weights $\Lambda_{n,m}$ can be determined using

$$\omega_{n,m} = \pi c \sqrt{(n/l_x)^2 + (m/l_y)^2} \tag{3.8}$$

$$\Psi_{n,m}(x,y) = \cos(n\pi x/l_x)\cos(m\pi y/l_y) \tag{3.9}$$

$$\Lambda_{n,m} = \int_0^{l_y}\int_0^{l_x} \Psi_{n,m}^2 \,\mathrm{d}x\,\mathrm{d}y. \tag{3.10}$$

By integrating the expression for the modal weights Λ one obtains

$$\Lambda_{n,m} = \begin{cases} 1 & n = m = 0 \\ 0.5 & n = 0,\ m > 0 \text{ or } m = 0,\ n > 0 \\ 0.25 & n > 0,\ m > 0 \end{cases}. \tag{3.11}$$

The sum in formula (3.2) should be over all modes, but since there are infinitely many, the sum has to be truncated somewhere. A common practice in structural

acoustics is to use modes with eigen-frequencies up to three or four times as large as the frequency of interest. When the frequency is close to a resonance the denominator in Eq. (3.2) becomes very small for the mode that corresponds to the resonance frequency, and the other terms in the sum will be small in comparison. Therefore it is sufficient to include only one or a few modes close to the resonance. Far from any resonance peaks the situation is reversed and many modes contribute to the solution.

When determining which modes to include in the summation there are two common approaches, either all modes up to a certain order m and n, or all modes with eigen-frequencies up to a certain value. These approaches are illustrated in Fig. 3.3, where all modes within the square are up to a certain order, and all modes within the circle are of eigen-frequencies less than a certain frequency. The domain in the diagram is what is known as a k-space, with the wavenumber $n\pi/l_x$ along the x-axis and $m\pi/l_y$ along the y-axis. The difference in the result between the methods is relatively minor, and depends on the source and receiver positions. Here the square method has been used.

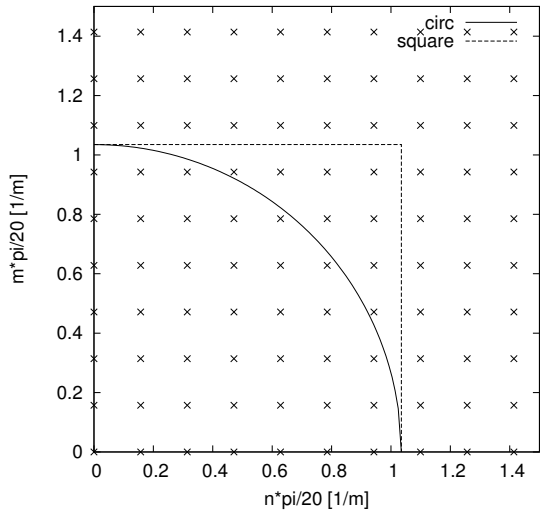

Figure 3.3: Illustration of summation of modes/eigen-frequencies in a 20×20 m^2 closed cavity in k-space.

An alternative way to calculate the Green function G_1 is to use an image source method, where the contributions from many image sources are added. It seems reasonable that such an approach would be more efficient than modal summation if the damping is relatively high. Then a large number of modes would be needed, but few image sources since those representing many reflections in the walls of the closed canyon would be attenuated by the damping. The main interest in this text

is relatively undamped canyons though, and therefore the method is more time consuming than the modal summation. In Fig. 3.4 a calculation using image sources is compared to a modal summation. The canyon is 17×20 m^2, and the damping $\eta = 0.004$, corresponding to approximately 0.005 dB/m in the frequency range plotted. The total number of image sources included is 25,600 (reflections up to order 160), and in spite the relatively high damping there is a small deviation compared to the modal approach. The very low frequencies were chosen to speed up the calculations, the results look similar at higher frequencies.

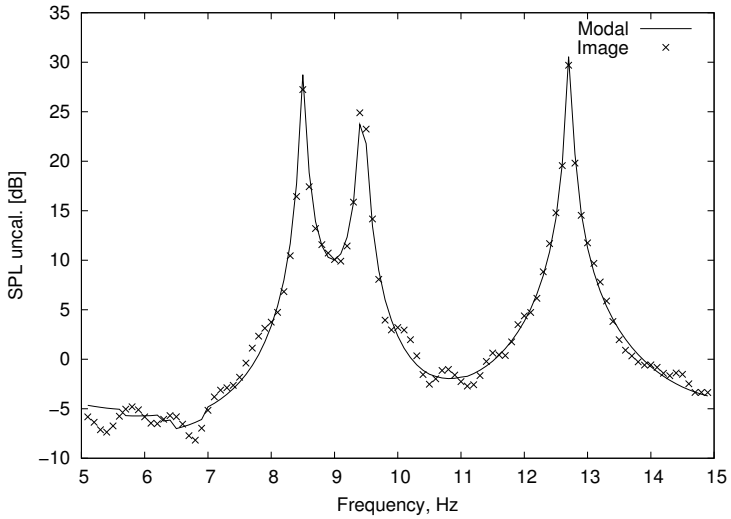

Figure 3.4: Comparison between a frequency response calulated using a modal approach and an image source approach using images of order up to 160.

When implementing the modal summation as computer code one can gain computational efficiency by ensuring that no calculations are repeated unnecessarily. For instance the eigen-frequencies of the modes are the same irrespective of position and frequency, and can be pre-calculated.

3.3 Building the matrix

Determining the strength of the boundary source density $q(x)$ that couples the solutions in the two domains D_1 and D_2 gives the solution to the total problem, and the pressure can be calculated at any position in the two domains using this information.

There are two approaches. Either one chooses large elements and describes the solution on each element using many coefficients for discretizing the boundary, or small elements with few coefficients. Here an element length of one tenth of

the wavelength is used ($\lambda/10$), and the complex source strength is assumed to be constant on each element, i.e. described by one coefficient.

This is a rather crude approach, a zeroth order approximation one could say, but it is used because of its simplicity. For future and more efficient implementations perhaps a linear function on each element would give more accurate results. It might also be more optimal to make the element length dependent on the position. A finer discretization close to the corners seems like a natural choice, which might give the same accuracy with fewer elements, i.e. with less computational effort.

The most straightforward way of matching the pressure and velocity above and below every element is to set them equal at the center points of each element

$$(x_1, y_1), (x_2, y_2), \ldots, (x_N, y_N), \tag{3.12}$$

a method often referred to as collocation or point matching. This approach ensures a perfect match at the center points, and if the elements are small enough compared to the wavelength, the deviation at other points on the boundary should be small.

In order to make an equation system of the matching of the pressure above and below the boundary Γ we introduce the functions

$$g_1(n \to m) = \int_{\Gamma_n} G_1(x, y | x_m, y_m) \, \mathrm{d}x \tag{3.13}$$

$$g_2(n \to m) = \int_{\Gamma_n} G_2(x, y | x_m, y_m) \, \mathrm{d}x \,, \tag{3.14}$$

that describes the pressure at an element center point (x_m, y_m) as an integral over the source element times the Green function on the element assuming unity source strength. Since the source strength q_n is constant over the element it can be moved out of the integral, and we can set up a matrix equation

$$\mathbf{A}\,\mathbf{q} = \mathbf{b} \tag{3.15}$$

where the matrix $\mathbf{A}$ is defined as

$$\mathbf{A} = \begin{bmatrix} g_1(1 \to 1) + g_2(1 \to 1) & g_1(2 \to 1) + g_2(2 \to 1) & \ldots & g_1(N \to 1) + g_2(N \to 1) \\ g_1(1 \to 2) + g_2(1 \to 2) & g_1(2 \to 2) + g_2(2 \to 2) & \ldots & g_1(N \to 2) + g_2(N \to 2) \\ \vdots & \vdots & \ddots & \vdots \\ g_1(1 \to N) + g_2(1 \to N) & g_1(2 \to N) + g_2(2 \to N) & \ldots & g_1(N \to N) + g_2(N \to N) \end{bmatrix}.$$

(3.16)

The source strengths q_n are gathered in a column vector

$$\mathbf{q} = \begin{bmatrix} q_1 \\ q_2 \\ \vdots \\ q_N \end{bmatrix}, \tag{3.17}$$

and the column vector **b** describes the effect of the driving sources of the system

$$\mathbf{b} = \begin{bmatrix} \sum_{i=1}^{M} Q_i \, (-1)^{\alpha-1} \, G_\alpha(x_{si}, y_{si} | x_1, y_1) \\ \sum_{i=1}^{M} Q_i \, (-1)^{\alpha-1} \, G_\alpha(x_{si}, y_{si} | x_2, y_2) \\ \vdots \\ \sum_{i=1}^{M} Q_i \, (-1)^{\alpha} \, G_\alpha(x_{si}, y_{si} | x_N, y_N) \end{bmatrix}, \tag{3.18}$$

where α is one if the source is located inside the canyon, and two if it is located above the canyon

$$\alpha = \begin{cases} 1 & (x_m, y_m) \in D_1 \\ 2 & (x_m, y_m) \in D_2 \end{cases} . \tag{3.19}$$

Note that the source changes sign when it changes domain, since it will be on the left hand side in Eq. (3.4) when inside the canyon, and on the right hand side in Eq. (3.5), when above the canyon.

The integral over the Green function G_2 will give the same value for all elements when the receiver is on the center point of its own element, since all elements are of equal size. This can be expressed as

$$g_2(1 \to 1) = g_2(2 \to 2) = \ldots = g_2(N \to N). \tag{3.20}$$

The integral can be evaluated numerically, but care must be taken since it is singular when $n = m$. This is due to that the distance r goes to zero when the receiver is the center point of the source element itself. It is shown in [40] that a Gauss quadrature can be used, and in [37] a series expansion is suggested. Yet another approach is to use a Struve function, which is approximated by its series expansion for small values s, see 11.1.7 in [41]

$$\int_0^s H_0^{(2)}(x)\,\mathrm{d}x = H_0^{(2)}(s)\,\left(s - s^3/3 + o(s^5)\right) + H_1^{(2)}(s)\,\left(s^2 - s^4/9 + o(s^6)\right). \tag{3.21}$$

For an element size of $\lambda/10$ the error is 0.02% using Eq. (3.21), which can be decreased further if more terms are included in the series expansion. The integrations of the Green function G_1 are straight-forward and do not give a singularity when $n = m$.

The resulting matrix $\mathbf{A}$ is square, fully populated and symmetric, and the system can easily be solved with for instance Gaussian elimination. The values below the diagonal can be obtained through the symmetry if the values above it have been calculated. This will decrease the time used to build the matrix by almost 50% for large matrices.

3.4 Subspace methods

When the number of modes that has to be included is very high if the wavelength is small compared to the size of the canyon, it can be very time consuming to set up the matrix $\mathbf{A}$. The number of modes needed for calculating for the Green function G_1 increases as f^2, and the number of elements in the matrix also increases as f^2. Therefore the time to set up the equation system increases approximately as f^4. At high frequencies, the setting up the matrix dominates the total time consumption. Solving it takes less than 1% of the total CPU-time used at 1 kHz for a 20×20 m^2 canyon.

One way of reducing the number of modes that has to be included is to divide the canyon into sub-domains, and couple those domains together just as the domain above the canyon is coupled to its interior. It is easiest to implement a horizontal division as is illustrated in Fig. 3.5, but vertically divided sub-domains are also possible. If the sub-domains are chosen symmetrically, the Green functions in them are equal, which means that they only need to be computed once, further improving the computational efficiency of the approach.

In [42] it is demonstrated that division into sub-domains gives a faster setup time of the equation system, but increases the size of it. The reduced setup time is due to that the Green functions in smaller sub-domains can be calculated using fewer terms in the modal summation. However, this approach it is only efficient until the size of the equation systems becomes large enough so that the computers

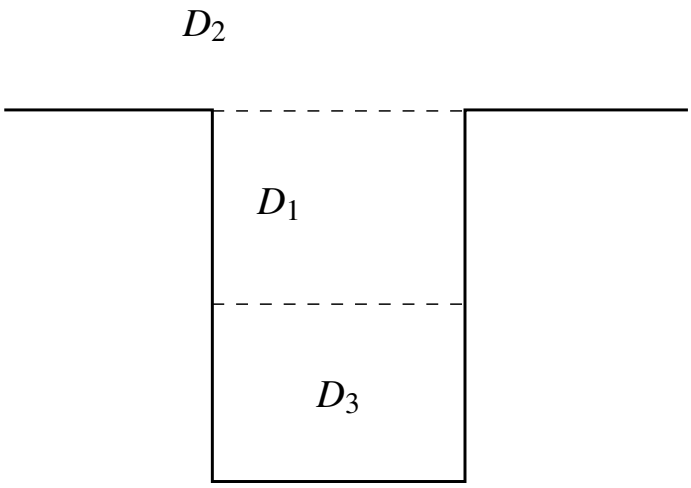

Figure 3.5: Division of the canyon into two equal subdomains D_1 and D_3.

cache memory, or even worse; primary memory, is full, causing it to have to swap information between different parts of the data storage system. In a case presented in [42] the optimum was to use six sub-domains, and it reduced the total time used for the computation by approximately 50%. Using more than six domains quickly increased the computation time.

$$\begin{bmatrix} G_1 + G_2 & -G_1 \\ -G_1 & G_1 + G_3 \end{bmatrix}$$

Figure 3.6: Illustration of the matrix for two horisontal sub-domains. $G_1 = G_3$ if the canyon sub-domains are choosen symmetrically.

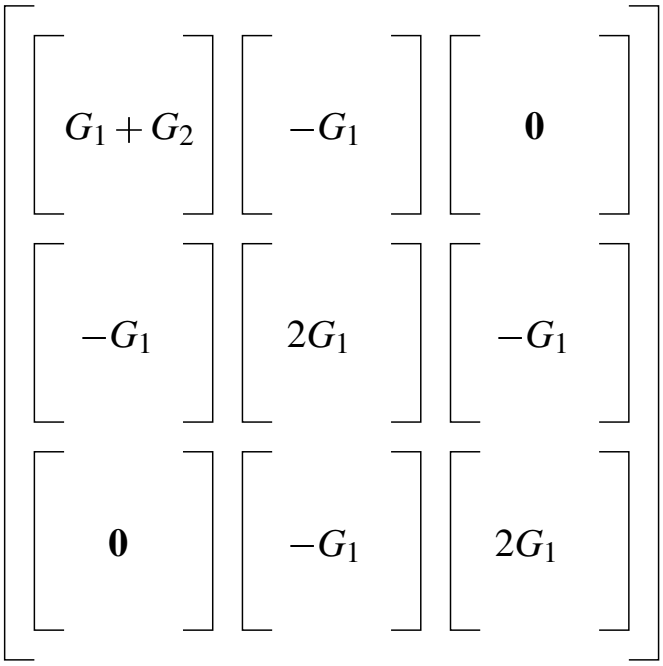

Figure 3.7: Illustration of the matrix for three horisontal sub-domains.

3.5 Impedance and sub-canyons

It is possible to include the effect of one or several patches with finite impedance on the canyon side walls, or on the plane surface above the canyon, when solving the equation system. Equivalent sources are placed on the patches, and instead of coupling two fields together via continuity, they ensure that the impedance boundary condition is fulfilled. This approach is explained and used successfully in [40] and [39].

The boundary condition for a locally reacting impedance is

$$p = Z v, \tag{3.22}$$

where v is the particle velocity normal to the surface. It is important to keep track of the direction of the normal, into or out of the surface. For many impedance models a normal directed into the surface is assumed, and then a positive real part of the impedance corresponds to power being transmitted into the surface. The sign of the imaginary part is not only related to the direction of the normal, but also to the sign of the harmonic time dependence.

The two dimensional volume velocity Q is equal to the velocity normal to the surface times the size of the element, if the velocity is assumed constant across the

element. On the other hand the source strength q is the volume velocity density along the element, i.e. equal to the normal velocity in this case.

If the impedance on the element is known we can relate the pressure on the element to the strength of the equivalent source inserted to fulfill the boundary condition, see [39]. Again we can calculate the pressure on the center point of an element in two ways, either as a sum of contributions from other sources, or as the impedance, which is assumed constant throughout an element, times the source strength on the element. This gives a new equation system for all elements on patches with an impedance surface, and again we can determine the source strength required to fulfill the desired impedance. The pressure at the center point of the impedance element i inside the canyon can be calculated as

$$p_Z = Z_i q_i', \tag{3.23}$$

where q_i' is the source strength, Z_i the impedance and Δx the length of the element. It can also be determined from the contribution of the other source strengths, both from the boundary Γ and from other impedance elements (including the element itself)

$$\begin{aligned} p_{int}(x_i, y_i) = &\sum_{j=1}^{N} q_j \int_{\Gamma_j} G_1(x, y|x_i, y_i)\,\mathrm{d}x + \\ &\sum_{j=N+1}^{N+M} q_j' \int_{\Gamma_j} G_1(x, y|x_i, y_i)\,\mathrm{d}x + p_{ol}, \end{aligned} \tag{3.24}$$

where M is the number of impedance elements, Γ_j, $j > N$, describes the impedance elements and p_{ol} is the contribution from any primary sources located inside the canyon. A similar set of formulas can easily be derived for a patch located outside the canyon.

Using these formulas a new equation system like (3.15) can be formed, now of size $(M+N) \times (M+N)$. The general formula for the matrix equation becomes prohibitively large, whereby an example gives better insight. Assume that we have a canyon where two elements describe the opening Γ, and another two elements describe an absorbing patch on one of the side walls as sketched in Fig. 3.8.

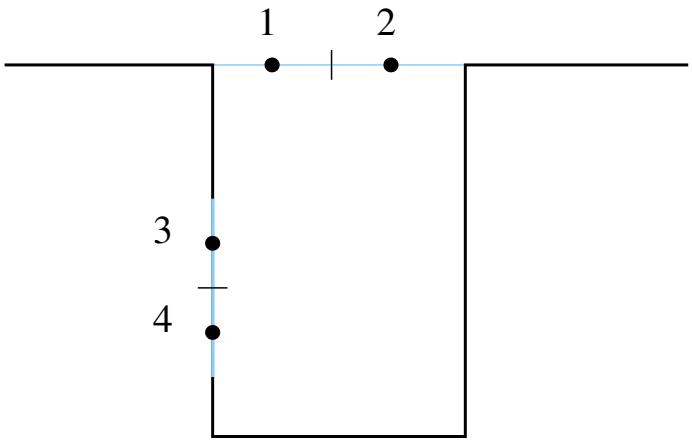

Figure 3.8: Example of a canyon with an absorbing patch on the left side wall.

The matrix corresponding to the problem in Fig. 3.8 is

$$\mathbf{A} = \begin{bmatrix} g_1+g_2 & g_1+g_2 & g_1 & g_1 \\ g_1+g_2 & g_1+g_2 & g_1 & g_1 \\ g_1 & g_1 & g_1-Z & g_1 \\ g_1 & g_1 & g_1 & g_1-Z \end{bmatrix}. \tag{3.25}$$

Here the notation from (3.13) and (3.14) is shortened somewhat: the position in the matrix determines n and m. The four elements in the upper left are the same as for the problem without the impedance patch included. The effect of the impedance is included on the diagonal elements in the lower right, and the remaining elements simply describe the coupling between elements inside the canyon. Using an infinite impedance causes the two lower diagonal elements to go to $-\infty$, which can only be satisfied if $q_3' = q_4' = 0$, and the problem is reduced to the case with hard walls.

The method can also be extended by including more domains that are coupled together to construct a more complex geometry than just a simple canyon. For instance the effect of a niche or inward bend might be modeled with equivalent sources as a smaller cavity coupled to the canyon cavity. Again it is perhaps more enlightening to use an example, than to give a complex general formula.

Consider a canyon with both an impedance patch and a small niche, see Fig. 3.9. The matrix corresponding to the problem in Fig. 3.9 is

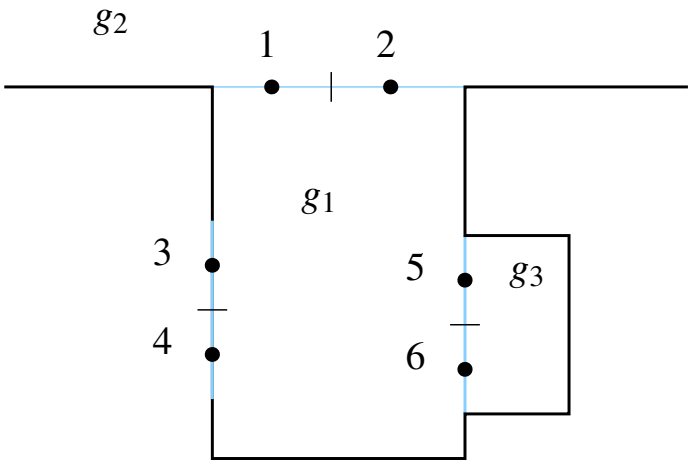

Figure 3.9: Example of a canyon with an absorbing patch and a small canyon connected to it.

$$\mathbf{A} = \begin{bmatrix} g_1+g_2 & g_1+g_2 & g_1 & g_1 & g_1 & g_1 \\ g_1+g_2 & g_1+g_2 & g_1 & g_1 & g_1 & g_1 \\ g_1 & g_1 & g_1-Z & g_1 & g_1 & g_1 \\ g_1 & g_1 & g_1 & g_1-Z & g_1 & g_1 \\ g_1 & g_1 & g_1 & g_1 & g_1+g_3 & g_1+g_3 \\ g_1 & g_1 & g_1 & g_1 & g_1+g_3 & g_1+g_3 \end{bmatrix}, \tag{3.26}$$

where g_3 is defined from a formula analogous to (3.13) but with the geometry and the Green function of the smaller cavity instead.

Including niches and impedance patches makes it possible to study the effect of diffusion in city street canyons, at least for two dimensional irregularities.

3.6 Including turbulence

When the atmosphere is homogeneous the contribution from each source element is multiplied with the Green function from the element to the receiver, and then all contributions are added up. Each contribution is a complex number, and adding them corresponds to adding up contributions from perfectly coherent sources. Turbulence effects will lead to decorrelation between sources, and the larger the propagation range, the larger the separation between the sources and the stronger the turbulence strength, the stronger the decorrelation becomes.

In propagation in a free field this decorrelation leads to both increased and decreased levels at certain time instances, but averaged out over time the intensity is

the same as in an homogeneous atmosphere. When there is an obstacle between the source and the receiver such as a noise barrier, the average level in the shadow behind the obstacle increases somewhat. This is usually viewed as an extra contribution, apart from the diffracted field, that reaches the receiver via scattering from the inhomogeneities in the air. This effect is studied in Paper I using measurements on a wide barrier and a theoretical model called scattering cross-section for the turbulence.

But studying a single house as a wide sound barrier is not relevant for situations with multiple reflections on the source and receiver sides. Therefore a version of the ESM including turbulence effects is useful. In Paper III such a method is described, based on the situation of two sources on a rigid plane displaced in the x-direction only, see Fig. 3.10. In a homogeneous atmosphere the pressure at the receiver would

Figure 3.10: Two sources on a ridgid plane in a turbulent atmosphere with separation Δx.

be the sum of the contributions from each source $p = p_1 + p_2$, but in a turbulent atmosphere we must take decorrelation into consideration, and we get

$$\langle |p|^2 \rangle = \langle p_1 p_1^* \rangle + \langle p_1 p_2^* \rangle + \langle p_2 p_1^* \rangle + \langle p_2 p_2^* \rangle. \tag{3.27}$$

Here $\langle\rangle$ denotes the ensemble average, which is equivalent to averaging over times much larger than the cycles of the sound waves. This can be expressed using the mutual coherence factor Γ_{ij}

$$\langle |p|^2 \rangle = \hat{p_1}\hat{p_1}^*\Gamma_{11} + \hat{p_1}\hat{p_2}^*\Gamma_{12} + \hat{p_2}\hat{p_1}^*\Gamma_{21} + \hat{p_2}\hat{p_1}^*\Gamma_{22}, \tag{3.28}$$

where $\hat{p}$ denotes the pressure without the effect of turbulence. Here the mutual coherence factor Γ_{ij} is assumed to be

$$\Gamma_{ij} = e^{-\gamma \Delta x}, \tag{3.29}$$

where γ is the extinction coefficient, which is dependent on the strength of the turbulence and the turbulence spectrum. Eq. (3.29) implies that $\Gamma_{11} = \Gamma_{22} = 1$, and that $\Gamma_{12} = \Gamma_{21}$. Using this, Eq. (3.28) can be rewritten

$$\langle |p|^2 \rangle = \hat{p_1}\hat{p_1}^* + \hat{p_2}\hat{p_2}^* + \Gamma_{12}(\hat{p_1}\hat{p_2}^* + \hat{p_2}\hat{p_1}^*), \tag{3.30}$$

which in turn can be simplified to

$$\langle |p|^2 \rangle = |\hat{p_1}|^2 + |\hat{p_2}|^2 + 2\Gamma_{12}\,\mathrm{Re}(\hat{p_1}\hat{p_2}^*). \tag{3.31}$$

This is an approximation[2] where it is assumed that the two sound waves travel through exactly the same atmosphere apart from the distance Δx, which is the only part that contributes to the decorrelation. This will underestimate the effect of turbulence, which can be explained as follows. Assume that the propagation from source to receiver occurs inside one Fresnel zone, and the decorrelation will be determined by the inhomogeneities present within this zone. A Fresnel zone, or perhaps more correct a Fresnel volume, is described by the ellipsoid formed between the source and the receiver when the propagation path is elongated by a fraction of the wavelength, see [43]. The two Fresnel zones will cover slightly different volumes, but not only along the common path of propagation, see Fig. 3.11. There is also an other error in the assumption that the atmosphere is the same along the common path since there is a small time difference between a sound wave emitted simultaneously from both sources. During this small time step the atmosphere will evolve slightly, and therefore it will not be identical for both waves.

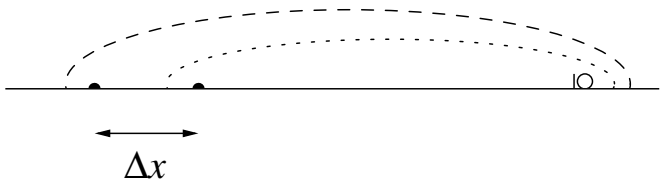

Figure 3.11: Sketch of the Fresnel zones for the two sources.

The above reasoning is valid for two sources, but can be generalised to work for a series of sources such as the equivalent sources used for the canyon calculations

[2]This model used here also assumes that the turbulence is homogeneous (independent of position) and isotropic (independent of rotation).

using the ESM. The effects for typical urban situations is small for low frequencies, and in the order of one or a few dBs at higher frequencies using the ESM method. Unfortunately no measurements have been published on the effect in typical urban geometries, but the effect measured for a wide barrier in Paper I is of the same order.

3.7 Rays and diffraction theory

Many prediction methods for road traffic noise use a combination of ray paths and diffraction theory to calculate the level in situations were shielding and reflections occur. The ray paths determine the interaction with the ground and reflections against obstacles, and diffracting edges are seen as secondary sources. Such a method for wedges and planes is described in [44], based on the diffraction theories from [45, 46, 47].

When using ray based methods to calculate the pressure in a canyon it is important to include many reflections. Consider a case with the source outside the canyon where the corner closest to the source will act as the diffracting wedge, see Fig. 3.12. Here the image sources in the diffracting wedge itself have been ignored; they are often included automatically in the diffraction model. It would appear that the only

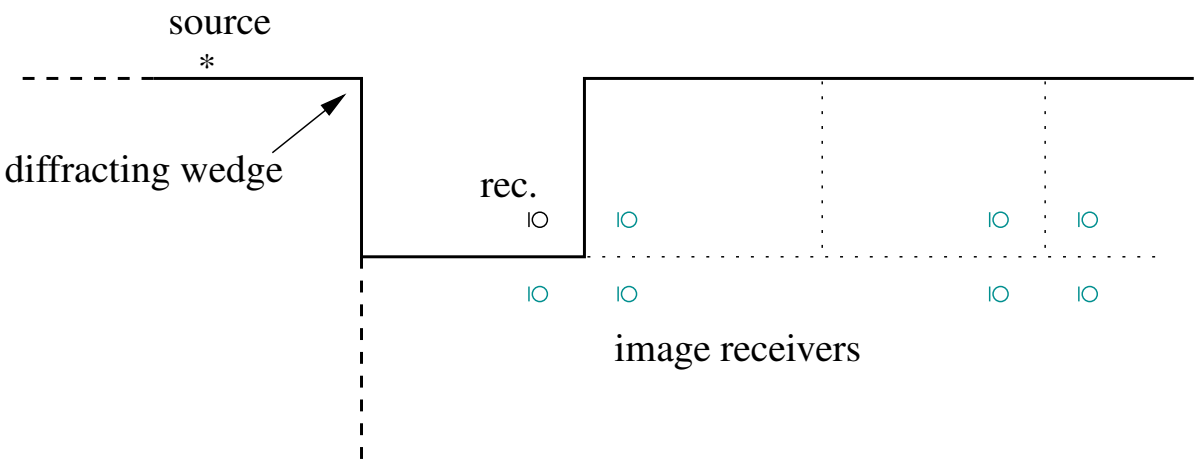

Figure 3.12: The canyon seen as a diffracting wedge.

thing that needs to be done is to calculate the pressure at the image receivers with the diffraction theory and sum it up, but then an important effect is ignored. The

reflection in the side walls of the canyon are not against an infinite plane. When drawing a Fresnel-zone around the source and an image receiver as in Fig. 3.13, it is clear that only part of the side wall is inside the Fresnel-zone if the image receiver is far from the canyon, so the reflection is typically weaker than for an infinite surface. The same applies every time the sound wave is reflected against the side wall, so for high order image receivers little is left of the contribution.

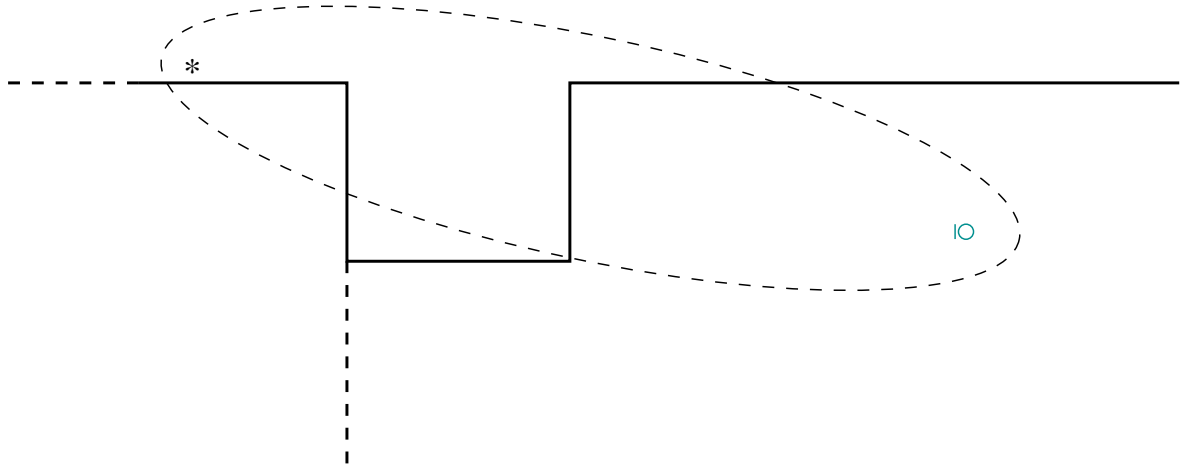

Figure 3.13: Illustration of a Fresnel-zone between the source and an image receiver.

An approximate way of calculating the strength of a reflection from a finite surface is to use what is known as the Fresnel zone method, where the size of the Fresnel zone projected on the surface compared to the size of the reflecting surface covered by the Fresnel zone gives an amplitude correction factor, as described for instance in [43]. The method includes an adjustable parameter, the wavelength fraction, that determines the size of the Fresnel zone as a function of the wavelength. A value of $1/8$ on this fraction is recommended in [43] for vertical surfaces. In Paper III this approach is used to calculate the pressure in a canyon which is 18 m high and 19 m wide, and the results are given in Fig. 3.14. The Fresnel zone solution is relatively similar to the ESM, but it is smoother close to the resonance frequencies. In Fig. 3.14 the effect of turbulence is included for both models, for details see Paper III.

An alternative way to model the reflection is to include high order diffraction. Instead of making a correction with the Fresnel zone, the diffraction from each edge that limits the reflecting surfaces be taken into account. This means that diffraction up to the same order as the number of reflection must be included, and since every diffracted ray can be reflected one or more times, the number of rays to be included will quickly grow very large. It also puts high demands on the diffraction model to

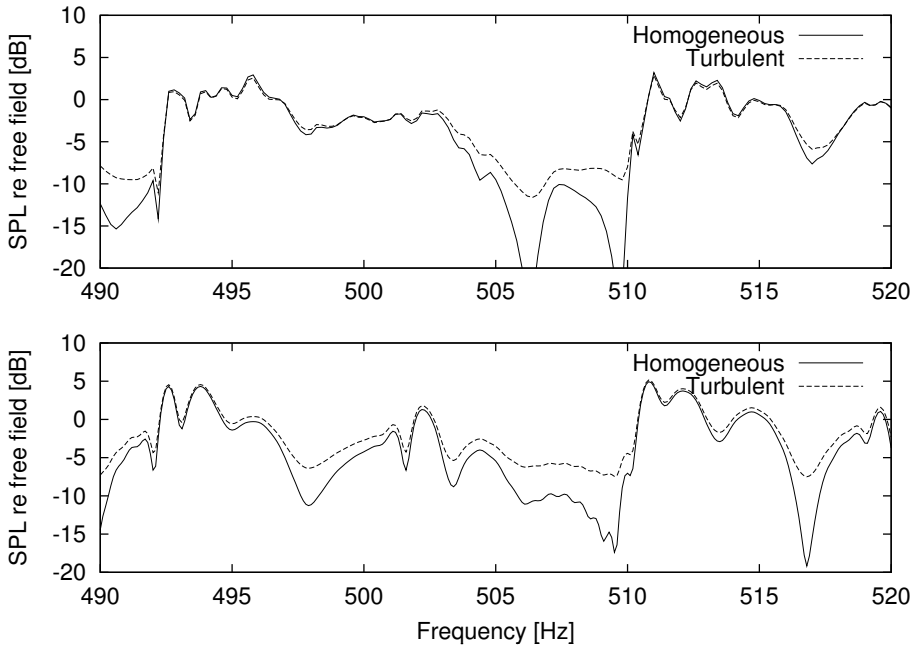

Figure 3.14: Frequency response relative free field for a canyon of width 19 m and height 18 m. The receiver is outside the canyon at (500,18). The upper figure is calculated using the equivalent sources method, and the lower using the ray-based model.

give correct results for rays that are diffracted many times.

3.8 Coupling two canyons

To get a more complete model of the sound propagation in city environments it is not sufficient to study street canyons or backyards alone, the two must be combined to form a system where the source is located in one canyon and the receiver in another canyon. The sound propagates from the source canyon out into the half-space above and then into the receiving canyon.

The total problem with the source in one canyon and the receiver in another can be solved in a way similar to including a secondary canyon in the first as explained in 3.5. However, if the source canyon and the receiver canyon are separated by a distance which is larger than the width of the canyons, a more effective method is to make a two step solution. Start by solving the source canyon, ignoring the effect of the receiving canyon, see Fig. 3.15. Then the equivalent sources of the source canyon are used as primary sources on the rigid plane of the second problem, solving the equivalent sources that determines the radiation into the receiving canyon.

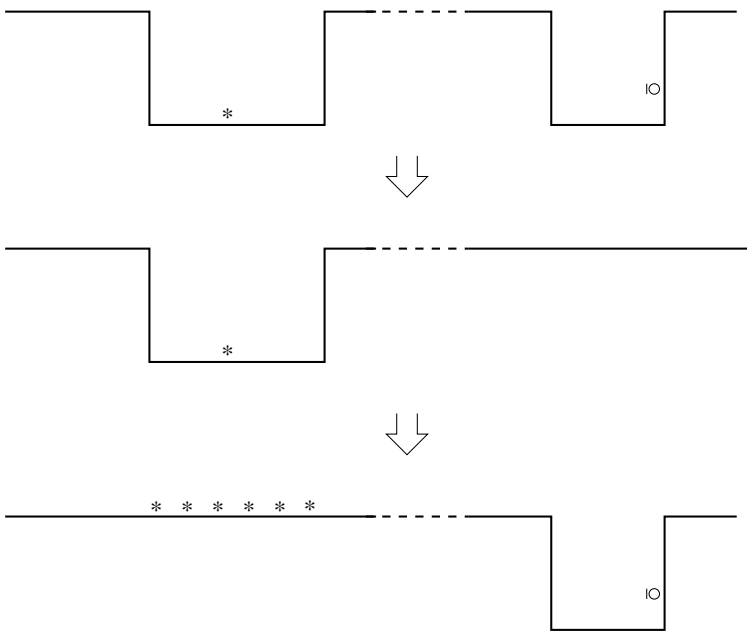

Figure 3.15: Solving a problem with the source in one canyon and the receiver in another by two steps.

This approach is the same as to see the equivalent sources of the source canyon as unaffected by the presence of the receiving canyon. The energy that is reflected back to the source canyon by the receiving canyon is neglected. For the sound pressure in the receiving canyon the effect of ignoring this interaction is very small as long as the separation is large enough compared to the widths of the canyons.

3.9 Validation

In Paper II the ESM is validated against the BEM for a 20 m wide and 18 m high canyon with hard walls. Unfortunately the BEM code was very slow and consumed large amounts of computer memory, so comparisons were only possible up to 400 Hz. The results showed a perfect match at and around the resonance peaks, but deviations were found at or close to anti resonances, see Fig. 3.16. Here infinitely many modes are needed to describe the sound field, so the truncation leads to errors. It is important to note that the BEM solution also is an approximation, and it is unclear if the accuracy is affected at anti resonances.

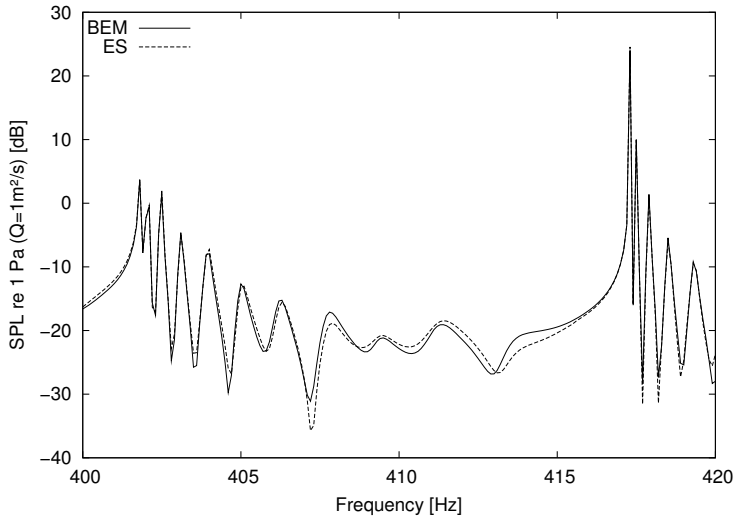

Figure 3.16: Comparison between BEM and ESM for a 20 m wide and 18 m high canyon with hard walls.

There are a number of well documented scale model measurement results published [19, 8], but unfortunately they are difficult to use for validating the ESM since they mainly focus on propagation along the length of the street canyon. Since the implementation of the ESM used here assumes a coherent line source, the pressure will be constant along the length of the canyon.

When there is absorbing material in the canyon the scale model results from [19] can be used to validate the insertion loss compared to a hard canyon. The impedance of the felt used in the scale model is described in [48], and can be modeled using the impedance model by Voronina [49, 50] or Attenborough [51]. For the felt used as an absorber in the measurement M3 in [19] the Voronina model gives slightly better fit to measured results, therefore it has been used for the ES calculations. Note that the scale factor must be taken into account, which is 20 in this case.

The geometry expressed as full scale equivalents is 17 m high and 17 m wide, with absorption added on the lowest 3 m of the side walls. Multiple point sources were used to simulate the traffic, and the spectrum of the sources were adjusted to fit that of light traffic according to [52]. The measured insertion loss is 4 dB for a light traffic spectrum, and the ESM using the same data gave 4.2 dB.

Validation against full scale data is difficult since the source is difficult to control. Measurements using ordinary traffic as a source are possible, but are best performed on the exposed façade. Nevertheless a comparison to a measurement on the quiet side is made in Paper II, which gives a relatively good match. However, the absorption of the canyon is chosen arbitrarily, and many source canyons are included, making it difficult to judge the validity in this case.

CHAPTER 4

The Flat City Method

4.1 Fast and approximate or slow and exact?

Solving the wave equation, or indeed an even more fundamental and complete equations, for sound propagation in cities is possible in increasingly complex environments. Micro-climate can be included, and, by using smart techniques, larger and larger geometries can be tackled. The computational power available in desktop systems is rapidly increasing. But even so it is unlikely that a complete city environment can be modeled in the near future. Apart from the size of the problem, the information required as input data is massive. Exact geometries of houses and streets, data on façade absorption, window locations, typical wind speeds and directions etc. Even if absurd details such as the positions and properties of thrash-cans or bus stop shelters are left out, there is simply too much data.

This does not mean that we should not attempt to understand the complex physical processes that determine sound propagation in urban environments. It is this understanding that can be used to produce the calculation methods of tomorrow. One way of using complex methods is to make calculations of interesting cases and store the results in a database. These results can later be accessed and processed by a simpler and faster program to predict the level by applying scaling rules, assuming typical values for unknown input data and so on.

Another way of using advanced methods is by inventing a simpler empirical approach based on comparisons with the more advanced method. Comparisons against scale model results or full scale measurements are also useful, but are more difficult to control. To change the turbulence strength or wind direction is easy in a theoretical model, but on a real measurement site it might be impossible. Therefore well

validated theoretical methods are in a way more useful than measurements, at least in the first stage of creating an empirical approach.

4.2 Measurements on the quiet side

Within the MISTRA programme a large number of measurements have been carried out in urban areas. Some were located on exposed positions, but the measurements presented here were all from the quiet side. The quiet sides were both closed courtyards and positions screened from major roads by buildings but not totally surrounded. A number of long-term (one week) and short-term (30 minutes) measurements were made in each of the areas studied.

The results presented here are the A-weighted equivalent sound pressure levels without corrections for positions, since the usual free field correction factor is ambiguous at closed courtyards, see section A.1. For the long-term measurements the equivalent level is an estimate of the 24 hour equivalent level ($L_{AEq,24h}$).

All positions were selected so they would not be disturbed by fans or other noisy equipment, which was the case for many inner city courtyards investigated. Extreme events have been removed from all measurements, the short-term measurements were supervised and the long-term measurements have been edited afterwards. The measurements were carried out by many different parties, which has lead to some degree of confusion in the measurement reports, and measurements lacking important information have been omitted here.

Area	position	L_{AEq} [dB]
Stockholm	1-3 m from façade	48
Stockholm	1-3 m from façade	50
Stockholm	1-3 m from façade	50
Stockholm	1-3 m from façade	51
Stockholm	on façade	51
Örebro	on façade	52
Örebro	1-3 m from façade	54
Göteborg, Johanneberg	on façade	53
Göteborg, Björkekärr	on façade	52
Göteborg, Björkekärr	on façade	51

Table 4.1: Some of the long-term measurement results from the MISTRA programme at shielded courtyards in Swedish cities.

4.3 The flat city method

The level is surprisingly constant at shielded positions as can be seen from the measurements in Tab. 4.1. In order to explain this effect a very simple prediction method was tested, were the city was seen as perfectly flat and rigid with the sources and receivers placed directly on the rigid ground as explained in Paper V. This geometry makes the calculations very simple indeed, and testing it shows that the level in the centre of the rectangles formed by the streets, the level is relatively constant.

But the levels are of course to high, since the effects of all buildings and absorption is omitted. By comparing to measurements it was noticed that the levels predicted were often 6–10 dB too high. The proposal for a very simple prediction method is then to calculate the pressure at shielded positions using the flat city method and then lower the results by a correction term obtained from measurements.

It would be nice if the correction term could be determined theoretically instead, and one possible approach can be to use the directivity calculations in Paper II. The directivity in Fig. 4.1 for a source at the bottom of the canyon to a receiver on the rigid plane is between -4 dB and -7 dB. At least for the inner city the source is located in one canyon, the street canyon, and the receiver in another, the courtyard. So when the source is modeled as on a hard surface instead of in a canyon, it will be 4–7 dB stronger, and because of reciprocity the receiver will be shielded by the same amount, giving a theoretical correction factor of 8–14 dB.

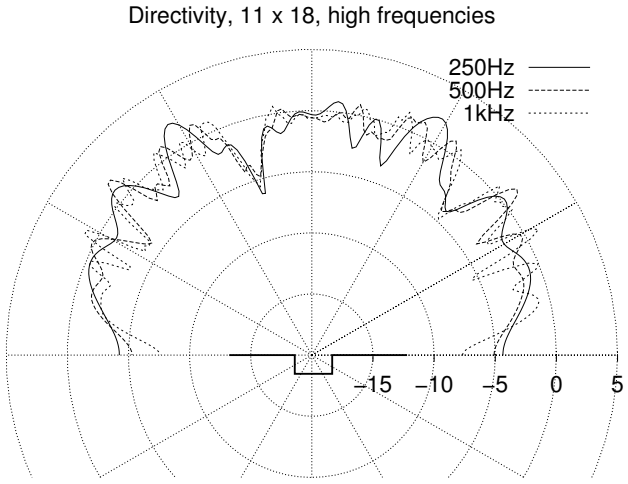

Figure 4.1: Directivity for a point source in a 11 m wide and 18 m high canyon from Paper II.

However, the directivity is dependent on the geometry of the canyon and the position of the source/receiver. The absorption in the canyon is also very important, and the calculations in Paper II assumes a very simplified model for absorption. The more advanced methods for including absorption presented in Paper IV and turbulence in Paper III would give better results provided that the input data needed (typical façade absorption and turbulence strength) can be provided for the city part in question.

CHAPTER 5

Results and Conclusions

5.1 Results

An important result of the theoretical calculations using the equivalent sources method (ESM) is that the sound field is more or less the same throughout the canyon on the quiet side. Although most measurements in the research programme were made with only one microphone in the courtyard, some were made with two microphones, one located at the center of the courtyard and the other on the inner façade. The results show that the A-weighted equivalent level is 2-3 dB higher on the façade than at the center of the courtyard. This indicates that the sound field behaves like a diffuse sound field, and is even throughout the canyon. Even though the results in [53, 54] are for the exposed side, they show almost no variation of the sound level with height for similar situations. This indicates that the sound level is constant also when a source is present in the canyon, except when the source is close to the receiver.

Another result of interest is that introducing diffusion into a canyon reduces the sound level. This suggests that rectangular courtyards with smooth and hard façade materials should be avoided. Introducing absorption also reduces the level, but the potential for reduction is determined by the amount of absorption already present in the courtyard. The sound level in a courtyard with only hard surfaces could be reduced by more than 10 dB at 1 kHz according to the ESM calculations in Paper IV. For a courtyard with a grass ground surface and perhaps other absorbing materials, the effect of introducing absorbers would be less dramatic.

In Paper III the effect of scattering from turbulence into the canyon is investigated for a few examples. For the highest frequencies investigated (1.6 kHz) the

increase in level is in the order of 2–5 dB, but for lower frequencies it is less, and below 500 Hz there is almost no effect at all. Although the method used is expected to underestimate the effect somewhat, the effects are still small. The effect on the A-weighted equivalent level assuming a traffic noise spectrum is at most 1 dB in the calculated examples.

5.2 Conclusions

The sound pressure level at well shielded positions such as courtyards in cities is difficult to predict with existing methods. A theoretical approach must take the damping in the courtyard and the diffusive properties of the façades into account. Since the closest source is shielded it will not dominate the level as on most exposed positions, therefore many sources within a large distance from the receiver must be included.

For engineering purposes extensive simplifications are possible. In fact, most measurements available for shielded positions in cities fall within a relatively narrow region. A very simplified model has been developed. It is the flat city model, where all sources and receivers are placed on a rigid plane, and a correction term for the effect of buildings and absorption is determined from measurements. The correction term for the A-weighted equivalent level is in the region of 6–10 dB.

The equivalent sources method presented here is one possible theoretical model that can include absorption, diffusive effects and scattering from turbulence. It can also be extended to include refraction due to temperature and wind gradients. Computationally it is slightly more efficient than competitors such as the boundary element method and finite difference time domain method, but it is still too slow for use in engineering tools.

Noise abatement for the quiet side requires other approaches than for the exposed façade. Traditional measures such as screening the closest source will have little effect on the quiet side, since many sources are contributing to the total level. A more global approach is needed for measures close to the source, such as redistributing the traffic into a larger grid of main roads or reducing the emission levels. In addition, local gains are possible in courtyards by introducing absorption or diffusion.

In future work the equivalent sources method can quite easily be improved to include effects from refraction by including it when calculating the Green functions for the half-space above the canyons. For instance this could be achieved by using the fast field program method. These improvements can in turn be verified against more advanced and generally applicable methods that can take a more complex atmosphere into account, possibly determined from fluid dynamic models.

APPENDIX A

A.1 Free field correction on courtyards

The sound level near a façade increases when the receiver moves closer to it. For a perfectly hard surface the sound pressure is doubled when the receiver is positioned on the façade itself, compared to if the surface was not present. This gives an increase of approximately 6 dB in the sound pressure level, see Fig. A.1.

In many countries the limit value is formulated as a maximum free field value that is not to be exceeded on the exposed façade. In other words, the values measured or calculated at the façade is lowered by 6 dB before being compared to the limit value. This is partly because the real sound level is not monotonically decreasing the distance from the source, and partly because the free field level is often used as an input when calculating the indoor level via the façade insulation.

In Fig. A.2 a simulated sound pressure level is calculated both with and without the effect of the reflecting façade. A few meters from the façade the free field level is 3 dB lower than the level including the reflection, which corresponds to an uncorrelated reflection. Relatively close to the façade the final increase from +3 dB to +6 dB takes place, corresponding to a in-phase reflection. This distance is dependent on the dominating frequency: the lower the frequency the bigger the +6 dB zone. For a source spectrum described by C_{tr} from [55], corresponding to road traffic at 50 km/h, the +6 dB zone is approximately 3 cm assuming a perfectly hard and infinite reflecting surface. The same has been shown in laboratory measurements [56], where a distance of one tenth of the wavelength gives just a small deviation from +6 dB. At 1 kHz this corresponds to 3.4 cm.

It is important to understand that the above reasoning is only valid for a directly exposed surface. For a courtyard, removing the reflecting surface will not only remove the primary reflex, but also any multiple reflections, see Fig. A.3. The question

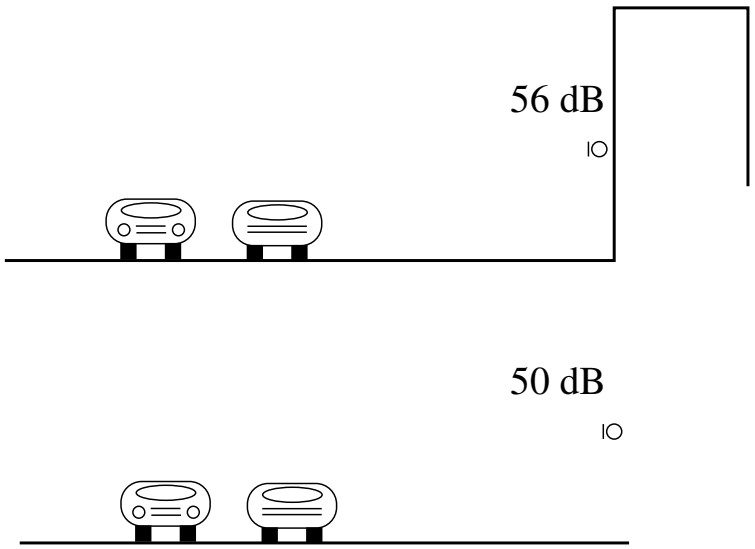

Figure A.1: Free field correction for an exposed façade.

is if there is a free field level at all inside courtyards. It might be defined as the sound pressure at the façade minus 6 dB, but then there is no direct link such as removing the effect of the reflecting surface anymore. For an exposed façade the free field level can be used for calculating the indoor level, since the sound reduction index is defined as the ratio of incident and transmitted acoustic power. But a shielded courtyard will act more like a diffuse sound field, and the reduction index for a partition between two diffuse sound fields is determined by the average sound pressure level in the two fields.

If the sound field in the courtyard is assumed to be diffuse, the increase close to the inner façade is 3 dB compared to the level in the center of the canyon [57], see Fig A.4. Again the distance where the level is increased is dependent on the frequency of interest. In a real courtyard the sound field is not diffuse, nor free. It is somewhere in between, determined by the geometry and the damping present in the courtyard.

In order to avoid the problem with the free field level at shielded positions, it might be convenient to use another correction for shielded positions than for directly exposed ones, or perhaps no correction at all. But this will give confusing data when comparing levels from different positions. Imagine the case of a house with one exposed façade, and one shielded side. The difference between the level at the exposed façade and the shielded façade could then include two different corrections. Therefore all levels given in this text are “uncorrected” unless otherwise noted. That means that if the free field level at a directly exposed position is desired, the value

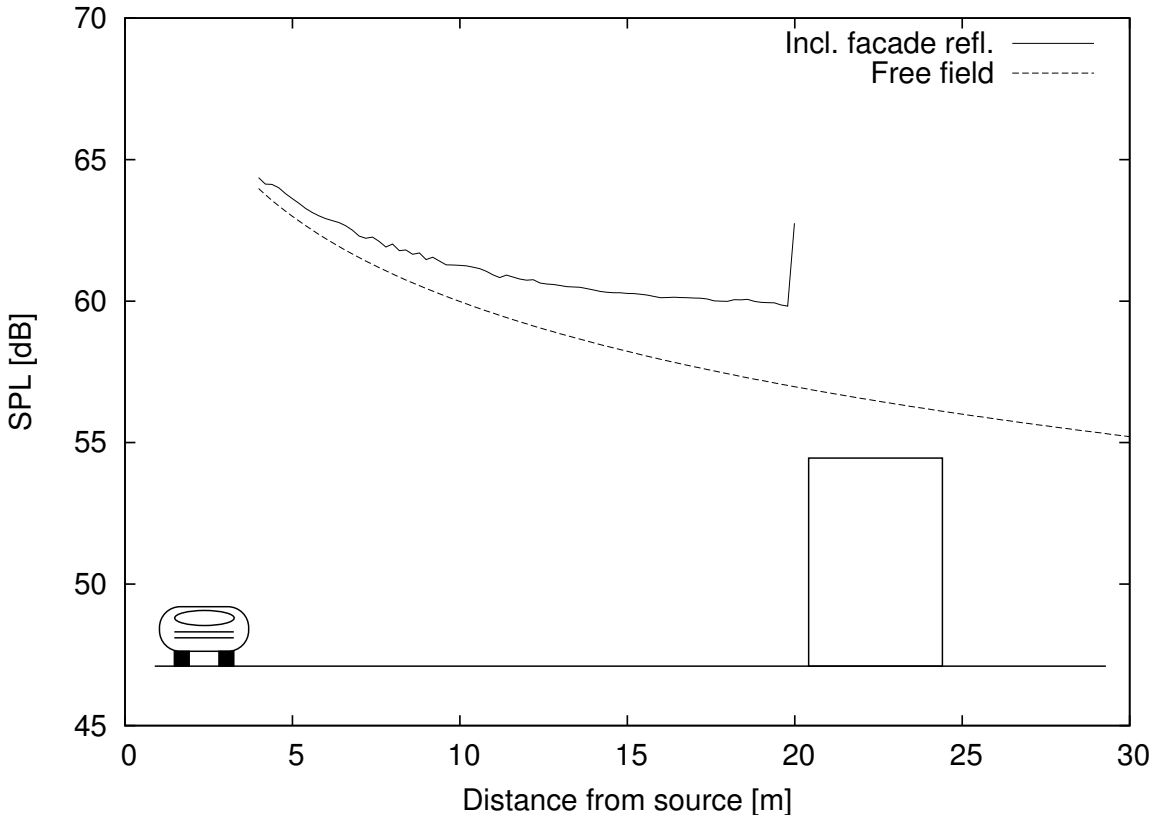

Figure A.2: Simulated SPL with and without the influence of a reflecting surface 20 m from the source.

given here should be reduced by 6 dB for a position on a façade, and by 3 dB for a directly exposed position a short distance away from the façade.

A.2 Buildings as Screens

The standardized methods for the prediction of road traffic noise levels include well tested and reliable models for calculating the effect of inserting screens between the source and the receiver, since this is a common noise abatement method. Therefore it is very convenient to see buildings as large screens when trying to predict the level at shielded positions. The first approximation would be to just model the shielding building by a simple screen as in Fig. A.5.

This approach would underestimate the level substantially, since the multiple reflections on the source and receiver side are ignored. But including reflections is easy if image sources are used, and in the Nordic method [6] (section 2.6.8 in part

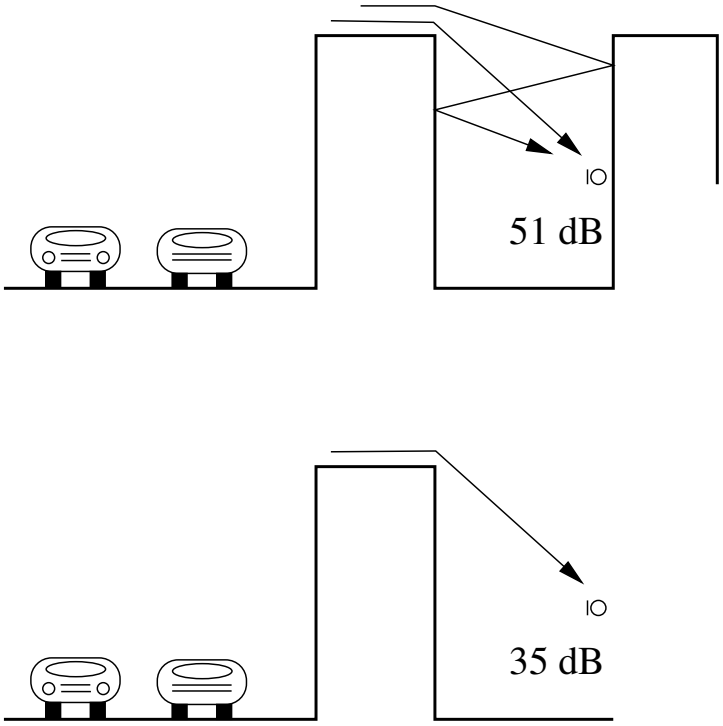

Figure A.3: Removing one reflecting surface for a courtyard.

2) it is stated that only one image source is necessary if the source and receiver are close to the ground. If the receiver is elevated a special correction is applied which can give 2 dB extra at the most. So then the situation could be solved by using just a few image sources and receivers.

However, it is important to understand that a few reflections are enough on the exposed side, but not on the shielded side. On the shielded side there is no direct field from the source, only a reverberant field excited via diffraction over the roof of the shielding building. A simplified example is given in Fig. A.6. The width of the canyon is 20 m, and the effect of diffraction at the canyon opening is assumed constant for all angles. Again the source spectra is described by C_{tr} in [55], and the side walls are assumed to have a reflection coefficient of 0.9. In Fig. A.7 the increase of the sound pressure level as a function of the number of image receivers is displayed. For the case with the source inside the canyon it is evident than only a few are needed, but this is not the case when the source is located 100 m to the left of the canyon.

This is due to the geometrical spreading (-3 dB per distance dubling for a line source) has a smaller effect for each order of image receivers when the source is located far from the canyon. When the source is inside the canyon the image receiver

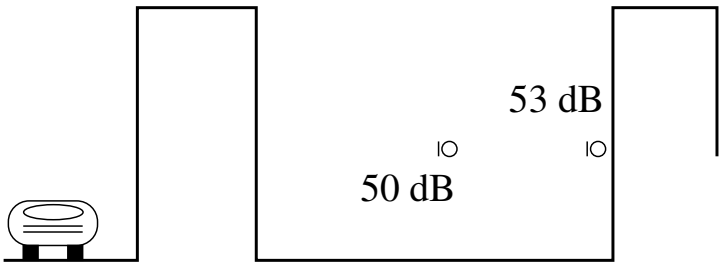

Figure A.4: Sound pressure level increase close to façades on a courtyard with a diffuse sound field.

of the first order is far from the source compared to the original receiver. If the sources is very far from the canyon instead, the distance is approximately the same to the primary receiver and to the first image receiver.

The diffraction into the canyon in the second case is assumed to be the same in all directions. In a better model more obtuse diffraction angles, corresponding to rays reflected many times, will have an even stronger contribution. Note that this is an over-simplified calculation example, but it serves to demonstrate that a few reflections are not enough for predictions at shielded positions.

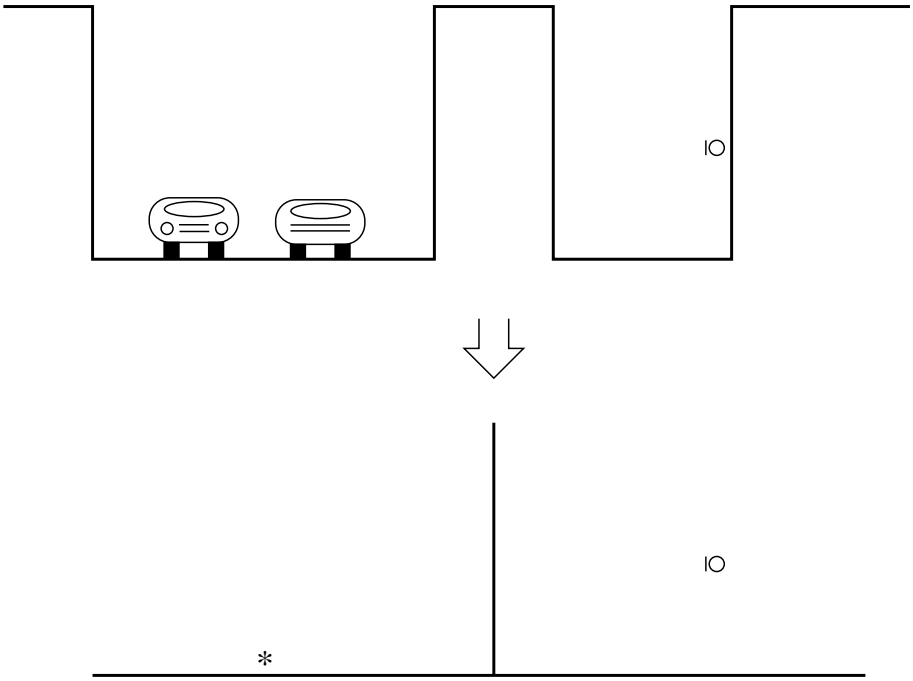

Figure A.5: Replacing a shielding house with a screen.

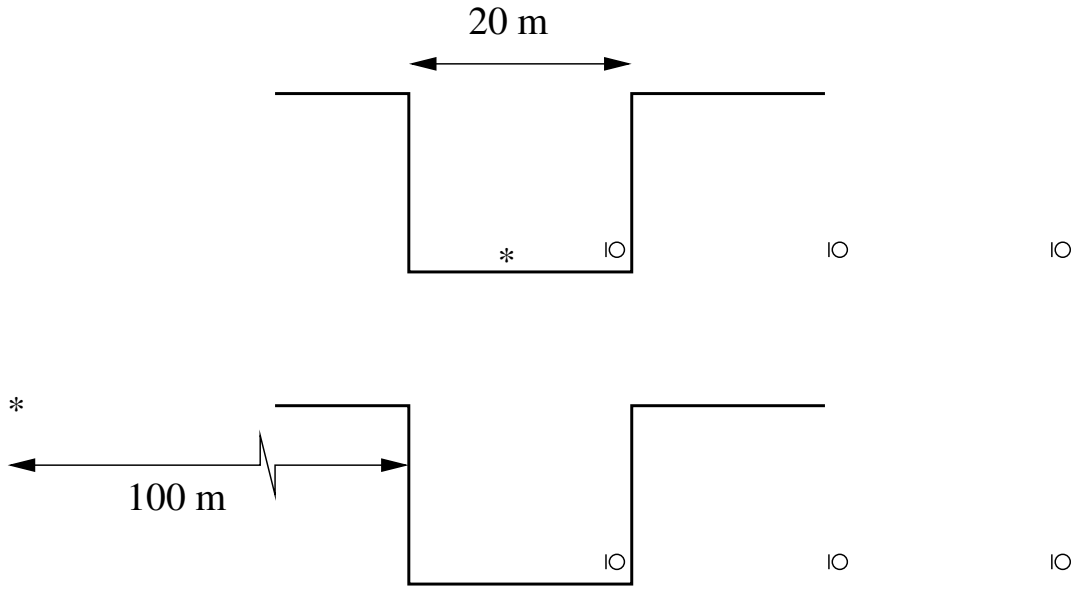

Figure A.6: Calculation geometry for a simplfied model for multiple reflections on an exposed façade and a shielded side.

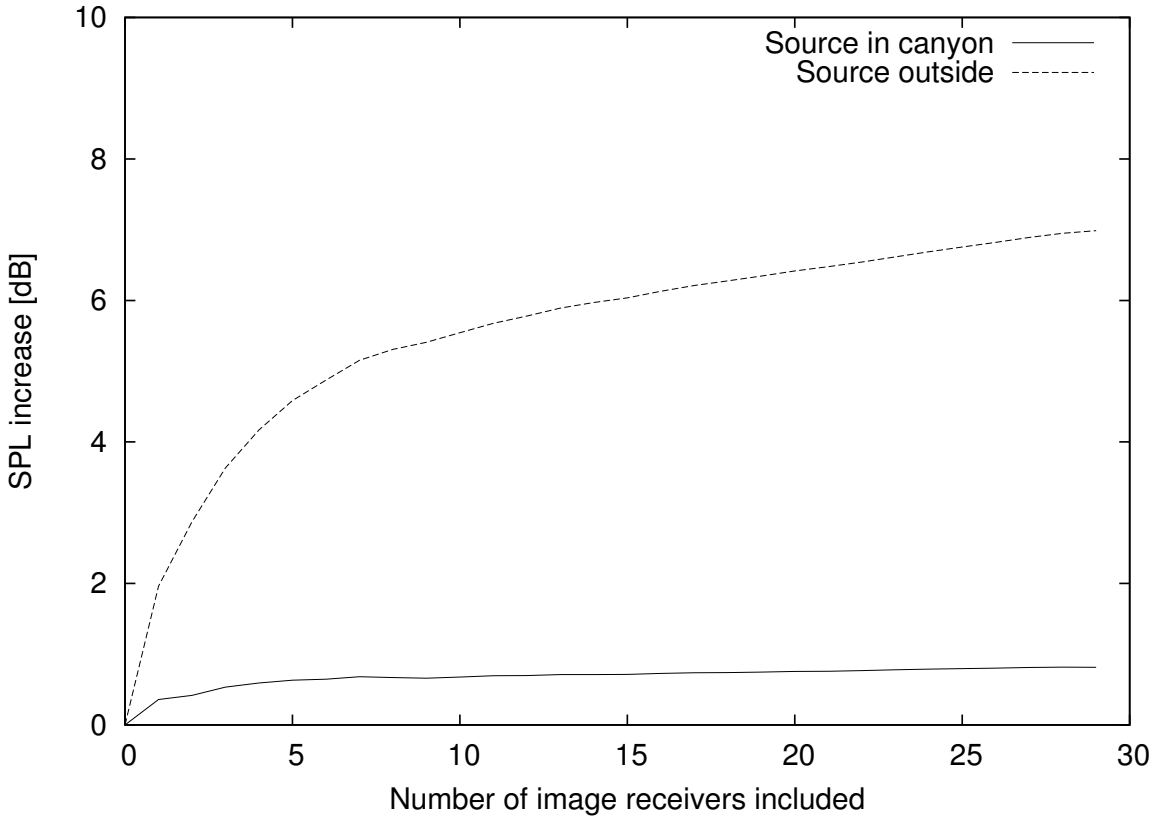

Figure A.7: The importance of including multiple reflections if the source is located inside or outside the canyon.

Bibliography

[1] Tor Kihlman. *National Action Plan against Noise*. Allmänna Förlaget, Stockholm, Sweden, 1993. Summary of "Handlingsplan mot buller" (in Swedish).

[2] Tor Kihlman and Wolfgang Kropp. City traffic noise – a local or global problem? *Noise Control Engineering Journal*, 49:165–169, 2001.

[3] Soundscape support to health, programme description. Published online at www.soundscape.nu, 2004.

[4] Tor Kihlman, Evy Öhrström, and Annbritt Skånberg. Adverse health effects of noise and the value of access to quietness in residential areas. In *Proceedings of Internoise*, Dearborn, USA, 2002. Paper 484.

[5] Annbritt Skånberg and Evy Öhrström. Adverse health effects in relation to urban residential soundscapes. *Journal of Sound and Vibration*, 250(1):151–155, 2002.

[6] H. Jonasson and H. Nielsen. Road traffic noise – nordic prediction method. TemaNord 1996:525, Nordic Council of Ministers, Copenhagen, Denmark, 1996. ISBN 92-9120-836-1.

[7] Pontus Thorsson. Application of linear transport to sound propagation in cities. *Acustica – Acta acustica*, 2004. Submitted for publication.

[8] R. Bullen and F. Fricke. Sound propagation in a street. *Journal of Sound and Vibration*, 46(1):33–42, 1976.

[9] Huw G. Davies. Multiple-reflection diffuse-scattering model for noise propagation in streets. *J. Acoust. Soc. Am.*, 64(2), 1978.

[10] J. Kang. Sound propagation in street canyons: Comparison between diffusely and geometrically reflecting boundaries. *J. Acoust. Soc. Am.*, 107(3):1394–1404, 2000.

[11] Bengt-Inge Dalenbäck, Mendel Kleiner, and Peter Svensson. A macroscopic view of diffuse reflection. *J. Audio Engineering Soc.*, 42:873–907, 1994.

[12] Erik Salomons, Alex C. Geerlings, and Denis Duhamel. Comparison of a rays model and a fourier-boundary element method for traffic noise situations with multiple diffractions and reflections. *Acustica – Acta acustica*, 83(1):35–47, 1997.

[13] D. Ouis. Noise shielding by simple barriers: comparison between the performance of spherical and line sound sources. *Journal of Computational Acoustics*, 8(3):495–502, 2000.

[14] K. Horoshenkov, S. Chandler-Wilde, and D. Hothersall. An efficient method for the prediction of sound propagation in a canyon. In *Proceedings of the International Congress on Acoustics*, Rome, 2001.

[15] H. Kuttruff. Zur berechnung von pegelmittelwerten und schwankungsgrößen bei straßenlärm. *Acustica*, 32, 1975.

[16] P. Steenackers, H. Myncke, and A. Cops. Reverberation in town streets. *Acustica*, 40:115–119, 1978.

[17] K. W. Yeow. Room acoustical model of external reverberation. *Journal of Sound and Vibration*, 67(2):219–229, 1975.

[18] Reinhard Neubauer. Prediction of reverberation time in rectangular rooms with non uniformly distributed absorption using a new formula. In *Proceedings of Congreso Nacional de Acústica – TechniAcústica*, Madrid, Spain, 2000.

[19] K. V. Horoshenkov, D. C. Hothersall, and S. E. Mercy. Scale modelling of sound propagation in a city street canyon. *Journal of Sound and Vibration*, 223(5):795–819, 1999.

[20] J. Kang. Numerical modelling of the sound fields in urban streets with diffusely reflecting boundaries. *Journal of Sound and Vibration*, 258(5):793–813, 2002.

[21] D. Fitzroy. Reverberation formula which seems to be more accurate with nonuniform distribution of absorption. *J. Acoust. Soc. Am.*, 31:893–897, 1959.

[22] Bengt-Inge Dalenbäck. The importance of diffuse reflection in computerized room acoustic prediction and auralization. In *Proceedings of the Conference of the Institite of Acoustics*, pages 24–34, Great Britain, 1995. ISBN 1-873082-770.

[23] Shuoxian Wu. On the relevance of sound scattering to the prediction of traffic noise in urban streets. *Acustica*, 81:36–42, 1995.

[24] K. Heutschi. A simple method to evaluate the increase of traffic noise emission level due to buildings for a long straight street. *Applied Acoustics*, 44:259–274, 1995.

[25] Conny Larsson and Sven Israelsson. Influence of the meteorological parameters on the sound propagation from a traffic road. In *Proceedings - International Conference on Noise Control Engineering*, volume 2, pages 513–516, Warsaw, Poland, 1979.

[26] Bengt Hallberg, Conny Larsson, and Sven Israelsson. Outdoor sound level variations due to fluctuating meteorological parameters. *Applied Acoustics*, 26(3):235–240, 1989.

[27] F. W. Embleton. Tutorial on sound propagation outdoors. *J. Acoust. Soc. Am.*, 100, 1996.

[28] Jong-Jin Baik and Jae-Jin Kim. On the escape of pollutants from urban street canyons. *Atmospheric Environment*, 36:527–536, 2002.

[29] M. W. Rotach. Profiles of turbulence statistics in and above an urban street canyon. *Atmospheric Environment*, 29(13):1473–1486, 1995.

[30] R. G. Harrison P. Louka, S. E. Belcher. Coupling between the air flow in streets and the well-developed boundary layer aloft. *Atmospheric Environment*, 34:2613–2621, 2000.

[31] T. R. Oke. *Boundary Layer Climates*. Routledge, 2 edition, 1992. ISBN 0-415-04319-0.

[32] Erik Salomons. *Computational atmospheric acoustics*. Kluwer Academic Publishers, Dordrecht, The Netherlands, 2001. ISBN 0-7923-7161-5.

[33] Timothy Van Renterghem. *The finite-difference time-domain method for simulation of sound propagation in a moving medium*. PhD thesis, Universiteit Gent, Belgium, 2003.

[34] Erik Salomons, Reinhard Blumrich, and Dietrich Heimann. Eulerian time-domain model for sound propagation over a finite-impedance ground surface. comparison with frequency-domain models. *Acustica – Acta acustica*, 88:483–492, 2002.

[35] Erik Salomons. Reduction of the performance of a noise screen due to screen induced wind speed gradients. numerical computations and wind-tunnel experiments. *J. Acoust. Soc. Am.*, 105:2287–2293, 1999.

[36] Martin Ochmann. The source simulation technique for acoustic radiation problems. *Acustica – Acta acustica*, 81(6):512–527, 1995.

[37] François-Xavier Bécot. *Tyre noise over impedance surfaces – Efficient application of the Equivalent Sources method*. PhD thesis, Chalmers, Gothenburg, Sweden, 2003. Report F03-03, ISBN 91-7291-313-4.

[38] A. Cummings. The effects of a resonator array on the sound field in a cavity. *Journal of Sound and Vibration*, 154(1):25–44, 1992.

[39] J. Bérillon and W. Kropp. A theoretical model to consider the influence of absorbing surfaces inside the cavity of balconies. *Acustica – Acta acustica*, 86:485–494, 2000.

[40] François-Xavier Bécot, Pontus Thorsson, and Wolfgang Kropp. An efficient application of equivalent sources to noise propagation over inhomogeneous ground. *Acustica – Acta acustica*, 88:853–860, 2002.

[41] M. Abramowitz and I. A. Stegun. *Handbook of mathematical functions*. Dover Publications, New York, 1972.

[42] Wolfgang Kropp and Mikael Ögren. Hilfsquellen zur kopplung von schallfeldern. In *DAGA '03*, Aachen, March 2003.

[43] B. Plovsing and J. Kragh. Comprehensive outdoor sound propagation model. part 1: Propagation in an atmosphere without significant refraction. Technical Report Delta report AV 1849/00, Delta, Lyngy, Denmark, 2000.

[44] Erik Salomons. Sound propagation in complex outdoor situations with a non-refracting atmosphere: Model based on analytical solutions for diffraction and reflection. *Acustica – Acta acustica*, 83:436–454, 1997.

[45] R. G. Kouyoumjan and P. H. Pathak. A uniform geometrical theory of diffraction for an edge in a perfectly conducting surface. *Proceedings of IEEE*, 62:1448–1461, 1974.

[46] A. D. Pierce. Diffraction of sound around corners and over wide barriers. *J. Acoust. Soc. Am.*, 55:941–955, 1974.

[47] W. J. Hadden and A. D. Pierce. Sound diffraction around screens and wedges for arbitrary point source locations. *J. Acoust. Soc. Am.*, 69(5):1266–1276, 1981.

[48] K. V. Horoshenkov, D. C. Hothersall, and K. Attenborough. Porus materials for scale model experiments in outdoor sound propagation. *Journal of Sound and Vibration*, 194(5):685–708, 1996.

[49] N. Voronina. Acoustic properties of fibrous materials. *Soviet Physics – Acoustics*, 31:402–404, 1985.

[50] N. Voronina. Acoustic properties of fibrous materials. *Applied Acoustics*, 42:165–174, 1994.

[51] K. Attenborough. Acoustical impedance models for outdoor ground surfaces. *Journal of Sound and Vibration*, 99(4):521–544, 1985.

[52] R. Jones. *An investigation of road traffic noise characteristics in restricted flow situations*. PhD thesis, University of Bradford, 1979.

[53] C. H. Chew and K. B. Lim. Facade effects on the traffic noise from the expressway. *Applied Acoustics*, 41:47–62, 1994.

[54] T. J. Schultz. Variation of the outdoor noise level and the sound attenuation of windows with elevation above the ground. *Applied Acoustics*, 12:231–239, 1979.

[55] Acoustics – rating of sound insulation in buildings and of building elements – part 1: Airborne sound insulation. ISO 717-1:1996, The International Organization for Standardization, 1996.

[56] J. D. Quirt. Sound fields near building facades. In *Proceedings of Inter-noise*, Edinburgh, 1983. ISBN 0-946731-02-0.

[57] Richard V. Waterhouse. Interference patterns in reverberant sound fields. *J. Acoust. Soc. Am.*, 27(2):247–258, 1955.

Paper I

Barrier noise-reduction in the presence of atmospheric turbulence: Measurements and numerical modelling

Jens Forssén and Mikael Ögren

Abstract

Atmospheric turbulence causes scattering of sound, which can reduce the performance of sound barriers. This is important to include in prediction models to get a correct picture of the sound reduction at higher frequencies. Here a prediction method is applied that uses the strengths of the wind and temperature turbulence to estimate the scattered power into the shadow zone of a barrier. The predictions are compared to full-scale measurements on a thick barrier, where both acoustic and meteorological data were recorded simultaneously under both calm and windy conditions. Comparison between the measurements and the predictions indicate that the method gives reasonably accurate results for mid to high frequencies and a slight overestimation at very high frequencies.

1 Introduction

When trying to predict the sound reduction obtained with a noise barrier in an outdoor environment, the inhomogeneous nature of the atmosphere can be of importance to consider. Wind speed and temperature that vary with height cause refraction and the atmospheric turbulence causes scattering and decorrelation of the sound waves. The turbulence scattering can significantly decrease the sound reduction obtained with a noise barrier, especially for high frequencies and large scale geometries [1, 2]. An example of a situation with a large scale geometry is a large building along a road side.

There exist other models than the one used here for predicting the influence of atmospheric turbulence on noise barrier performance. A parabolic equation method has been applied to situations with flat geometries [3], i.e. when the source and the receiver are far away from the barrier in relation to the height of the barrier. Also a model called the substitute-sources model has been developed [4]. In this model a surface of sources represents the field behind the barrier and a mutual coherence between all source-pairs is used which describes the decorrelation due to the turbulence. Also this model has so far only been implemented for flat geometries.

The model used here for predicting the effects of a turbulent atmosphere on the sound reduction by a barrier on ground is based on a model by Daigle [5] and has been further extended. In Daigle's model the power scattered by the turbulence is calculated using a sound scattering cross-section [6, 7] and is then added to the diffracted power in the acoustic shadow of the barrier. With this model Daigle investigated a few different geometries and the predictions were compared with measured data [5]. The comparison showed a fairly good agreement between predictions and measurements, and that neglecting the turbulence scattering would yield a poor prediction, especially at higher frequencies, which is also concluded in Ref. [8].

Using the physically based Kolmogorov spectrum for the description of the turbulence allows for a straight forward transformation of the results from one frequency to other frequencies. Moreover, the results when enlarging or diminishing the geometry in scale can also be predicted using straight forward transformations. These transformation properties are adopted and the predictions for many situations can be made from a small set of pre-calculated data, as shown in Refs. [1, 2], and as described in the following. In the further extended model used here, also the interference effects due to a ground surface are taken into account, in an approximate way.

2 Measurement setup

Two sets of measurements were carried out with identical measurement setups. One set of measurements was carried out during calm weather conditions with rather low wind speeds (1–3 m/s) and weak turbulence. During the other set the wind speeds were higher (4–7 m/s) and the turbulence was stronger. Unfortunately the wind direction had changed between the two sets, so during the calm set there was predominately upwind propagation, and downwind for the windier set.

The barrier was constructed using two standard containers, one 12 m and one 6 m long, forming an 18 m long barrier, 2.55 m high and 2.44 m thick. The containers were placed on a wide asphalt road strip, and mineral wool absorbing material was

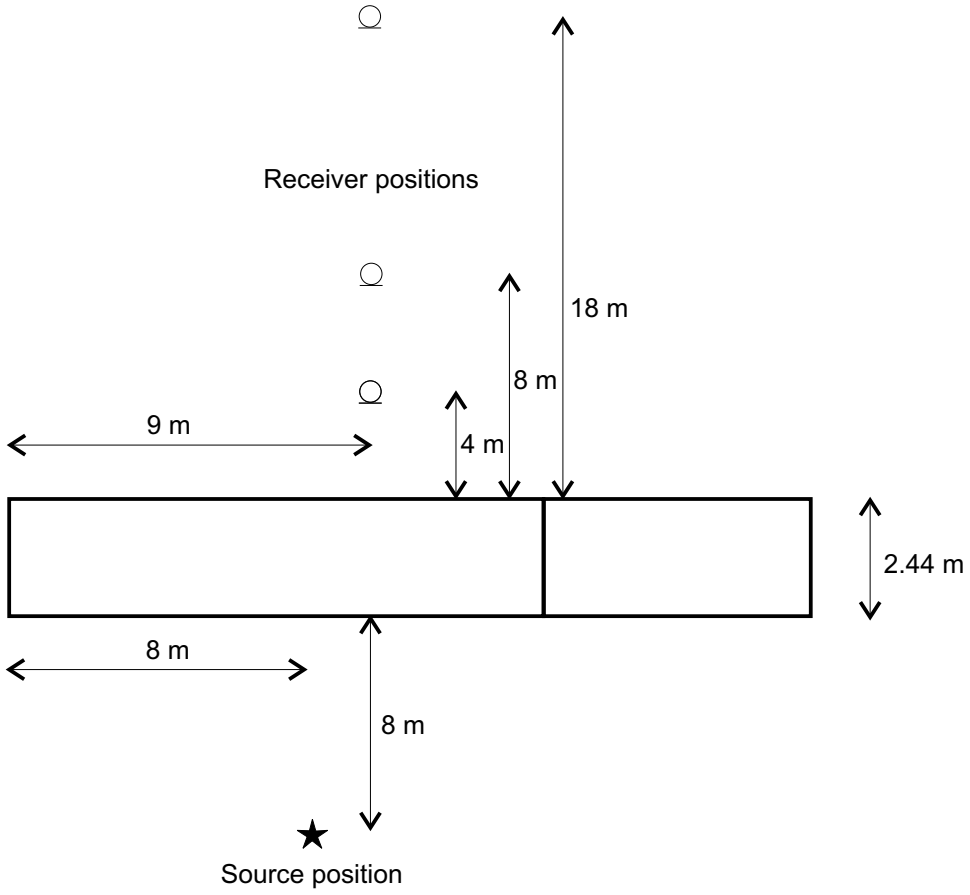

Figure 1: Measurement setup.

used to seal the gap between them. The source was positioned 8 m from the barrier during all measurements, and the receiving microphone was placed at a distance of 4, 8 or 18 m from the barrier. The geometry is described in detail in Figure 1. The microphone and the source were placed either on the ground or at a height of 1.25 m above ground.

A point source was simulated using a compression driver feeding into a flexible hose with a diameter of 25 mm at the opening. A CD-player supplied a filtered pink noise signal trough an amplifier to the driver. One 1/4" microphone was placed close to the source to monitor the emitted sound, and a second 1/2" microphone was used to measure the sound pressure at the receiving positions. The signals were recorded using a DAT recorder at a sampling frequency of 48 kHz, and were later transformed to power spectra using the Welch method with a Hanning window of length 2048

points and 50% overlap.

The wind speed was measured using a conventional instrument with rotating cups. The sensor was placed far away from the barrier to avoid disturbances, at a height of 5 m. The turbulence was measured using an ultrasound anemometer with a sampling frequency of 18 Hz. The anemometer was placed at a height of 3.7 m, 7 m from the barrier, and 5 m in from the edge.

The sound power level of the source was determined through measurements in an anechoic chamber at a specified input voltage. This voltage was later kept during the measurements in order to get the same output, and thereby be able to find the sound reduction obtained with the barrier. The source spectrum contained rather sharps peaks due to resonances in the flexible hose that were spaced about 200 Hz apart. In order to avoid this effect, all the measured spectra were averaged over 200 Hz.

3 Theory

The spatial and temporal fluctuations in temperature and wind velocity, i.e. the atmospheric turbulence, cause the sound waves to be scattered into acoustic shadow regions and to be decorrelated. Decorrelation effects are usually of interest for line-of-sight propagation.

The model for calculating the influence of the turbulence scattering for barrier situations is based on the model by Daigle [5]. A further developed model [8] uses a small set of precalculated data to predict the scattered power for different geometrical configurations and frequencies. This prediction scheme is here extended to be applicable to a more general barrier shape, and also interference effects due to a ground surface are taken into account.

The sound scattering cross-section used for the scattered power due to the turbulence is a single-scattering approximation where the field incident on a scattering object is assumed to be well approximated by the field calculated for a non-turbulent atmosphere. This means that the model is restricted to situations where the propagation distance is not too large and the fluctuations of the medium not too strong.

The atmospheric turbulence is approximated as homogeneous and isotropic, which means that it is described by the same statistics in all points independent of direction. It is also assumed that the source and receiver are in the far field. This means that they are far away from where the dominant scattering is produced in relation to the largest scale L_0 of the inhomogeneities of the medium and to the size L of the dominant-scattering volume. It is also assumed that $L \gg \lambda$, $L \gg L_0$, and $R \gg kLL_0$

are fulfilled, where λ is the acoustic wavelength, k the acoustic wave number, and R the distance from a scattering volume element to the source or to the receiver [6]. Using the correlation length l of the turbulent atmosphere (usually assumed to be around one meter), the last inequality can be relaxed to

$$R \gg l^2/\lambda, \tag{1}$$

as established in Ref. [7]. (See also Ref. [5].) The last inequality says that the radius of the first Fresnel zone $(R\lambda)^{1/2}$ is large compared to l, which is a condition for treating the scattering from different points as being uncorrelated.

Then the time average of the total received scattered power can be written as [5]

$$W_s = \int_V p_0^2 \frac{\sigma(\theta)}{\rho^2} dV, \tag{2}$$

where p_0 is the amplitude of the incident pressure, $\sigma(\theta)$ the scattering cross-section, θ the scattering angle, and ρ the distance from a volume element to the receiver. See Figure 2. The volume of integration V consists of all points in line of sight from both source and receiver (i.e. the striped area in Figure 2).

For the locally homogeneous and isotropic turbulence in the inertial range, following the Kolmogorov spectrum, the structure parameters can be defined from the structure functions

$$D_{v,T}(x) = C_{v,T}^2 x^{2/3}, \tag{3}$$

where C_v and C_T are the structure parameters of the wind turbulence and of the temperature turbulence, respectively.

For the fluctuating velocity v in the direction of x and temperature T, and two points, x_1 and x, the structure functions can be defined as

$$D_v(x) = < [v(x_1+x) - v(x_1)]^2 >, D_T(x) = < [T(x_1+x) - T(x_1)]^2 >, \tag{4}$$

where $< \cdot >$ denotes an ensemble average. The time average can be used instead of the ensemble average when the hypothesis of frozen turbulence is used. For a given scattering angle θ and acoustic wave number k, the wave number κ of the turbulence that causes the scattering is found from the Bragg condition

$$\kappa = 2k \sin \frac{\theta}{2}. \tag{5}$$

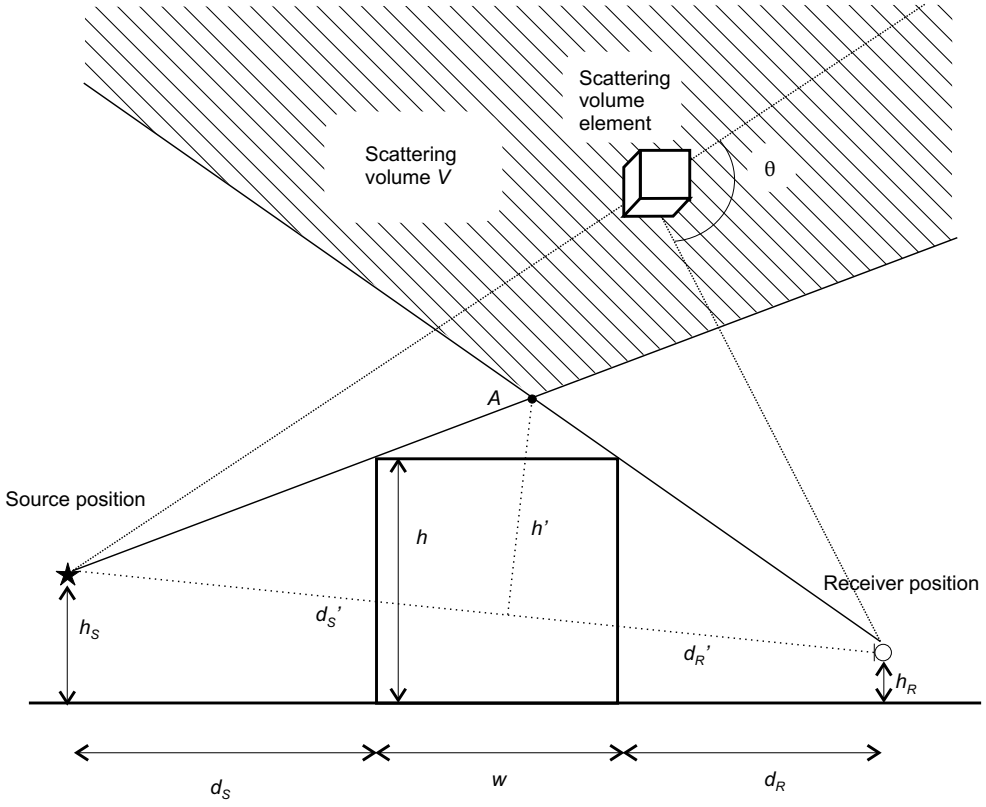

Figure 2: Geometry for the sound scattering cross-section.

For these conditions the scattering cross-section can be written as [6]

$$\sigma(\theta) = 0.03k^{1/3}\frac{\cos^2\theta}{[\sin(\theta/2)]^{11/3}}\left[0.14\frac{C_T^2}{T_0^2}+\frac{C_v^2}{c_0^2}\cos^2\frac{\theta}{2}\right], \tag{6}$$

where T_0 is the mean temperature in Kelvin and c_0 the mean sound speed. In Eq. (6) it can be seen that the scattering increases with frequency as $f^{1/3}$.

According to this model the scattered power will, relative to free field, change with the same factor as the geometry is scaled. To see this let the height of the screen, as well as its distance from source and receiver, be doubled. Substituting for these new variables in the integral (2) will cause an increase by a factor eight in dV and a factor four in ρ^2, whereas p_0^2 will stay constant relative to free field. As a result the scattered power will be doubled, i.e. increased by 3 dB, relative to free field.

The turbulence scales larger than in the source range have strengths that are influenced by the large-scale structures of the terrain, and are not easily determined. Since the scattering into barrier shadows has been concluded to influence the mean sound power only at higher frequencies, only the smaller wave numbers of the turbulence are considered (see the Bragg condition (5)). The turbulence spectrum in the source range and in a part of the inertial range is omitted, and L_0=1 m is assumed instead of a typical value in the order of 100 m. This limits the application of the prediction scheme to high enough frequencies and steep enough geometries. The limitation to steep geometries is in accordance with the other model assumptions because for flatter geometries more power will come via multiple scattering. The dissipation range of the turbulence includes scales smaller than about a few millimetres and therefore will not be of importance in the audio range.

Concerning the measurements of the turbulence, the structure parameters C_v and C_T were estimated from the longitudinal turbulence spectrum in the direction of the mean wind. A least square fit in the range 0.5–5 Hz of the turbulence fluctuations was made of

$$W_{v,T}(\omega) = \frac{6\pi}{5}AC_{v,T}U^{2/3}\omega^{-5/3}, \tag{7}$$

where $A \approx 0.0330$, U is the mean wind speed, ω is the angular frequency of the fluctuations, and W_v and W_T are the power spectra of the velocity and the temperature fluctuations, respectively. (See e.g. [6, 9] for more thorough descriptions of the theory and the measurements of the structure parameters.)

For a ground reflected wave the spherical reflection coefficient [10] is used with the ground impedance being modelled using the Delany/Bazley model [11] and a

flow resistivity of 20 000 kNm/s^4. The diffraction effect for a single edge is modelled by Hadden/Pierce [12] and the two edges on the barrier are then combined using the scheme from Ref. [13]. This procedure gives four ray paths with complex pressures normalized to a free field reference.

Decorrelation

When the receiver position is not in an acoustic shadow region, the situation is usually referred to as line-of-sight propagation. For line-of-sight propagation in a fluctuating medium the decorrelation causes interference patterns to be less pronounced. (See e.g. Ref. [14].)

For two sources oscillating with the frequency f and contributing with the complex-valued pressure amplitudes p_1 and p_2, the time signal of the total pressure in a homogeneous atmosphere can be written

$$p_{tot} = p_1 \mathrm{e}^{\mathrm{j}2\pi ft} + p_2 \mathrm{e}^{\mathrm{j}2\pi ft}, \tag{8}$$

where t is time. (The convention $\mathrm{e}^{\mathrm{j}\omega t}$ is used.) For a turbulent atmosphere, the long-term average of the squared absolute value of the total pressure amplitude can be written [15]

$$\langle |p_{tot}|^2 \rangle = |p_1|^2 + |p_2|^2 + 2|p_1 p_2| \cos\left[\arg\left(\frac{p_2}{p_1}\right)\right] \Gamma_{12}, \tag{9}$$

where Γ_{12} is the mutual coherence function fulfilling $0 \leq \Gamma_{12} \leq 1$.

For N sources we get [16]

$$\langle |p_{tot}|^2 \rangle = \sum_{i=1}^{N} |p_i|^2 + 2 \sum_{i=1}^{N-1} \sum_{j=i+1}^{N} |p_i p_j| \cos\left[\arg\left(\frac{p_j}{p_i}\right)\right] \Gamma_{ij}. \tag{10}$$

For the turbulence model used here, we have [6, 17]

$$\Gamma = \exp\left[-\frac{3}{8} D \left(\frac{C_T^2}{T_0^2} + \frac{22}{3}\frac{C_v^2}{c_0^2}\right) k^2 \rho_\Gamma^{5/3} L_\Gamma\right], \tag{11}$$

where $D \approx 0.364$, ρ_Γ is the transversal separation between the sources and L_Γ is the longitudinal distance to the receiver. For a direct and a ground reflected wave, the maximum vertical separation between their paths is chosen as the transversal

separation [17]. With the heights h_S and h_R above the ground of the source and the receiver this implies that $\rho_\Gamma = 2h_S h_R/(h_S + h_R)$.

The measured values of C_v and C_T are taken as input when calculating the mutual coherence between direct and ground reflected waves, both for the diffraction and for the scattering. For the diffraction all the paths are taken as going along the top of the barrier; the direct and ground reflected waves from the source meet at the top barrier edge closest to the source, and vice versa on the receiver side. The diffraction can be seen as contributions along four paths, and Eq. (10) is used.

How the decorrelation is applied to the calculation of the scattering is explained in the following subsection.

Prediction scheme

The Tables A1 and A2 (in Appendix A) with the data for the prediction scheme contain the scattered power at a chosen frequency $f_0 = 2$ kHz, for different geometries, and for a given unit strength of the velocity fluctuations or of the temperature fluctuations. The data come from a numerical calculation of the integral (2), where the incident pressure p_0 is calculated without taking into account the reflections from a ground surface, or the field diffracted by the screen. For a complete description of the calculation see Ref. [1] or [2].

The tabulated values are then transformed for other values of frequency or for a scaling of the geometry. If the frequency f is changed, $\frac{10}{3}\log(f/f_0)$ is added, and if the geometrical length scale is changed a factor s, $10\log(s)$ is added (i.e. if the distances between source and screen, screen and receiver, and the screen height are all changed with the same factor s).

When modelling the effect of a ground surface, a good way would be to include the ground reflected wave in p_0 when the integral (2) is calculated, as well as the ground reflection on the receiver side and the decorrelation between direct and ground reflected waves. However, in order to avoid recalculating the integral (2) for each height above the ground of the source and receiver and for each frequency, a point A is chosen, around which the dominating part of the scattering is assumed to be produced. All the direct and ground reflected paths via all scattering volume elements are thereby approximated by the single set of paths that go through A. The single set of sound paths from source to receiver via the point A consists of four paths, as seen from mirroring the source and the receiver in the ground surface. If W_0 is the scattered power when omitting the ground (corresponding to the values in the Tables A1 and A2), then the total power can be approximated as $W_0 \cdot C_S \cdot C_R$. Here C_S and C_R are correction factors, both with values between 0 and 4. The factors C_S

and C_R are the expected powers relative to free field at A without the barrier, with the ground, and where a decorrelation between direct and ground reflected sound waves is included. C_S is calculated from the source and the image source to the point A, and C_R is to the same point A, but from the receiver position. The decorrelation considers the atmospheric turbulence, but for a better prediction it should also take into account ground and terrain properties and a correction that models the dominating scattering as coming from a small volume around the point A rather than only from that point. The last statement is of most importance at high frequencies where the interference pattern has room to vary significantly inside the volume where the dominating scattering is produced.

The point A is chosen to be the lowest point in line of sight from both the source and the receiver. For a thin screen, A is at the screen edge. (See Figure 2.) This choice of the point A is motivated since the scattering cross-section (6) in general becomes large when the scattering angle becomes small. If $\theta = 90^\circ$ at A, however, there is no scattering, and another choice of A would be motivated. Moreover, for A very close to the source and far away from the receiver (or vice versa) the scattered power from A will be low due to the large difference in the distances (see Eq. (2)).

The presented prediction scheme is applied in the following for the comparison with the measured data.

4 Comparison between predictions and measurements

Measurements of the sound reduction obtained with a thick barrier were performed simultaneously with turbulence measurements on two different days.

The results for six different geometries are presented in Figures 3–8. The distance from the barrier to the receiver is varied ($d_r = 4$, 8, and 18 m) and the heights of the source and the receiver are changed. The situation with a high source position (1.25 m) and the receiver on the ground is exchanged for a high receiver position (1.25 m) and the source on the ground. When the source is on the ground a source height h_S of around 3 cm is used as input in the model (see each figure caption for the exact value used for h_S). For the receiver on the ground the height h_R is taken to be 3 mm.

The results to the left are from the calmer situations, and to the right are those from the more windy situations. The measured values of the structure parameters are shown in each figure caption.

In the calculated results the air absorption is taken into account using ISO 9613-1:1993, based on the mean temperature that was about 19°C and the relative humidity that was about 50% during the measurements. The atmospheric pressure was

assumed to be 1013 hPa.

In the plots the measured results are represented by a thick solid line and the total predictions, including diffraction, decorrelation and scattering, are represented by a thick dashed line. The thin dash-dotted line represents the turbulence scattering only and the thin solid line represents the diffraction only, without considering the decorrelation.

At frequencies lower than about 2 kHz the results show little influence of turbulence scattering. The measurements are in fairly good agreement with the calculations in this range. It does, however, look like an offset in some situations. These offsets may be due to refraction caused by the mean wind speed profile. For the downwind situations (right) the measured values are mainly higher than the predictions and for the upwind situations (left) the measured values are mainly lower than the predictions.

For frequencies above 2 kHz strong scattering effects, up to 10 dB, are shown in the more windy and turbulent situations, especially for the longer receiver distances. For these high-frequency data the agreement between the predictions and the measurements is fairly good. The model does, however, seem to overpredict the scattered power for the highest frequencies, i.e. above 6-8 kHz. This may partly be the error due to the single-scattering approximation, i.e. considering multiple scattering could mean a change in the incident pressure wave p_0 in Eq. (2).

The decorrelation in the predictions seems in general to be stronger than in the measurements. This can be seen for example in Figure 5 (right), where the prediction shows no interference effects above 2 kHz, whereas the measurements do, up to about 3 kHz. This is probably due to that the strength of the turbulence is measured above the barrier and that the main part of the medium that influences the decorrelation is closer to ground, and there the turbulence may be weaker.

For the low source position the field in the neighborhood of the barrier top experiences an interference minimum at high frequencies, around 10 kHz (see Figures 6–8). In the model predictions, this minimum leads to a larger interference dip than is shown by the measurements. If the interference is included in p_0 when the integral (2) is calculated, the interference dip would be much less pronounced since at these high frequencies, the volume from which the dominating scattering comes will not be occupied by a field described mainly by destructive interference. Therefore, the decorrelation should increase faster at higher frequencies in order to compensate for the spatially narrower interference pattern compared to the size of the dominant-scattering volume. This problem appears not only for the scattering. It could be seen as a general difficulty at high frequencies for most acoustic prediction

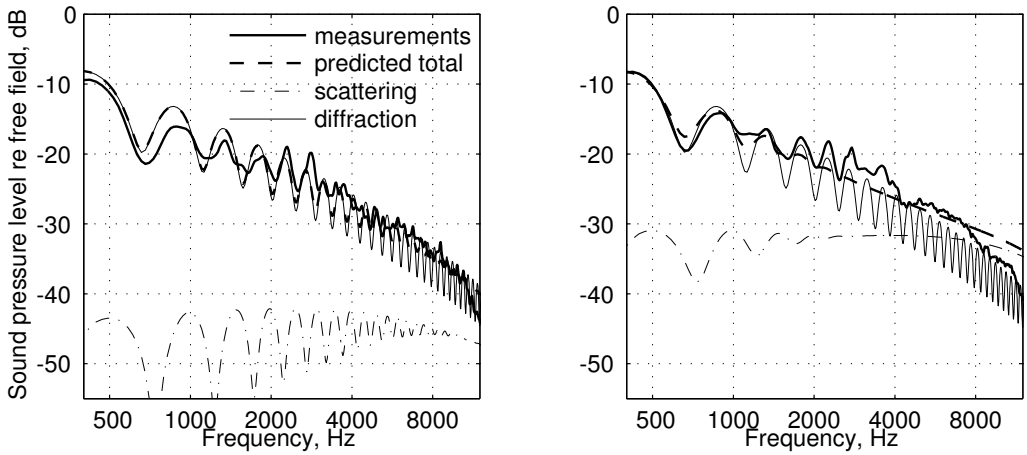

Figure 3: Measurement and prediction for $h_S = 1.25$ m, $h_R = 0.3$ cm, and $d_R = 4$ m. To the left $C_v^2 = 0.4$ m$^{4/3}$/s^2 and $C_T^2 = 0.2°$K/m$^{2/3}$; to the right $C_v^2 = 8$ m$^{4/3}$/s^2 and $C_T^2 = 3.5°$K/m$^{2/3}$. (The same units are used in the following Figures.)

methods. Also the source and the boundary will contain details that are difficult to describe, but are important at high frequencies. For example when the wavelength is about the size of the source, the point source model may be a poor representation. The usual approach to handle this would be to model the details in a statistical way in a wide-band analysis.

5 Conclusions

Looking at the overall results for both the calm and for the windy situations, the predictions agree fairly well with the measurements.

The influence of the turbulence scattering on the sound reduction obtained with a barrier increases when the frequency is increased or when the geometry is increased in scale (as shown in comparison to earlier measurements [5, 18, 8]).

The scattering due to turbulence is shown to be able to significantly increase the noise level behind a barrier. The increase shown here is up to about 5 dB at 4 kHz and up to about 10 dB at 8 kHz. For larger geometries even stronger effects are assumed to be possible.

The model includes many approximations and conditions that are not always fulfilled. For instance, assuming that the turbulence is homogeneous, so that it needs to be measured in one point only, is probably a crude approximation. Moreover, the condition (1) that motivates the volume integration of the scattered power is not met

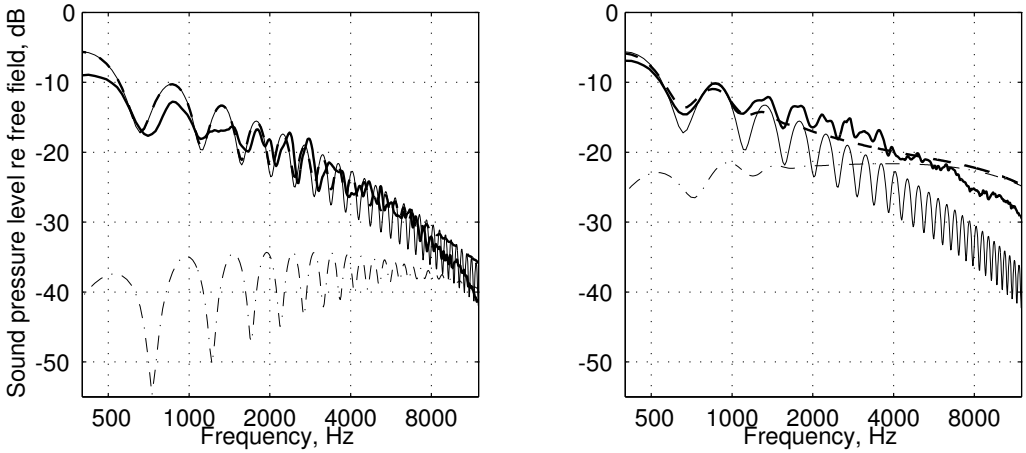

Figure 4: Measurement and prediction for $h_S = 1.25$ m, $h_R = 0.3$ cm, and $d_R = 8$ m. To the left $C_v^2 = 0.4$ and $C_T^2 = 0.3$; to the right $C_v^2 = 15$ and $C_T^2 = 4$.

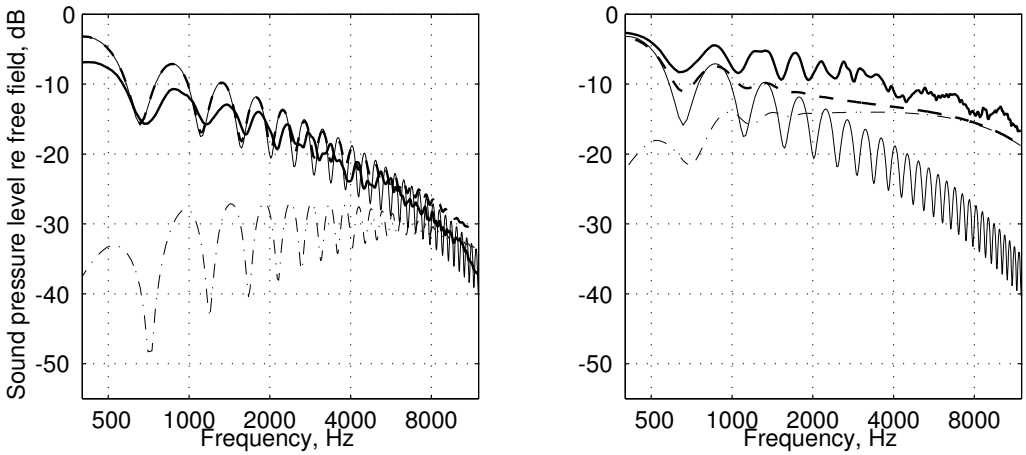

Figure 5: Measurement and prediction for $h_S = 1.25$ m, $h_R = 0.3$ cm, and $d_R = 18$ m. To the left $C_v^2 = 0.4$ and $C_T^2 = 0.2$; to the right $C_v^2 = 15$ and $C_T^2 = 3.5$.

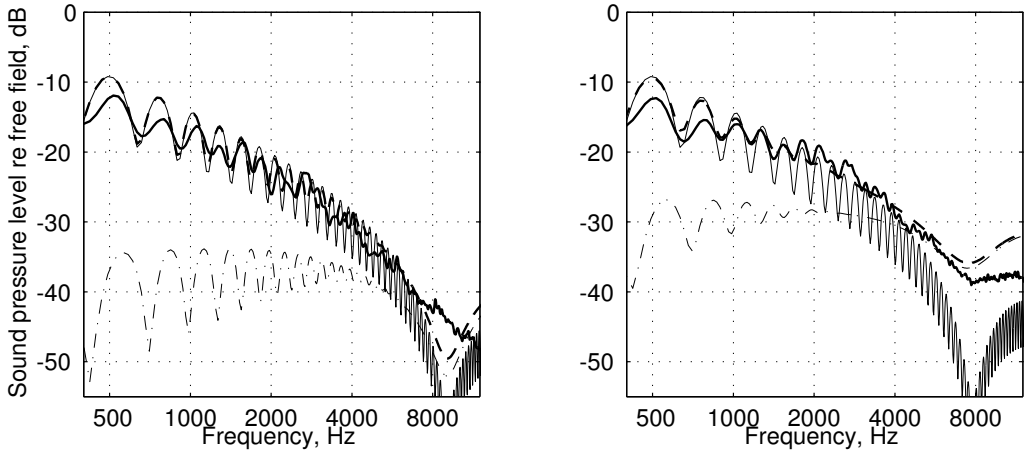

Figure 6: Measurement and prediction for $h_S = 2.9$ cm (left), and 3.4 cm (right), $h_R = 1.25$ m, and $d_R = 4$ m. To the left $C_v^2 = 2$ and $C_T^2 = 1$; to the right $C_v^2 = 15$ and $C_T^2 = 2$.

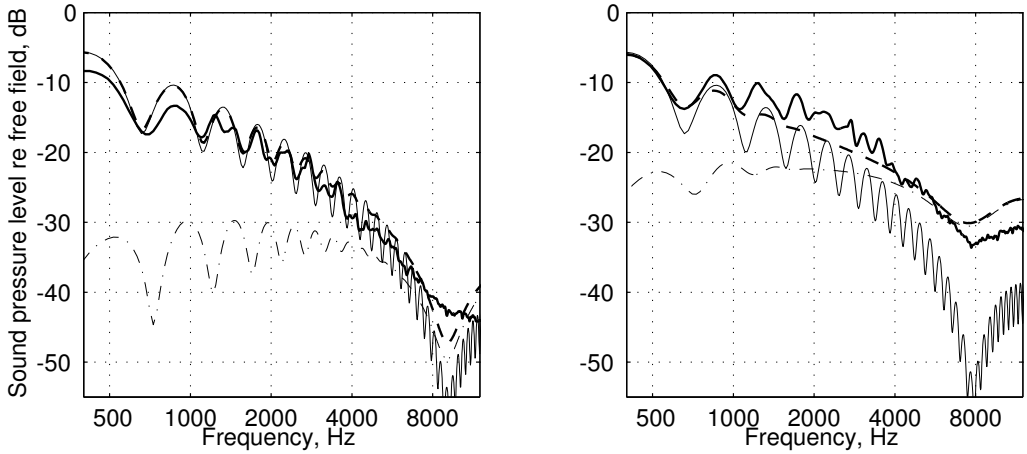

Figure 7: Measurement and prediction for $h_S = 2.9$ cm (left), and 3.4 cm (right), $h_R = 1.25$ m, and $d_R = 8$ m. To the left $C_v^2 = 1.5$ and $C_T^2 = 0.8$; to the right $C_v^2 = 17$ and $C_T^2 = 2$.

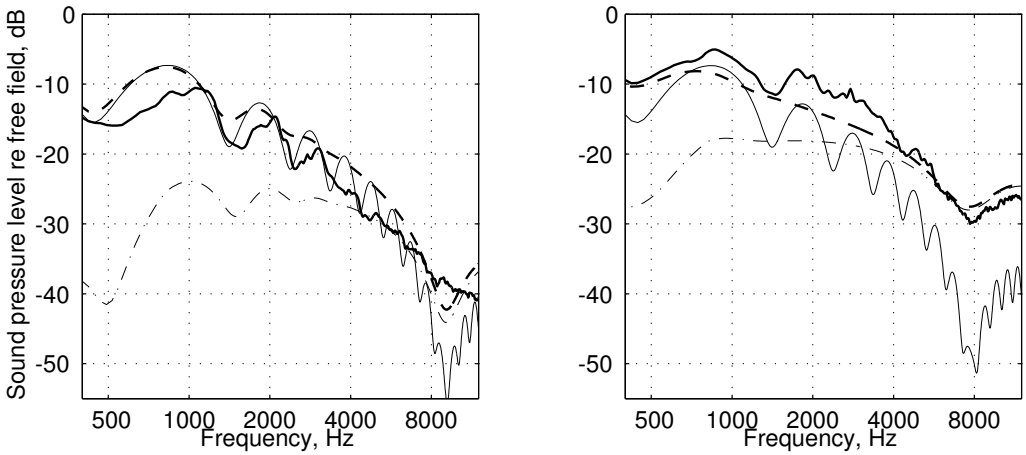

Figure 8: Measurement and prediction for $h_S = 2.9$ cm (left), and 3.4 cm (right), $h_R = 1.25$ m, and $d_R = 18$ m. To the left $C_v^2 = 2$ and $C_T^2 = 1$; to the right $C_v^2 = 14$ and $C_T^2 = 2$.

at the higher frequencies. Also, neglecting the diffracted field in the wave irradiating the scattering volume (p_0 in Eq. (2)) could cause a significant error. This problem is connected to the approximation that the scattered and the diffracted fields are uncorrelated. Moreover, the error due to the single-scattering approximation might grow large at the higher frequencies, where the scattering cross-section is larger, which may cause the overprediction in the model at the highest frequencies, here above about 6–8 kHz. The fairly good agreement between the predictions and the measurements does, however, indicate that the model is applicable.

For future work a model similar to the one used here can be developed to take into account barriers of finite length, a non-constant sound speed profile, and inhomogeneous and anisotropic turbulence.

Acknowledgements

The authors wish to thank Wolfgang Kropp for fruitful discussions and critical reading. This work was financially supported by MISTRA (Swedish Foundation for Strategic Environmental Research).

Appendix A

The Tables A1 and A2 contain the scattered power, in dB relative to free field, calculated for the frequency $f_0 = 2$ kHz, without the influence of a ground. In Table A1, $C_v^2 = 1$ m$^{4/3}$/s^2 and $C_T^2 = 0$. In Table A2, $C_v^2 = 0$ and $C_T^2 = 1°$K/m$^{2/3}$. The screen height h' is the height of the *equivalent* thin screen, which has the edge at the point A. The distance d_R' between screen and receiver is varied as well as h'. The distance $d_S' = 40$ m between source and screen is kept constant. (See Figure 2.) The scattered power for other frequencies and geometries is found using transformation properties, as described in the paper.

	d_R'=10	20	30	40	50	60	70	80	90	100
$h' = 5$	-41.6	-33.9	-30.2	-27.9	-26.2	-24.9	-23.9	-23.1	-22.4	-21.8
10	-49.9	-44.0	-39.5	-36.7	-34.7	-33.1	-31.8	-30.9	-30.1	-29.3
15	-52.1	-48.9	-45.8	-42.9	-40.7	-39.1	-37.7	-36.6	-35.5	-34.7
20	-53.8	-51.0	-48.8	-46.8	-45.0	-43.5	-42.1	-40.9	-39.9	-39.1
25	-55.4	-52.4	-50.4	-48.8	-47.5	-46.2	-45.1	-44.0	-43.1	-42.2
30	-57.0	-53.8	-51.5	-50.6	-48.9	-47.8	-46.8	-45.9	-45.2	-44.4
35	-58.6	-55.1	-52.7	-51.1	-49.8	-48.8	-47.9	-47.1	-46.4	-45.7
40	-59.9	-56.5	-53.9	-52.1	-50.7	-49.6	-48.7	-48.0	-47.3	-46.6

Table A1. Scattered level due to a unit strength of velocity turbulence for different values of the screen height h' and the screen–receiver distance d_R' (both in meters).

	d_R'=10	20	30	40	50	60	70	80	90	100
$h' = 5$	-44.0	-39.1	-36.0	-34.0	-32.5	-31.3	-30.4	-29.6	-28.9	-28.3
10	-47.4	-44.7	-42.4	-40.5	-39.1	-37.9	-36.9	-36.0	-35.3	-34.7
15	-48.9	-46.7	-45.1	-43.6	-42.4	-41.4	-40.5	-39.7	-39.0	-38.4
20	-50.2	-48.0	-46.4	-45.2	-44.1	-43.2	-42.4	-41.7	-41.1	-40.5
25	-51.4	-49.0	-47.4	-46.2	-45.2	-44.3	-43.6	-42.9	-42.3	-41.8
30	-52.5	-50.0	-48.3	-47.0	-46.0	-45.1	-44.4	-43.7	-43.2	-42.6
35	-53.6	-51.0	-49.2	-47.8	-46.7	-45.8	-45.0	-44.4	-43.8	-43.3
40	-54.6	-52.0	-50.0	-48.5	-47.4	-46.4	-45.6	-44.9	-44.3	-43.8

Table A2. Scattered level due to a unit strength of temperature turbulence for different values of the screen height h' and the screen–receiver distance d_R' (both in meters).

References

[1] Forssén J. Influence of atmospheric turbulence on sound reduction by a thin, hard screen: A parameter study using the sound scattering cross-section. *Proc. 8th Int. Symp. on Long-Range Sound Propagation*, The Pennsylvania State University, 1998, pp. 352-64.

[2] Forssén J. Calculation of sound reduction by a screen in a turbulent atmosphere. Report F 98 - 01, Chalmers University of Technology, Göteborg, Sweden (ISSN 0283 - 832X), 1998.

[3] Forssén J. Calculation of sound reduction by a screen in a turbulent atmosphere using the parabolic equation method. *Acustica* 1998, Vol. 84, pp. 599-606.

[4] Forssén J. Calculation of noise barrier performance in a turbulent atmosphere by using substitute sources above the barrier. *Acustica* 2000, Vol. 86, pp. 269-75.

[5] Daigle GA. Diffraction of sound by a noise barrier in the presence of atmospheric turbulence. *J Acoust Soc Am* 1982, Vol. 71, pp. 847-54.

[6] Ostashev VE. Acoustics in moving inhomogeneous media. E & FN Spon (an imprint of Thomson Professional), London, 1997.

[7] Tatarskii VI The effects of the turbulent atmosphere on wave propagation. Keter Press, Jerusalem, 1971.

[8] Forssén J, Ögren M. Approximative model for the influence of atmospheric turbulence on sound reduction by a thin screen. *Proc. 6th International Congress on Sound and Vibration*, Technical University of Denmark, Lyngby, 1999, pp. 713-20.

[9] Panofsky HA, Dutton JA. Atmospheric turbulence. John Wiley & sons, New York, 1984.

[10] Chein CF, Soroka WW Sound propagation along an impedance plane *Journal of Sound and Vibration* 1975, Vol. 43, pp. 9-20.

[11] Delany ME, Bazley EN Acoustical properties of fibrous absorbent materials *Applied Acoustics* 1970, Vol. 3, pp. 309-322.

[12] Hadden JW, Pierce AD Sound diffraction around screens and wedges for arbitrary point source locations *J. Acoust. Soc. Am* 1981, Vol. 69, pp. 1266-1276.

[13] Salomons EM Sound Propagation in Complex Outdoor Situations with a Non-Refracting Atmosphere: Model Based on Analytical Solutions for Diffraction and Reflection *Acustica / Acta Acustica* 1997, Vol. 83, pp. 436-454.

[14] Chevret P, Blanc-Benon Ph, Juvé D A numerical model for sound propagation through a turbulent atmosphere near the ground. *J Acoust Soc Am* 1996, Vol. 100, pp. 3587-99.

[15] Clifford SF, Lataitis RJ. Turbulence effects on acoustic wave propagation over a smooth surface. *J Acoust Soc Am* 1983, Vol. 73, pp. 1545-50.

[16] L'Espérence A, Herzog P, Daigle GA, Nicolas JR. Heuristic model for outdoor sound propagation based on an extension of the geometrical ray theory in the case of a linear sound speed profile. *Applied Acoustics* 1992, Vol. 37, pp. 111-39.

[17] Ostashev V, Clifford S, Lataitis R, Blanc-Benon P, Juve D. The effects of atmospheric turbulence on the interference of the direct and ground reflected waves. *Proc. 29th Inter-Noise*, Nice, 2000, pp. 217-222.

[18] Ögren M, Forssén J. Measurements of sound reduction by a noise barrier in the presence of wind and atmospheric turbulence. *Proc. 6th International Congress on Sound and Vibration*, Technical University of Denmark, Lyngby, 1999, pp. 721-26.

Paper II

Road Traffic Noise Propagation between Two Dimensional City Canyons using an Equivalent Sources Approach

Mikael Ögren and Wolfgang Kropp

Abstract

The sound pressure level at courtyards from road traffic noise is difficult to predict using standardised methods. A simple model for a courtyard is a two dimensional city canyon, where a second canyon represents the street with vehicles. Here an equivalent sources approach is used to couple the canyons and the free half-space above them. The strengths of the virtual sources that couples the different domains can be determined by solving an equation system. After that the level can be calculated anywhere inside or outside the canyons. Unfortunately the method is rather computationally heavy, but less so than the standard boundary element method (BEM) or the finite difference – time domain method (FDTD). The method is verified against BEM in a simple case, and against full-scale measurements in the field. The comparisons show that the agreement is acceptable if sufficiently many streets are included as sources.

1 Introduction

Courtyards are a typical feature in many European cities. Since these courtyards are shielded from direct traffic noise exposure by the surrounding buildings, they represent relatively quiet areas. The noise level on an exposed facade can be predicted with reasonable accuracy using available methods (e.g. the Nordic calculation method [1]). However, the noise level in shielded areas seems to be more difficult to predict. The existing prediction methods for road traffic noise underestimate the noise level in these areas [2]. This is probably due to that the sound propagation in an urban environment is a complex process not sufficiently described in existing

prediction schemes. Sound waves travel from the source to the receiver via many paths, and the waves can be reflected and diffracted many times. A complex micro climate with inhomogeneous atmosphere together with many scattering objects lead to diffusive and absorptive effects. The shortcomings of the present schemes might also be due to the fact that normally only sources in the vicinity of the receiver are taken into account.

This paper attempts to contribute to the clarification of these questions by proposing a very first approach of a prediction method for shielded areas, i.e. the sound propagation between different street canyons.

Different methods for sound propagation in urban areas can be found in literature. A ray based solution for diffraction and reflection may be used for such situations [3]. The limitations of such a model is that it is not valid for low frequencies, it might require high order reflections and diffractions, and in situations with uneven surfaces or surfaces which are not perfectly hard some form of approximations must be used. Diffusive effects are difficult to take into account, but recent efforts show promising results with methods based on radiosity [4] or on the diffusion equation [5].

Models using statistical methods for propagation in complex urban environments were developed some twenty years ago [6, 7], but are most relevant for positions far from the source. They were designed to give the average level in an area with a random distribution of buildings. At positions close to the source, either exposed directly to the source, or in deep shadow behind one or several objects, such models fail.

The situation of a depressed road, or a road surrounded by tall buildings, can be seen as a two dimensional (2-D) problem, where the traffic will act as a line source and the road together with the buildings' façades will form a "city canyon". This geometry has been studied extensively [8, 9, 10, 11, 12], but with a focus on propagation along the street or into side streets, not out of one canyon and into another.

Recently the FDTD method (Finite Difference – Time Domain) has been applied to similar geometries [13], and other methods like the BEM (Boundary Element Method) are also applicable. However, one can expect a high computational effort using BEM, since large geometries have to be considered in a frequency range up to one or a few kHz. The FDTD method is computationally heavy since the whole domain must be discretized, including an area above the canyon, and if the damping in the canyon is low many time steps have to be used in order to include all important reflections. In canyons where sources are located, i.e. on exposed façades, only a few reflections are neccesary [14], but this is not the case at shielded positions where

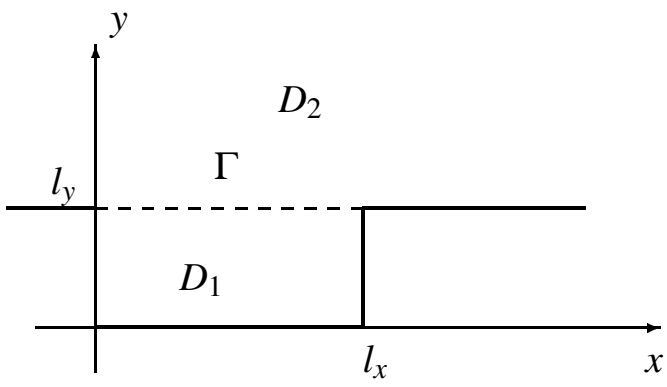

Figure 1: Sketch of the 2D canyon geometry.

no direct field is present.

2 Theory

In [15] the method of equivalent sources was used to calculate the insertion loss of balconies including absorbing surfaces. The main idea of the method is to reduce the problem to a simplified geometry with boundary conditions which are easy to handle. On boundaries with different conditions, sources are placed. The strengths of these sources are adjusted so that the boundary conditions are fulfilled everywhere. Applications of this can be found in [16, 15, 17], and a good theoretical background can be found in [18]. The method has been shown to be robust and computationally efficient and is therefore suitable for the problem considered here.

Consider the street canyon shown in Figure 1.

In order to apply the equivalent sources method, the geometry is divided into two parts, the domain inside the canyon and the half space above $y = l_y$. The boundary between the two domains is denoted as Γ. In this way the problem is reduced to two subproblems, which can easily be handled; radiation into a half space by a Rayleigh integral, and a sound field in a rigid cavity by a modal approach. The coupling between the half space and the cavity is obtained by the set of equivalent sources which correct the field impedance along the boundary Γ. Although the mathematical derivation of the method has been described elsewhere [15], some details are repeated here for clarity.

In the following harmonic time dependence described by $\exp(\mathrm{j}\omega t)$ is assumed. The wave equation for the complex pressure p in a two dimensional domain, assum-

ing a source of strength q, is

$$\nabla^2 p(x,y) + k^2 p(x,y) = -\mathrm{j}\omega\rho_0 q(x,y), \tag{1}$$

where the strength q is a volume velocity, or in the two dimensional case what might be called a surface velocity. In this text q denotes a distributed source, and Q a point source, both in 2-D. Taking into account the boundaries of the two domains the Green functions can be found for instance in [19] and [20], and they are

$$G_1(x_s,y_s|\,x_r,y_r) = \mathrm{j}\omega\rho\frac{c^2}{l_x l_y}\sum_n\sum_m \frac{\Psi_{n,m}(x_s,y_s)\Psi_{n,m}(x_r,y_r)}{\Lambda_{n,m}(\omega_{n,m}^2(1+\mathrm{j}\eta)-\omega^2)}, \tag{2}$$

$$G_2(x_s,y_s|\,x_r,y_r) = \mathrm{j}\omega\rho\,\frac{-\mathrm{j}}{2}H_0^{(2)}(kr). \tag{3}$$

The Green function G_1 is a modal summation where the eigen frequencies $\omega_{n,m}$, modal shapes $\Psi_{n,m}$ and modal weights $\Lambda_{n,m}$ can be determined using

$$\omega_{n,m} = \pi c\sqrt{(n/l_x)^2 + (m/l_y)^2} \tag{4}$$

$$\Psi_{n,m}(x,y) = \cos(n\pi x/l_x)\cos(m\pi y/l_y) \tag{5}$$

$$\Lambda_{n,m} = \int_0^{l_y}\int_0^{l_x} \Psi_{n,m}^2\,\mathrm{d}x\,\mathrm{d}y, \tag{6}$$

where c is the sound speed, η the loss factor, l_x and l_y the dimensions of the canyon and Γ the boundary between the canyon D_1 and the free space above it D_2, see Figure 1. The modal summation must be truncated somewhere, and here eigen frequencies up to three times as large as the frequency of interest were included in order to ensure convergence. Note that the damping expressed as η applies to the covered canyon only, the effect of power being transfered into the field above the canyon is described by the coupling of the two domains. In the same way the modes of the covered canyon are orthogonal, but the modes of the combined system might be coupled since the opening might be seen as an unevenly distributed absorption.

The Green function G_2 contains the Hankel function of the second kind, and describes a line source in front of a rigid surface. The distance between the source and the receiver is denoted $r = \sqrt{(x_s-x_r)^2+(y_s-y_r)^2}$, and k is the wavenumber. The Green function contains no losses, but if necessary the losses due to atmospheric absorption in the propagation from the canyon to an external receiver can be included at a later stage in the computations.

The coupling between the two domains is introduced by assuming boundary source distributions. Using a combination of the primary source of strength Q located inside the canyon at $(x_s, y_s \in D_1)$, and the boundary source distribution $q_l(x)$ below the boundary and $q_u(x)$ above it, the pressure can be calculated as

$$p_l(x_r, y_r) = QG_1(x_s, y_s|x_r, y_r) + \int_\Gamma q_l(x) G_1(x, l_y|x_r, y_r)\,\mathrm{d}x \tag{7}$$

inside the canyon $(x_r, y_r \in D_1)$ and

$$p_u(x_r, y_r) = \int_\Gamma q_u(x) G_2(x, l_y|x_r, y_r)\,\mathrm{d}x \tag{8}$$

above the canyon $(x_r, y_r \in D_2)$. The source is assumed to be located inside the canyon for brevity.

At the boundary Γ between the two domains, the pressure and the velocity fields must be continuous. As a consequence p_l equals p_u and q_l equals $-q_u$ along Γ, and we can drop the subscripts l and u. The resulting equation system can be discretized by dividing the boundary Γ into a number of equally sized elements $\Gamma_1, \Gamma_2, \ldots, \Gamma_N$, and approximate the source strength along the boundary by a piecewise constant complex source strength $q_1, q_2, \ldots, q_N$ on each element. The pressure at the centre points of the elements $x_1, x_2, \ldots, x_N$ must be equal, which gives the equation system

$$Aq = b \tag{9}$$

where

$$A_{i,j} = \int_{\Gamma_j} G_1(x, l_y|x_i, l_y)\,\mathrm{d}x + \int_{\Gamma_j} G_2(x, l_y|x_i, l_y)\,\mathrm{d}x \tag{10}$$

and

$$b_i = Q\,G_1(x_s, y_s|x_i, l_y). \tag{11}$$

The length of the elements is set to one tenth of the wavelength. The size of the equation system will be $N \times N$, and A is a symmetric matrix. Solving equation (9) one obtains the strengths of the boundary sources q, and can calculate the pressure using

$$p(x_r, y_r) = \sum_{i=1}^{N} q_i \int_{\Gamma_i} G_1(x, l_y|x_r, y_r)\,\mathrm{d}x + QG_1(x_s, y_s|x_r, y_r) \tag{12}$$

inside the canyon $(x_r, y_r \in D_1)$ and

$$p(x_r, y_r) = -\sum_{i=1}^{N} q_i \int_{\Gamma_i} G_2(x, l_y | x_r, y_r)\, \mathrm{d}x \tag{13}$$

above the canyon $(x_r, y_r \in D_2)$.

The integrations of the free Green function G_2 in equation (10) can be evaluated numerically, except for the case of $i = j$, which gives a singularity. One way of going around this problem is to make a numerical integration that avoids the singular part. Another way is to use

$$\int_{-a}^{a} H_0^{(2)}(|x|)\, \mathrm{d}x = 2 \int_0^a H_0^{(2)}(x)\, \mathrm{d}x \tag{14}$$

and

$$\begin{aligned} \int_0^a H_0^{(2)}(x)\, \mathrm{d}x = {} & H_0^{(2)}(a)\, \left(a - a^3/3 + o(a^5)\right) \\ & + H_1^{(2)}(a)\, \left(a^2 - a^4/9 + o(a^6)\right) \end{aligned} \tag{15}$$

derived from 11.1.7 in [21] ($a > 0$), where the integral over a Hankel function is expressed in terms of Hankel and Struve functions. In equation (15) the Struve functions have been approximated by polynomials according to 12.1.4 and 12.1.5 in [21], and the accuracy is better than 0.02% if the elements are smaller than one tenth of the wavelength. If a higher accuracy is required, more terms can be included.

In equation (10) the Green function G_1 can be integrated analytically. The case $i = j$ does not require any special consideration. Assuming that the order of the integration and summation can be reversed, one can move everything that does not depend on x out of the integral. Integrating over one element starting at x_1 to x_2 at $y = l_y$ for each n, m in the modal summation yields

$$\begin{aligned} & \int_{x_1}^{x_2} \cos(n\pi x/l_x) \cos(m\pi y/l_y)\, \mathrm{d}x = \\ & \qquad \left[\sin(n\pi x/l_x)\, l_x/(n\pi)\right]_{x_1}^{x_2} (-1)^m \end{aligned} \tag{16}$$

unless $n = 0$, then

$$\begin{aligned} & \int_{x_1}^{x_2} \cos(n\pi x/l_x) \cos(m\pi y/l_y)\, \mathrm{d}x = \\ & \qquad (x_2 - x_1)(-1)^m. \end{aligned} \tag{17}$$

Canyon	Width l_x (m)	Height l_y (m)	Source position (m) x_s	y_s
A	11	18	5	0
B	19	18	9	0
C	20	18	0.5	0.5
D	11	18	0.5	0.5
E	20	18	–	–

Table 1: Canyon geometries.

The approach of assuming a piecewise constant complex source distribution over each element is rather crude, it might be thought of as a zeroth order polynomial approximation. Assuming a linear or higher order polynomial on each element might give better numerical properties, i.e. a faster and more accurate method, but this is not studied further in this work.

3 Results

3.1 Initial tests

The natural starting point for validating the model is to ensure that it gives a field which is continuous across the boundary of the two domains. Using a geometry with a 19 m wide and 18 m deep canyon, the pressure was calculated in, and above, the canyon. The source was located at $(9,0)$, i.e. nine meters from the left wall on the floor of the canyon. The source is located slightly off centre in order to excite both even and odd modes in the x-direction. This geometry is summarised in Table 1 as **B** together with other canyon geometries used later in this article.

The sound field is always continuous at the points $x_1, x_2, \ldots, x_N$ since this is required by the solution method, but at positions in between there might be a small deviation. This effect is most visible close to the edges, i.e. close to $x = 0$ and $x = l_x$, where the field has large gradients. In Figure 2 the pressure 1 mm above and below the boundary Γ for a source position inside the canyon $(9,0)$ has been calculated at a frequency of 40 Hz. The matching points are also indicated in the Figure. As expected the discrepancy is largest close to the corners. The low frequency was chosen in order to make the effect more visible.

Another way to study the continuity is to calculate the pressure level in the entire canyon including an area above it, and show the results as a surface plot. In Figure 3

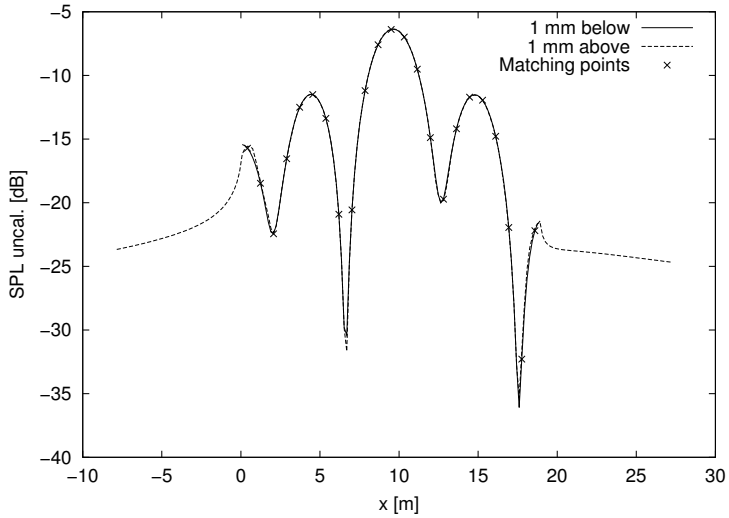

Figure 2: Sound pressure level in canyon **B** just above and just below the intersection at 40 Hz.

such a plot can be seen for the canyon mentioned above (**B** in Table 1) at a frequency of 20 Hz. The field is clearly continuous. Also note that no sharp increase is visible close to the source at $(0, 9)$. Very close to the source a large number of modes have to be included in the summation in order to get the correct solution.

In order to validate the method calculations with the boundary element method for different canyons and source/receiver positions were carried out, and the agreement is acceptable. Unfortunately the BEM implementation was very computationally heavy, so comparisons were only possible at frequencies up to 400 Hz. Figure 4 shows a comparison plotted against frequency for canyon **D**. The receiver is located inside the canyon at $(10.5, 0.5)$, which is opposite to the source.

The curves are identical at the resonance frequencies of the canyon, but differ somewhat in the regions in between. Close to resonance frequencies the modal summation will be determined by one or a few terms, but more terms are needed for positions between resonance peaks. Therefore the effect of truncating the modal summation becomes visible here. On the other hand, if the sound pressure is averaged over frequency bands that include a few resonances, the sound pressure level will be dominated by the values close to the resonances.

The BEM used here assumes no damping, but the proposed method includes a little damping ($\eta = 10^{-9}$) in order to avoid the singularity at internal resonance frequencies. This does not influence the peak value at resonance for relatively low canyons though, since the largest part of the dissipated power is due to radiation

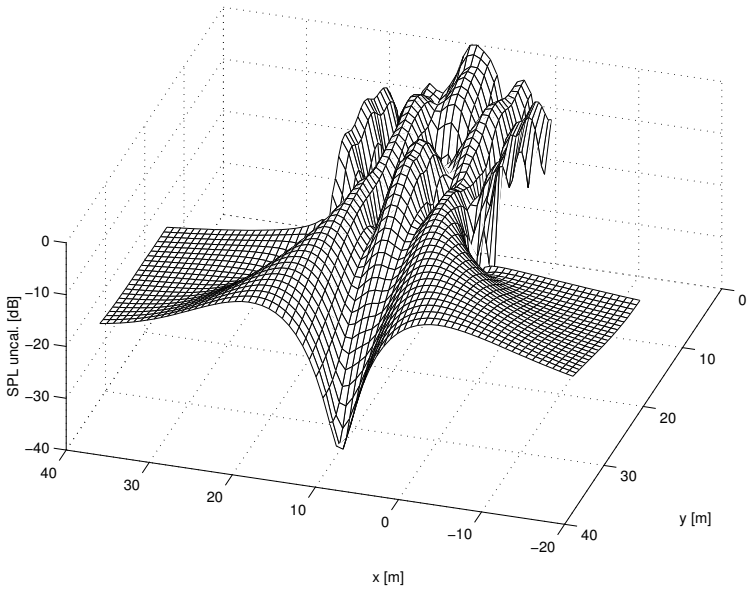

Figure 3: Surface plot of sound pressure level in the canyon **B** at 20 Hz, normalised to 0 dB for the maximum level.

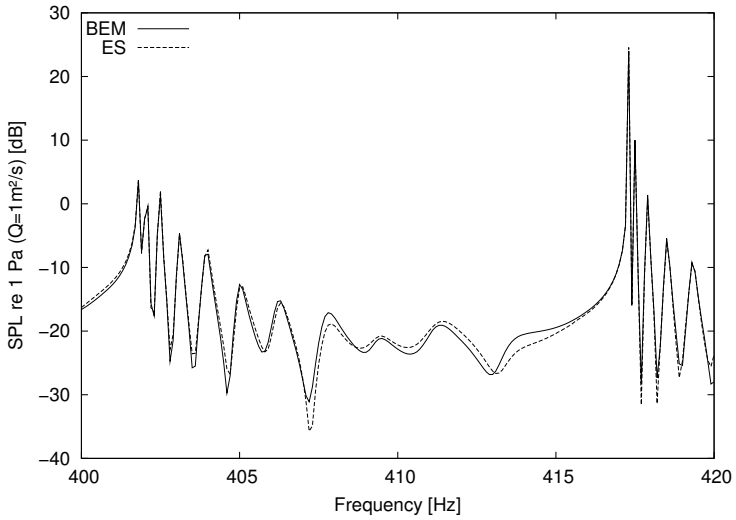

Figure 4: Comparison between BEM and the proposed method for canyon **C**.

from the opening of the canyon.

For solving the equation system and evaluating the pressure at one receiver point at 400 Hz the ES implementation used approximately 60 s of CPU-time and 10 Megabytes of memory[1] for 130 elements and 4500 modes in the modal summation. The BEM implementation used 220 s and 370 Megabytes for 790 elements. These data are of limited value though, since none of the implementations were optimised for high performance.

The large dissipation for low canyons makes the resonance peaks less pronounced, and slightly shifted to higher frequencies, which is visible in Figure 5, where a number of calculations for varying canyon heights are presented. The frequency response between 15 and 50 Hz for the 20 m wide canyon **C** was calculated for canyon heights between 2 m (a very shallow canyon) and 30 m (a very deep canyon). In Figure 5 the response is plotted as a contour with the frequency along the x-axis and the height along the y-axis. Dark contours indicate high levels, so the ridges going in the y-direction are the resonances that become more prominent as the height of the canyon increases. The receiver is positioned at (19.5,0.5) opposite to the source and at the same height. Note that for low canyon heights, only the simple resonances are visible (standing waves in the x-direction), but for higher canyons there will be more complicated effects involving dips and peaks between those frequencies.

3.2 Directivity

A source inside a canyon will have a different radiation pattern compared to a source on a rigid plane. Canyon **A** from Table 1 has been used for calculating the directivity. This geometry corresponds to typical distances between buildings and typical building heights for the area Söder in Stockholm, Sweden, which will be used later for comparisons with measurements. Again the source is located slightly off centre in order to excite both even and odd modes.

The equivalent sources in the model represent the radiation from the canyon to the surroundings. Their directivity describes how sound power is distributed in different directions. The directivity is normalised by the result for a source on a hard ground. Due to the canyon more power is radiated up-wards, and less to the sides, see Figure 6. This means that the reduction due to the canyon can be estimated to be 5–7 dB at high frequencies for sound propagation parallel to the city. If we consider a case where the source is in one canyon, and the receiver in a similar canyon, the total effect would be twice as much, giving a reduction of 10–14 dB for high frequencies, assuming reciprocity.

[1] Dual Pentium III at 866 MHz

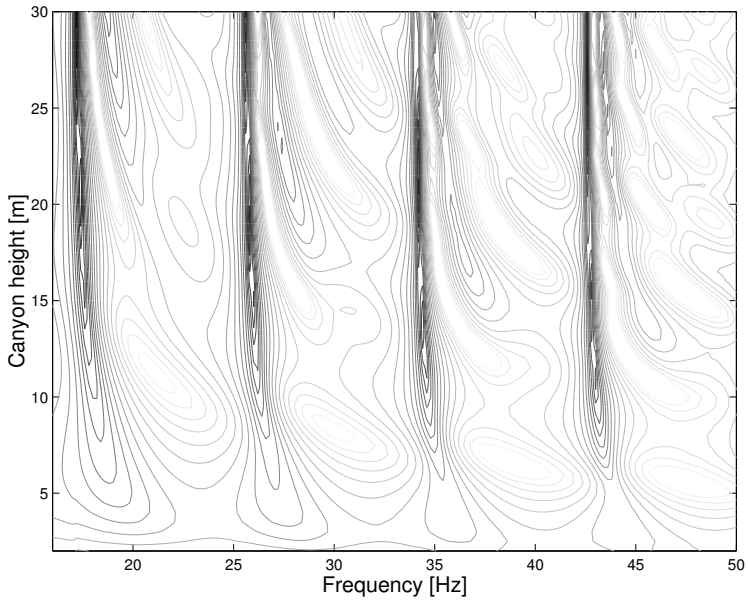

Figure 5: Contour plot of the frequency response in the canyon **C** for different canyon heights. Dark contours indicate high levels.

The two minimas that can be observed for certain angles at all the high frequencies correspond to the line of sight from the source out of the canyon, i.e. the line from the source and through one of the edges of the canyon.

3.3 Damping

The loss factor η is important for the noise level inside the canyon if the side walls of the canyon are relatively high. If the loss factor is determined assuming air absorption only it will be too low. In reality the effect of finite impedances on the walls of the canyon will give higher losses. For future predictions the loss factor can be determined from measurements on real courtyards, or from measurements of properties of typical façade materials, but for now a simpler approach has been chosen. The loss factor is taken from measurements of the intrinsic damping in the reverberation chamber at Chalmers University of Technology. The volume of the chamber is 240 m^3, and a logarithmic least squares fit of the damping as a function of frequency, based on reverberation time measurements, gives

$$\eta(f) = 10^{-0.94} f^{-0.84}, \tag{18}$$

for the frequency range 100 Hz – 1 kHz. In this way the damping is underestimated, and can be seen as a kind of minimum damping for a courtyard, since the walls of the

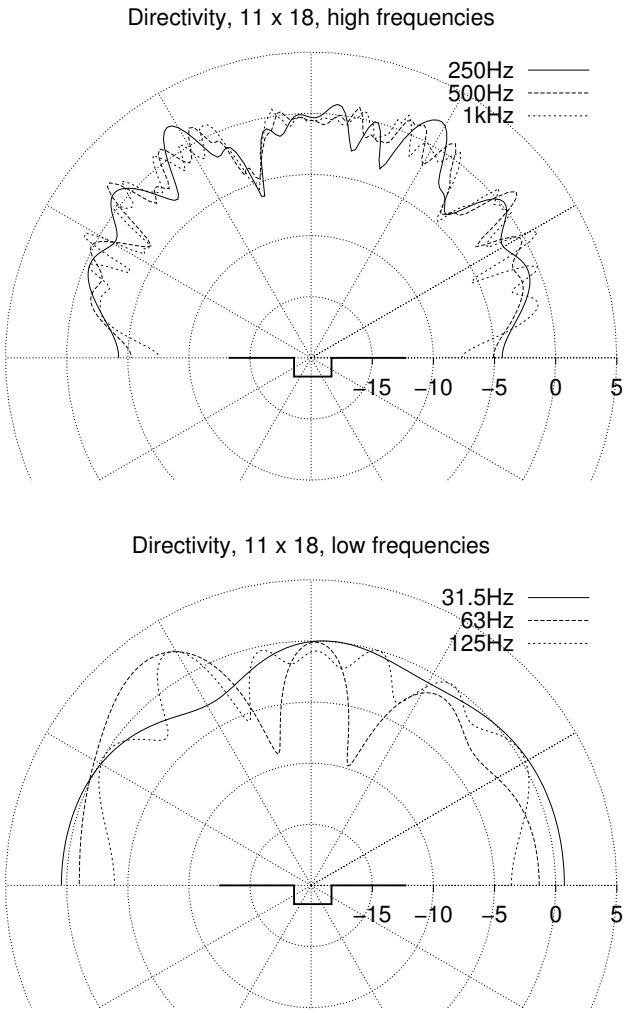

Figure 6: Directivity for the canyon **A** from Table 1 in third octave bands.

reverberation chamber is likely to have lower damping than real façade materials.

3.4 Source and receiver canyons

The calculations are divided into two steps. First the source canyon is treated as if the receiving canyon was not present. Then the source strengths calculated in the first step are seen as sources on a rigid plane for the receiving canyon, and the pressure at the receiving point is calculated. This approach is valid as long as the waves that are reflected at the receiving canyon back to the source canyon, and then back again to the receiving canyon, can be neglected.

In Figure 7 a contour plot is given for a source canyon of type **A** and a receiver canyon of type **E** as given in Table 1. The distance between the canyons was 14 m, corresponding to the width of the house that separates the street and the backyard. Each third octave band level has been estimated using 20 frequencies. The plots have been normalised to 0 dB at the mean value of the level in the source canyon, and are divided into 5 dB steps, where "0" corresponds to levels from +2.5 to -2.5, "-5" corresponds to -2.5 to -7.5 and so on.

For the third octave band 1 kHz the levels in the receiving canyon are approximately 31 dB below the mean level in the source canyon, but for the third octave 63 Hz this effect is only about 22 dB. So the insertion loss of the canyons increases with frequency, as does the insertion loss of a screen.

3.5 Comparisons with measurements

The measurements are from courtyards in the area Söder in Stockholm. The area consists of buildings with 5–7 floors, and the streets close to the courtyards of interest are between 11 and 20 m wide. The courtyards themselves are of different shapes and sizes. Courtyards with fans or other noisy machinery have been excluded from the study. The results of 5 short term measurements (approximately 30 minutes) and 5 long term measurements (one week) show that the equivalent sound level is surprisingly constant in the courtyards throughout the area. The long term measurements are in the range 48–51 dB, and the short term measurements 48–55 dB. All long term measurements were made a few meters from the inner façade at a height of 1.5–2 m. Some of the short term measurements were made on the façade, but have been corrected by -3 dB assuming a diffuse field inside the courtyard.

The traffic situation around one of the courtyards can be seen in Figure 8, numbers close to streets indicate traffic flows in vehicles per 24 h. Streets with traffic flows less than 1,000 vehicles/24 h have been neglected if they are not adjacent to the courtyard.

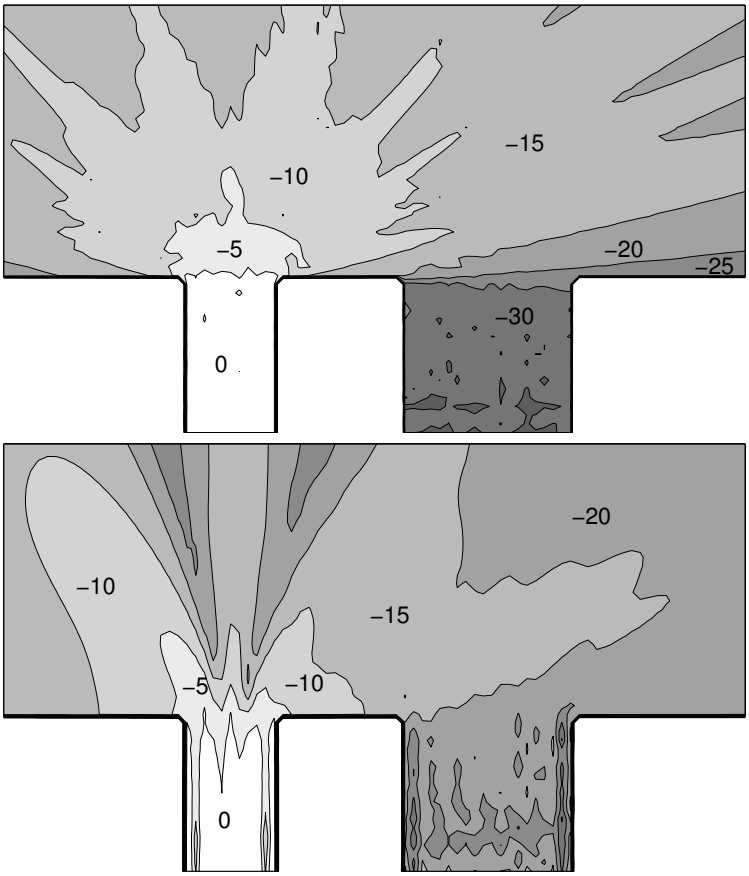

Figure 7: Contour plot of the sound pressure level normalised to 0 dB in the source canyon. The upper Figure is for the third octave band 63 Hz, the lower for 1 kHz.

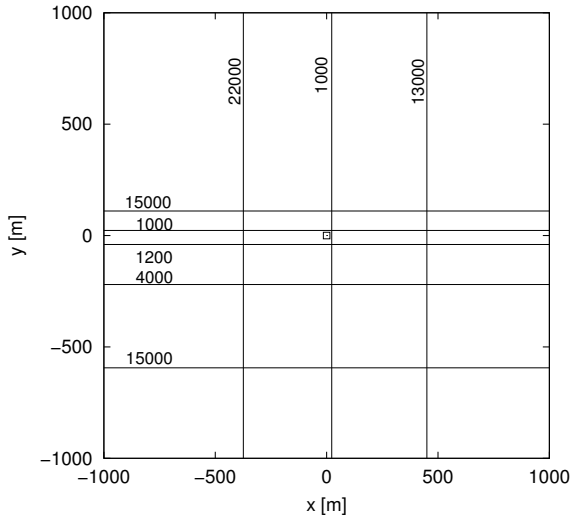

Figure 8: Traffic situation around the courtyard. The numbers indicate vehicle flow in vehicles per 24 h. Roads at longer distances with small traffic volumes have been neglected.

The two nearest streets are calculated using a width of 11 m (**A**), the rest uses 19 m (**B**). The Figure is slightly misleading in the sense that in the calculations the courtyard is seen as an infinite (2D) canyon, and all source canyons are treated individually as parallel to the receiver canyon. The total sound pressure in the receiving canyon is then calculated as the uncorrelated sum of the contributions from each source canyon.

In order to reduce the computational effort, the calculations are simplified for all but the two closest roads by assuming that they can be scaled with distance according to cylindrical propagation. In other words the level in a canyon twice as far from the source as another identical canyon will be 3 dB lower. This is true if the distance between the canyons is large compared to the widths of the source and receiver canyons.

The strength of each source has been calculated using [1] under the assumption that there is 2% heavy traffic on all streets. The spectrum shape is taken from the C_{tr} spectrum in [22], which corresponds to road traffic at 50 km/h. No source data is available below the third octave band 100 Hz, since C_{tr} does not specify a level at lower frequencies.

In Figure 9 the calculated and measured sound pressure levels at a position 3 m in front of the inner façade closest to the nearest street are displayed. The measurement microphone was at a height of 1.5 m above the ground. Each third octave band

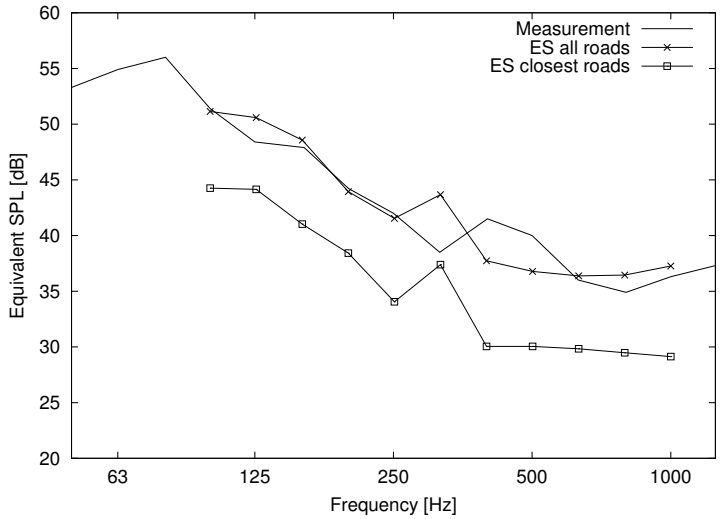

Figure 9: Comparison between two different calculations and one 30 minute measurement at Söder, Stockholm.

level is calculated using twenty frequencies within the band. The calculations using only the two closest streets underestimates the sound pressure level substantially. Including more sources, i.e. more roads, improves the result significantly. At low frequencies the level is dominated by the roads with high traffic volumes a bit further from the receiver, but for high frequencies the two closest streets are also important.

4 Discussion

4.1 Application to road traffic noise

The prediction of the equivalent level in Figure 9 is reasonably accurate using the proposed method and including more than just the closest sources. Sources more distant than those in figure 8 are, however, neglected, even though they may have even larger traffic flows. This might lead to an underestimation of the level. On the other hand the damping will be higher for real city canyons than what has been used here, which gives an overestimation.

The level predicted by the proposed method is rather constant in space in both the source and receiver canyons when averaged over a third octave band. The field can be seen as relatively diffuse at higher frequencies, since the damping is relatively low and the dimensions of the canyons large in comparison to the wavelength. Close to the canyon walls an increase of approximately 3 dB can be expected just as in a

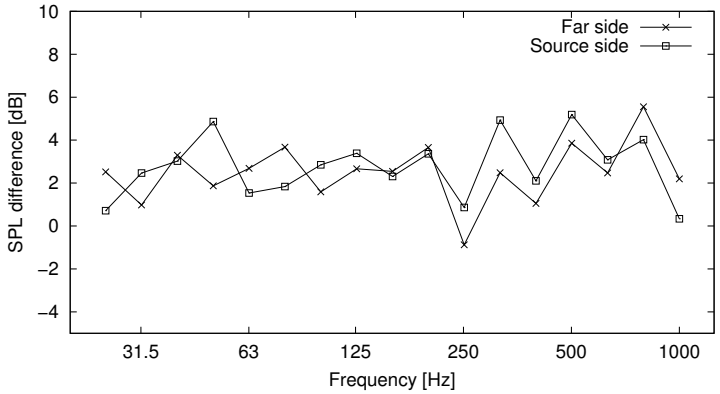

Figure 10: Calculated increase of sound pressure level close to canyon walls compared to the centre of the canyon in third octave bands. Receiver height 1.5 m inside canyon **E**.

reverberation chamber. Such an example is given in Figure 10, where the same geometry as in Figure 7 has been used. Note that it is difficult to calculate the reverberation time in the canyon since the damping is not evenly distributed. Most of it is concentrated to the opening of the canyon.

The wind speed gradient and the temperature gradient are very important for long range propagation, especially if the level is dominated by contributions from one direction. Then different wind directions can lead to both substantially higher and lower levels compared to the homogeneous case. This effect is probably less pronounced in inner city regions, because the influence of some sources will be enhanced and others reduced for all wind directions. The temperature gradient will still be very important though.

4.2 Calculation time

The method described here is rather computationally heavy, but the BEM and FDTD are even more so, since they have to discretize a large part of the canyon. A ray model including diffraction might be more efficient, but if the damping in the canyon is low, many image sources must be included. For low frequencies the accuracy will suffer, so perhaps a hybrid model with equivalent sources at low frequencies and rays at higher is a good approach.

The most time consuming process in the method is the building of the matrix A in equation (9). The number of elements along the boundary is proportional to one over the wavelength, so the number of elements in the matrix is proportional to the frequency squared. Since the number of terms in the modal summation also is proportional to the frequency squared, the total time used to build the elements of the matrix that depend on G_1 is proportional to f^4. For the G_2 part the evaluations of the integrals are not dependent on frequency, so the total time is proportional to f^2. So for high frequencies the modal summation will dominate. Consequently, the first part of the model to work on in order to reduce the calculation time should be the evaluation of the Green function G_1.

4.3 Further studies

Atmospheric turbulence can reduce the efficiency of a noise barrier by scattering sound into the shadow zone. This effect is most prominent at higher frequencies. The turbulence also reduces the interference pattern at the receiver by decorrelating different ray paths [23]. Both of these effects should be possible to introduce into the proposed method using a mutual coherence function for a random medium in a way similar to the approach used in [24].

Using more realistic values for the damping in courtyards and street canyons is important for the accuracy of the method. Measured reverberation times of typical cases would be useful if they could be translated into loss factors. These data could be used for an investigation of the improvement from introducing damping into existing backyards.

It is also very important to include the effect of diffusion for accurate predictions of the sound levels in backyards, as demonstrated in [4]. Diffusive elements can be included in the method presented here as patches with varying impedance, or as small niches in the side walls in the same manner as the balcony is modelled in [15]. This is not a random or statistical effect though, and it does increase the computational effort needed to solve the problem.

5 Acknowledgements

This paper is based on a study performed within the research programme “Soundscape Support to Health”, sponsored by the Swedish Foundation for Strategic Environmental Research (MISTRA), the Swedish Agency for Innovation Systems (Vinnova) and the Swedish National Road Administration (VV).

The help and support of Jens Forssén and Pontus Thorsson is gratefully acknowledged.

References

[1] H. Jonasson and H. Nielsen. Road traffic noise – nordic prediction method. TemaNord 1996:525, Nordic Council of Ministers, Copenhagen, Denmark, 1996.

[2] Tor Kihlman, Mikael Ögren, and Wolfgang Kropp. Prediction of urban traffic noise in shielded courtyards. In *Proceedings of Inter-Noise*, Dearborn, MI, USA., 2002.

[3] E. Salomons. Sound propagation in complex outdoor situations with a non-refracting atmosphere: Model based on analytical solutions for diffraction and reflection. *Acustica – Acta acustica*, 83:436–454, 1997.

[4] J. Kang. Numerical modelling of the sound fields in urban streets with diffusely reflecting boundaries. *Journal of Sound and Vibration*, 258(5):793–813, 2002.

[5] J. Picaut, L. Simon, and J. Polack. A mathematical model of diffuse sound field based on a diffusion equation. *Acustica – Acta acustica*, 83:614–621, 1997.

[6] H. Kuttruff. A mathematical model for noise propagation between buildings. *Journal of Sound and Vibration*, 85(1):115–128, 1982.

[7] R. Walerian and R. Janczur. Statistical description of noise propagation in a built up area. *Archives of Acoustics*, 19:201–225, 1994.

[8] Richard H. Lyon. Role of multiple reflections and reverberation in urban noise propagation. *J. Acoust. Soc. Am.*, 55(3):493–503, 1974.

[9] R. Bullen and F. Fricke. Sound propagation in a street. *Journal of Sound and Vibration*, 46(1):33–42, 1976.

[10] K. Heutschi. A simple method to evaluate the increase of traffic noise emission level due to buildings for a long straight street. *Applied Acoustics*, 44:259–274, 1995.

[11] K. V. Horoshenkov, D. C. Hothersall, and S. E. Mercy. Scale modelling of sound propagation in a city street canyon. *Journal of Sound and Vibration*, 223(5):795–819, 1999.

[12] K. Horoshenkov, S. Chandler-Wilde, and D. Hothersall. An efficient method for the prediction of sound propagation in a canyon. In *Proceedings of ICA*, Rome, 2001.

[13] Shinichi Sakamoto, Takuma Seimiya, and Hideki Tachibana. Visualization of sound reflection and diffraction using finite difference time domain method. *Acoustical Science and Technology*, 23(1):34–39, 2002.

[14] E. Walerian, R. Janczur, and M. Czechowicz. Practical description of diffraction at wedges. *Acustica – Acta acustica*, 88(1):65–76, 2002.

[15] J. Bérillon and W. Kropp. A theoretical model to consider the influence of absorbing surfaces inside the cavity of balconies. *Acustica – Acta acustica*, 86:485–494, 2000.

[16] A. Cummings. The effects of a resonator array on the sound field in a cavity. *Journal of Sound and Vibration*, 154(1):25–44, 1992.

[17] M. E. Johnson, S. J. Elliot, K-H. Baek, and J. Garcia-Bonito. An equivalent source technique for calculating the sound field inside an enclosure containing scattering objects. *J. Acoust. Soc. Am.*, 104(3):1221–1231, 1998.

[18] Martin Ochmann. The source simulation technique for acoustic radiation problems. *Acustica – Acta acustica*, 81(6):512–527, 1995.

[19] H. Kuttruff. *Room acoustics*. Applied science publishers Ltd., London, 2 edition, 1979.

[20] E. Skudrzyk. *The Foundations of Acoustics*. Springer – Verlag, New York - Wien, 1971.

[21] M. Abramowitz and I. A. Stegun. *Handbook of mathematical functions*. Dover Publications, New York, 1972.

[22] Acoustics – rating of sound insulation in buildings and of building elements – part 1: Airborne sound insulation. ISO 717-1:1996, The International Organization for Standardization, 1996.

[23] Jens Forssén and Mikael Ögren. Thick barrier noise-reduction in the presence of atmospheric turbulence: measurements and numerical modelling. *Applied Acoustics*, 63:173–187, 2002.

[24] Jens Forssén. Calculation of noise barrier performance in a three-dimensional turbulent atmosphere using the substitute-sources method. *Acustica – Acta acustica*, 88:181–189, 2002.

Paper III

Modelling of a city canyon problem in a turbulent atmosphere using an equivalent sources approach

Mikael Ögren and Jens Forssén

Abstract

The sound propagation into a courtyard shielded from direct exposure is predicted using an equivalent sources approach. The problem is simplified into that of a two-dimensional city canyon. A set of equivalent sources are used to couple the free half-space above the canyon to the cavity inside the canyon. Atmospheric turbulence causes an increase in the expected value of the sound pressure level compared to a homogeneous case. The level increase is estimated using a von Kármán turbulence model and the mutual coherences of all equivalent sources' contributions. For low frequencies the increase is negligible, but at 1.6 kHz it reaches 2–5 dB for the geometries and turbulence parameters used here. A comparison with a ray-based model shows reasonably good agreement.

1 Introduction

Courtyards are shielded from direct traffic noise exposure by the surrounding buildings, and thereby they represent relatively quiet areas in urban environments. On a directly exposed façade, i.e. toward a street, the noise level can be sufficiently well predicted by standard methods based on ray-tracing (e.g. the Nordic calculation methods [1, 2]). Shielded areas seem more difficult to model. The sound paths contain multiple reflections involving diffraction, and the influence of streets further away is increased. A model for this kind of problem using equivalent sources has recently been developed for a homogeneous atmosphere [3]. Here, a further development is described, which incorporates effects of a turbulent atmosphere. The basis is a substitute sources method using a mutual coherence function for turbulence [4].

The situation of a depressed road, or a road surrounded by tall buildings, can be seen as a two-dimensional (2-D) problem, where the traffic will act as a line source and the road together with the buildings' façades will form a "city canyon", the sending canyon. A shielded courtyard forms a second, receiving canyon.

The equivalent sources approach to the problem is field-based rather than ray-based, and thereby more easily captures the resonant behaviour of a city canyon. The original noise sources inside the sending canyon are exchanged for the equivalent sources at the top of the canyon. This can be seen as changing the position of a noise source from the canyon bottom to a typical roof height of the city, which also changes the strength and directivity of the source. The effect of turbulence is modelled on the equivalent sources on the canyon top, which is expected to be a more successful approach than using ray-based models including a scattering cross-section for turbulence. Such a scattering cross-section based method has been investigated previously and it was concluded that the turbulence influence increases at higher orders of the reflections inside the canyon [5]. This is because the higher order reflections correspond to ray directions that are more nearly horizontal, which makes the turbulence scattering stronger due to the smaller scattering angles. A precise calculation of the high order reflections together with turbulence scattering is difficult and the approach used here seems more promising.

2 Theory

2.1 A 2-D canyon solution using equivalent sources

In [6] the method of equivalent sources was used to calculate the insertion loss of balconies including absorbing surfaces. The main idea of the method is to reduce the problem to simplified geometries with boundary conditions which are easy to handle. On boundaries with different conditions, sources are placed. The strength of these sources are adjusted so that the boundary conditions are fulfilled everywhere. Applications of this can be found in [6, 7]. The method has been shown to be robust and computationally efficient and is therefore suitable for the problem considered here.

Consider the street canyon shown in Fig. 1. In order to apply the equivalent sources method, the geometry is divided into two parts, the domain inside the canyon and the half space above $y = l_y$. The intersection between the two domains is denoted C. In this way the problem is reduced to two subproblems, which can easily be handled; radiation into a half space by a Rayleigh integral, and a sound field in a rigid cavity by a modal approach. The coupling between the half space and the

cavity is obtained by the set of equivalent sources which correct the field impedance along the intersection. Although the mathematical derivation of the method has been described elsewhere [6], some details are repeated below for clarity.

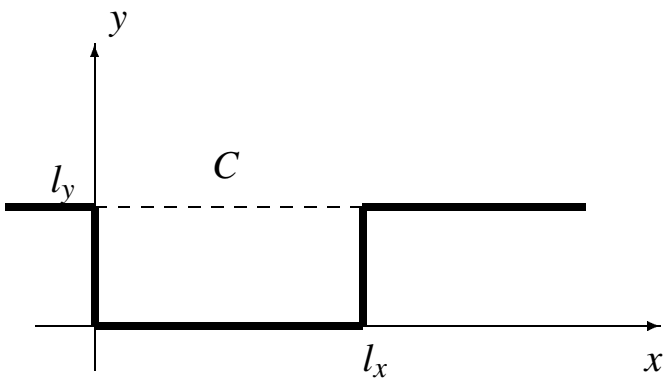

Figure 1: Sketch of a two-dimensional city canyon.

In the context of boundary element methods (BEM), one can view the modal approach as finding the Green function from a velocity point source inside the canyon to the pressure at a point on the intersection C. Concerning numerical performance, a BEM implementation with such specialised Green functions will be equally efficient as the model presented in this paper. The rigid cavity Green functions fulfil the boundary conditions for a canyon with open top together with the equivalent sources. (If instead there had been a zero impedance boundary condition at the top, another set of Green functions is needed. For further discussion see e.g. [6].)

In the following, harmonic time dependence described by $\exp(\mathrm{j}\omega t)$ is assumed. The wave equation for the complex pressure p in a two-dimensional domain, assuming a source of strength q, is

$$\nabla^2 p(x,y) + k^2 p(x,y) = -\mathrm{j}\omega\rho_0 q(x,y), \tag{1}$$

where the strength, q, is a volume velocity, or in the two-dimensional case what might be called a surface velocity, and where ρ_0 is the air density. In this text q denotes a distributed source, and Q a point source, both in 2-D. Taking into account the boundaries of the two domains, the Green functions can be found for instance in [8] and [9], and they are

$$G_1(x_s,y_s|x_r,y_r) = \mathrm{j}\omega\rho_0 \frac{c^2}{l_x l_y} \sum_n \sum_m \frac{\Psi_{n,m}(x_s,y_s)\Psi_{n,m}(x_r,y_r)}{\Lambda_{n,m}(\omega_{n,m}^2(1+\mathrm{j}\eta)-\omega^2)}, \tag{2}$$

and

$$G_2(x_s, y_s | x_r, y_r) = \mathrm{j}\omega\rho_0 \frac{-\mathrm{j}}{2} H_0^{(2)}(kr). \tag{3}$$

The Green function G_1 is a modal summation where the eigen frequencies $\omega_{n,m}$, modal shapes $\Psi_{n,m}$, and modal weights $\Lambda_{n,m}$ can be determined using

$$\omega_{n,m} = \pi c \sqrt{(n/l_x)^2 + (m/l_y)^2} \tag{4}$$

$$\Psi_{n,m}(x, y) = \cos(n\pi x/l_x) \cos(m\pi y/l_y) \tag{5}$$

$$\Lambda_{n,m} = \int_0^{l_y} \int_0^{l_x} \Psi_{n,m}^2 \, \mathrm{d}x \, \mathrm{d}y, \tag{6}$$

where c is the sound speed, η the loss factor, and l_x and l_y the dimensions of the canyon. The modal summation must be truncated somewhere, and here eigen frequencies up to three times as large as the frequency of interest were included in order to ensure convergence. This is a common truncation limit used in structural acoustics, and here it has been verified in a few test cases by increasing the number of modes and checking that the changes are small. Note that the damping expressed as η applies to the covered canyon only, the effect of power being transferred into the field above the canyon is described by the coupling of the two domains. The damping modelling assumes that the losses are evenly distributed within the canyon. For localised areas with high damping, such as absorbers, the damping can be modelled by equivalent sources placed in these areas, fulfilling the given impedance boundary condition, as in [6].

The Green function G_2 contains the Hankel function of the second kind, and describes a line source in front of a rigid surface. The distance between the source and the receiver is $r = \sqrt{(x_s - x_r)^2 + (y_s - y_r)^2}$, and k is the wave number. This Green function contains no losses, but if necessary the losses due to atmospheric absorption in the propagation from the canyon to an external receiver could be included in the computations.

The loss factor η is important for the noise level inside the canyon if the side walls of the canyon are high compared to the width. If the loss factor is determined assuming air absorption only, it will be too low. In reality the effect of finite impedances on the walls of the canyon will give higher losses. Here the loss factor is taken from reverberation time measurements at Chalmers University of Technology, in the reverberation chamber with volume 240 m^3. The results showed a power-law behaviour and a logarithmic least squares fit of the damping as a function of frequency gives

$$\eta(f) = 10^{-0.94} f^{-0.84}, \tag{7}$$

valid within the frequency range of interest here. In this way the damping is underestimated, and can be seen as a kind of minimum damping for a courtyard.

The coupling between the two domains is introduced by assuming an equivalent sources distribution on the boundary. Using a combination of the primary source of strength Q located inside the canyon at (x_s, y_s), and the boundary source distribution $q_l(x)$ below the boundary and $q_u(x)$ above it, the pressure can be calculated as

$$p_l(x_r, y_r) = QG_1(x_s, y_s|x_r, y_r) + \int_C q_l(x) G_1(x, l_y|x_r, y_r)\,\mathrm{d}x \tag{8}$$

inside the canyon and

$$p_u(x_r, y_r) = \int_C q_u(x) G_2(x, l_y|x_r, y_r)\,\mathrm{d}x \tag{9}$$

above the canyon. The source is assumed to be located inside the canyon for brevity.

At the intersection C between the two domains, the pressure and the velocity fields must be continuous. As a consequence p_l equals p_u and q_l equals $-q_u$ along C, and we can drop the subscripts l and u. The resulting equation system can be discretised by dividing the boundary C into a number of equally sized elements $C_1, C_2, \ldots, C_N$, and approximate the source strength along the boundary by a piecewise constant complex source strength $q_1, q_2, \ldots, q_N$ on each element. The pressure at the centre points of the elements, $x_1, x_2, \ldots, x_N$, must be equal, which gives the equation system

$$Aq = b, \tag{10}$$

where

$$A_{i,j} = \int_{C_j} G_1(x, l_y|x_i, l_y)\,\mathrm{d}x + \int_{C_j} G_2(x, l_y|x_i, l_y)\,\mathrm{d}x \tag{11}$$

and

$$b_i = QG_1(x_s, y_s|x_i, l_y). \tag{12}$$

The length of the elements is set to one tenth of the wavelength. The size of the equation system will be $N \times N$, and A is a symmetric matrix. Solving Eq. (10) one obtains the strengths of the boundary sources q, and can calculate the pressure anywhere inside or above the canyon using Eqs. (8) or (9), respectively.

The integrations of the free Green function G_2 in Eq. (11) can be evaluated numerically. Care has to be taken to avoid the singular part when $i = j$ (see e.g. [3]).

The Green function G_1 can be integrated analytically, and the case $i = j$ does not require any special consideration.

Assuming a piecewise constant complex source distribution over each element is a rather crude approach, which can be thought of as a zeroth order polynomial approximation. Using a linear or higher order polynomial on each element might give better numerical properties, i.e. a faster and more accurate method, but this is not yet studied further.

2.2 Modelling of turbulence effects

In the general case with contributions from two sources to one receiver, the two paths can have a transversal separation as well as different lengths. Here, all the paths follow a single line, along the intersection C, and only the lengths vary. The mutual coherences for such cases can be estimated using the extinction coefficient, γ, for a turbulent atmosphere.

Here, we assume that the turbulence is homogeneous and isotropic, i.e. has statistical properties independent of translation and rotation. This is a crude approximation; in reality we expect the canyons to affect the turbulence, in addition to the variations with height one gets over any surface. Such refinements should however be possible to include in the model. Yet another approximation is used, which is that there is no turbulence inside the canyon. It might be possible to extended the model to incorporate turbulence inside the canyon. As a result we would expect a larger effect of turbulence.

The ensemble average of the pressure amplitude, $\langle p \rangle$, decays exponentially as the wave propagates through a turbulent medium. This can be formulated as

$$\langle p \rangle = \hat{p} \mathrm{e}^{-\gamma x}, \tag{13}$$

where $\hat{p}$ is the amplitude in absence of turbulence and x is the distance of propagation [10]. The average pressure, $\langle p \rangle$, is also called the coherent field.

If the path from one source to the receiver is extended a distance Δ compared to the path from the other source, the mutual coherence factor of the two contributions is estimated as $\mathrm{e}^{-\gamma\Delta}$, as explained next. The definition used here of the mutual coherence factor for two contributions is

$$\Gamma_{12} = \frac{\langle p_1 p_2^* \rangle + \langle p_1^* p_2 \rangle}{\hat{p}_1 \hat{p}_2^* + \hat{p}_1^* \hat{p}_2}, \tag{14}$$

where the complex conjugate is denoted by an asterisk (*), p_1 and p_2 are the fluctuating pressure amplitudes in the turbulent atmosphere and $\hat{p}_1$ and $\hat{p}_2$ are the amplitudes for the same situation except that there is no turbulence (e.g. [11]). The

propagation for p_1 and p_2 follow the same paths all the way except along the extension with length Δ. Only the propagation along the extension causes decorrelation (i.e. reduced coherence) since the rest of the propagation goes through the same medium for both paths. Using Eq. (13) this results in $\langle p_1 p_2^* \rangle = \hat{p}_1 \hat{p}_2^* \mathrm{e}^{-\gamma\Delta}$ and $\langle p_1^* p_2 \rangle = \hat{p}_1^* \hat{p}_2 \mathrm{e}^{-\gamma\Delta}$, which gives $\Gamma_{12} = \mathrm{e}^{-\gamma\Delta}$. This estimate of the mutual coherence is equivalent to assuming turbulence only along the intersection above the canyon, and not further away. In a more accurate solution of the received pressure on the same line as the two sources, not only the propagation along the extension between the sources should affect the decorrelation if turbulence is present all the way to the receiver. In terms of Fresnel zones, the field from the source further away from the receiver will cover a larger volume of the atmosphere and thereby be more affected by turbulence. Hence, the model used here is assumed to underestimate the effect of turbulence.

Each equivalent source of the sending canyon gives a contribution $p_i, i = 1, \ldots, N$, to the received pressure. The total contribution including all mutual coherences can be written (e.g. [12])

$$\langle |p_{\mathrm{tot}}|^2 \rangle = \sum_i \sum_j \langle p_i p_j^* \rangle = \sum_i \sum_j \hat{p}_i \hat{p}_j^* \Gamma_{ij}, \tag{15}$$

where $\Gamma_{ij} = \mathrm{e}^{-\gamma\Delta_{ij}}$, with Δ_{ij} the distance between the equivalent sources i and j. Eq. (15) gives the expected value of the square of the pressure amplitude in the turbulent medium, and is used to estimate the equivalent level.

In a situation with two canyons (see Fig. 2), a sending and a receiving one, it can be shown that the decorrelation due to turbulence can be treated separately for the two canyons. For this, however, a far field condition needs to be fulfilled, i.e. that the widths of the canyons are small in comparison to the distance in between them.

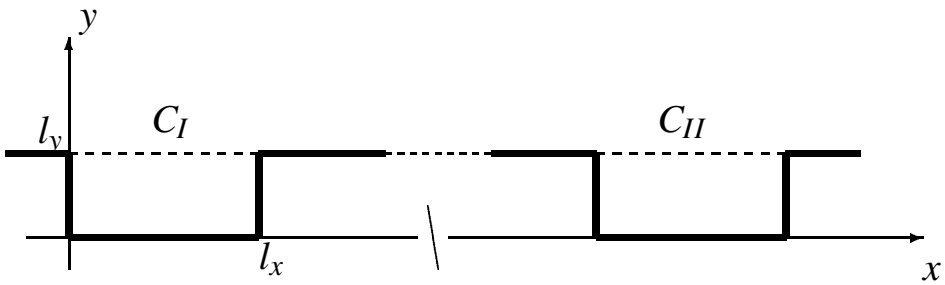

Figure 2: Sketch of two city canyons.

This results in an excitation from the sending canyon at the boundary, C_{II}, of the

receiving canyon. The excitation has constant amplitude, Q_1, and phase variation $\exp(-\mathrm{j}kx)$ along C_{II}. The amplitude is found from $Q_1^2 = \sum_i \sum_j q_i q_j^* \Gamma_{ij}$, where q_i and q_j are the contributions via the equivalent sources i and j on C_I, with coherence Γ_{ij}. The contributions via the different equivalent sources at C_{II} give rise to a similar double sum and the total result can be written

$$\langle |p_{\mathrm{tot}}|^2 \rangle = Q_1^2 \sum_i \sum_j g_i g_j^* \Gamma_{ij}, \tag{16}$$

where g_i and g_i are the Green functions, in absence of turbulence, from Q_1 to the received pressure inside the canyon via the equivalent sources i and j at C_{II}, with coherence Γ_{ij}. It could be noted that the Green functions in Eq. (16) are numerically found from the reciprocal problem, where the source position (i.e. where Q_1 was taken) and the receiver position are interchanged.

For the calculated results shown here, the von Kármán turbulence model is used, for which the extinction coefficient can be written [10]

$$\gamma = \gamma_T + \gamma_v = \frac{3}{10}\pi^2 A k^2 K_0^{-5/3} \left(\frac{C_T^2}{T_0^2} + \frac{4C_v^2}{c^2} \right). \tag{17}$$

In the above equation γ_T and γ_v are the extinction coefficients due to temperature and velocity fluctuations, respectively; $A \approx 0.0330$; $K_0 = 2\pi/L_0$, where L_0 approximates the outer scale of turbulence; C_T^2 and C_v^2 are the structure parameters describing the strengths of temperature and velocity fluctuations, respectively; T_0 is the mean temperature; and c is the mean sound speed.

3 Results

In the calculations, the canyons modelled are 18 m high and 19 or 11 m wide. All surfaces are acoustically hard. The source is on the bottom of the canyon, at position $x_s = 9$ or 5 m, for the 19 and 11 m wide canyon, respectively. (These data are summarised in Table 1.) For the single-canyon problems, the receiver is placed at $x = 500$ m, on the hard surface. The results apply equally well to the reciprocal problem, with the receiver in the canyon and the source 500 m away. For the double-canyon problems, the receiving canyon starts at $x = 500$ m. All results are plotted relative to free field.

The double-canyon problem models a sending canyon (road) and a receiving canyon (closed courtyard). The calculations are then divided into two steps. First the sending canyon is treated as if the receiving canyon is not present. Then the

Canyon	Width l_x m	Height l_y m	Source/receiver pos.
A	19	18	(9,0)
B	11	18	(5,0)

Table 1: Canyon geometries used for the calculations. The source/receiver positions are slightly off center in order to get contribution from modes with both odd and even orders in the x direction.

strengths of the equivalent sources calculated in the first step are seen as sources on a rigid plane for the receiving canyon, and the pressure at the receiving point is calculated. This approach is valid as long as the waves that are reflected at the receiving canyon back to the source canyon, and then back again to the receiving canyon, can be neglected.

For the turbulence modelling we have used velocity fluctuations with $C_v^2 = 10\ \mathrm{m}^{4/3}\mathrm{s}^{-2}$ and $L_0 = 10$ m. The value of C_v^2 is taken from measurements and chosen to model a strong turbulence condition [13]. The size of the largest scales of influence, L_0, can in general be much larger [14] but here propagation fairly close to ground is modelled and a smaller value is chosen, which results in a smaller value of the extinction coefficient and in a weaker turbulence influence. For these values of the turbulence parameters, examples of the mutual coherence factor, Γ, (see Eqs. 13 and 17) are plotted in Fig. 3 for different sound frequencies. The value of Γ is 1 at separation $x = 0$ and decays for larger absolute values of x.

The main results presented here are third octave band levels, each calculated using 20 frequencies, starting at 100 Hz and ending at 1.6 kHz. However, in Section 3.1 below the results are calculated for a higher resolution in frequency, near 500 Hz.

3.1 Comparison with a ray-based model

In Fig. 4 two different methods for estimating the influence of turbulence for a single 19 m wide canyon is presented. The upper figure is calculated using the equivalent sources method as described in section 2.1, and the lower is calculated using a ray-based model, where the diffraction and reflection modelling is described in [15]. The diffraction theory is combined with the concept of Fresnel zones to reduce the strength of reflections from the finite, vertical surfaces. Here, a parameter value of $1/8$ of a wavelength is used for the Fresnel zone approach, as recommended in the new Nordic sound propagation method for finite reflecting surfaces [2]. A maximum of 32 reflections are taken into account, and numerical tests showed small increase when including more reflections.

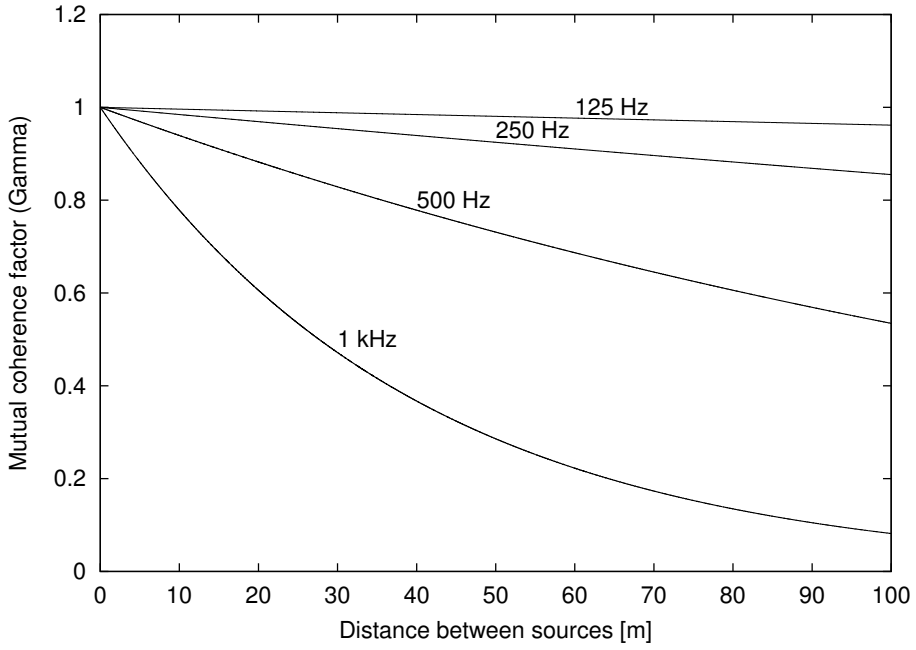

Figure 3: Calculation of the mutual coherence factor $\Gamma = \mathrm{e}^{-\gamma x}$ versus distance, x, for different frequencies.

The turbulence effect is estimated using the simplified scheme described in [13], which is based on a scattering cross-section for a turbulent atmosphere. Here the turbulence parameters together with geometry parameters such as the distance to and the height of the screening object is used to determine the scattered level. This level is then added incoherently to the diffracted level to produce the expected value of the total level behind the screen. This combination of reflections, diffractions and turbulence scattering has previously been used to estimate the influence of multiple reflections and distant sources in city environments [5].

For the equivalent sources approach (upper plot in Fig. 4), the turbulence can be seen to have two effects, working in opposite directions. First, the decorrelation weakens the positive interference slightly, as can be seen at the largest resonance peaks, which leads to a decreased level. Second, the strongest shadowing, in between the resonance peaks, is limited, which leads to an increased level. This can be seen as a weakened destructive interference of the equivalent sources' contributions.

For the ray-based model only the second effect is visible; since the scattered level is added incoherently, it can only lead to increased levels. The total effect for both approaches, averaged over several resonances, is however an increase due to the turbulence. In the case presented here the increase averaged over the third

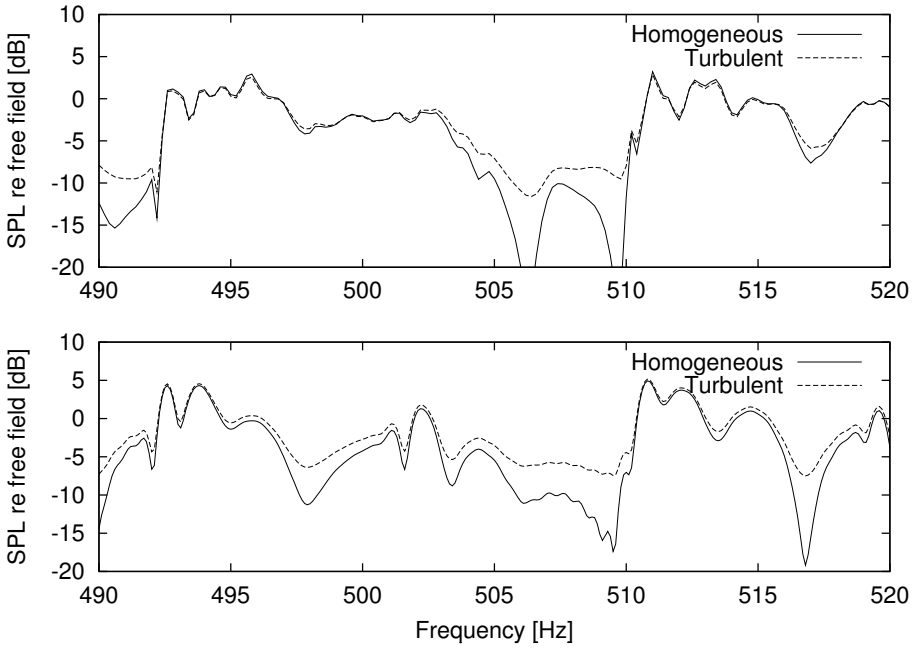

Figure 4: Frequency response relative free field for a canyon of width 19 m and height 18 m (A). The receiver is outside the canyon at (500,18). The upper figure is calculated using the equivalent sources method, and the lower using the ray-based model.

octave bands 1, 1.25 and 1.6 kHz is 1.6 dB for the equivalent sources method and 4.9 dB for the ray-based model.

In narrow bands the results from the two methods show the same trends at peaks and dips, but are far from perfectly matched. It should be stressed that the ray-based model has significant weaknesses. For instance, the Fresnel zone approach can be implemented with different parameters, and the diffraction theory has limitations at low frequencies and high diffraction orders. On the other hand, the equivalent sources method without the turbulence modelling has been validated against BEM, with good agreement [3], and is concluded to be more accurate than the ray-based model.

3.2 Results for single and double canyons

In Figs. 5 and 6 third octave band results are shown for the 19 and 11 m wide canyon, respectively (canyons A and B in Table 1). It can be seen that the increase in sound level due to turbulence is larger for the wider canyon (Fig. 5), where the strongest decorrelation takes place.

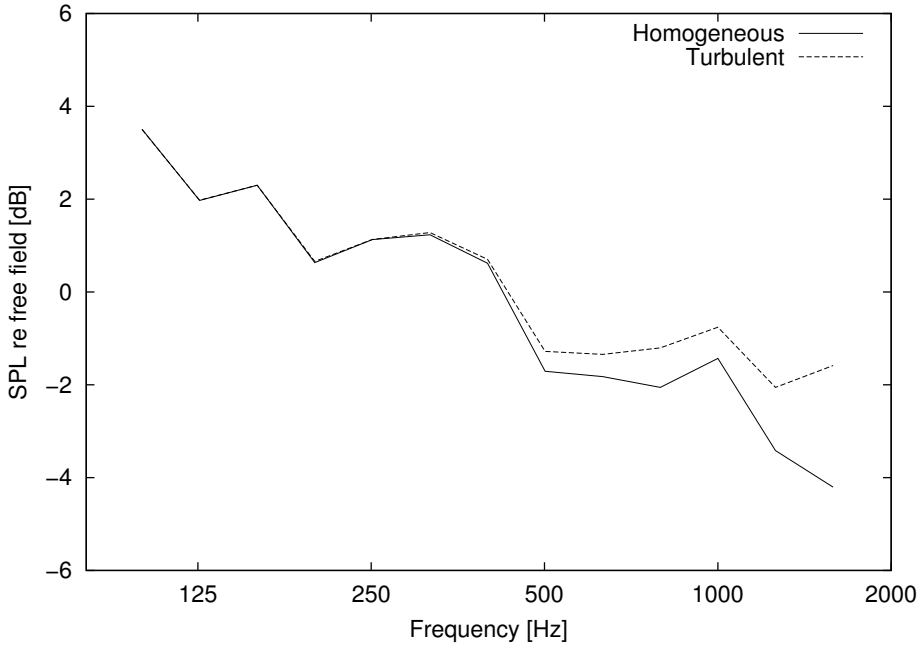

Figure 5: Frequency response in third octave bands relative free field for a canyon of width 19 m and height 18 m (A). The source is located at (9,0) and the receiver at (500,18).

Figs. 7–9 are for double-canyon problems. The receiver is at the bottom of a 19 or 11 m wide canyon, at a distance of 9 or 5 m from the wall closest to the sending canyon, respectively. Fig. 7 is for a sending canyon of 19 m width and a receiving canyon of 19 or 11 m width. The turbulence decorrelation is only modelled for the sending canyon and the calculations at each frequency should give the same increase due to turbulence since the width of the canyon with turbulence is the same. The effect on the third octave band levels in the receiving canyon is however not the same; the receiving canyon can be seen as filtering the input from the sending canyon before the third octave band levels are calculated. For two canyons of equal width, the turbulence caused level increase in between the resonance peaks of the sending canyon gets a reduced influence when the receiving canyon has the same resonance behaviour. We can see in Fig. 7 that the 11 m wide receiver canyon (B) gives a larger influence of turbulence.

Fig. 8 shows the results for two situations with turbulence at the sending canyon. The first situation has a 19 m wide sending canyon and an 11 m wide receiving canyon (A to B), whereas the second situation has the widths interchanged (B to A). The influence of the turbulence on the field from the sending canyon is filtered by

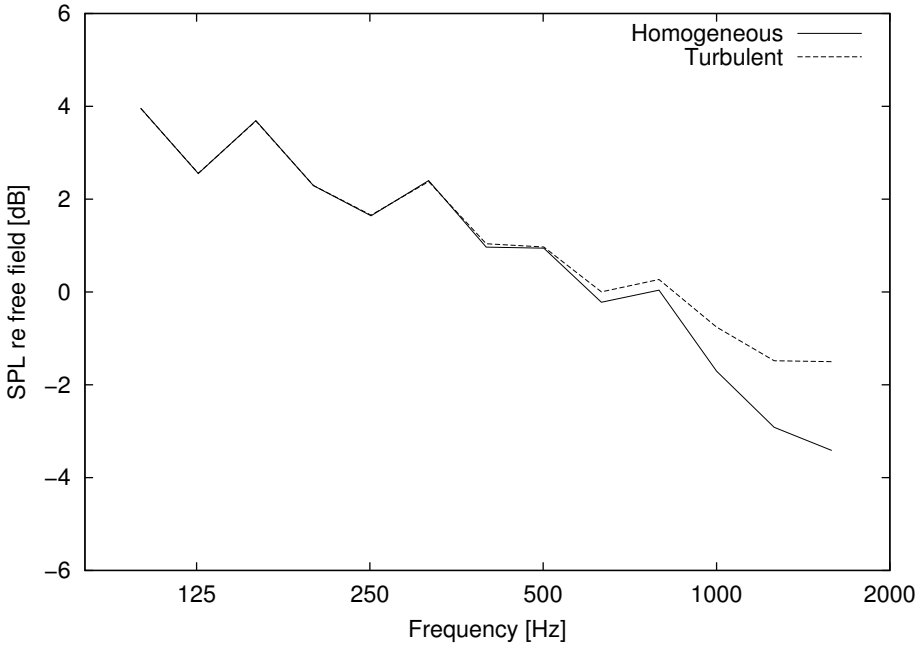

Figure 6: Frequency response in third octave bands relative free field for a canyon of width 11 m and height 18 m (B). The source is located at (5,0) and the receiver at (500,18).

the receiving canyon. Thereby the trend in the results that a wider canyon should be more sensitive to turbulence is less distinguished.

The results from modelling turbulence in both canyons (A and B) are shown in Fig. 9. The separate treatment of the turbulence effects here means that the increase would equal the sum of the increases in the two cases shown in Fig. 8 if single-frequency results were shown. The third octave band averaging can change this slightly, but we expect to get larger influence of turbulence when it is modelled in both canyons than in only one canyon. Here, the effect is more than 5 dB at 1.6 kHz.

4 Conclusions

The increase in the sound pressure level due to turbulence can be predicted for city canyons. The model is based on the mutual coherence factor for sources or receivers separated in space in a turbulent atmosphere, and assumes a homogeneous and isotropic turbulence described by the von Kármán model.

The equivalent sources approach to the problem is expected to more easily cap-

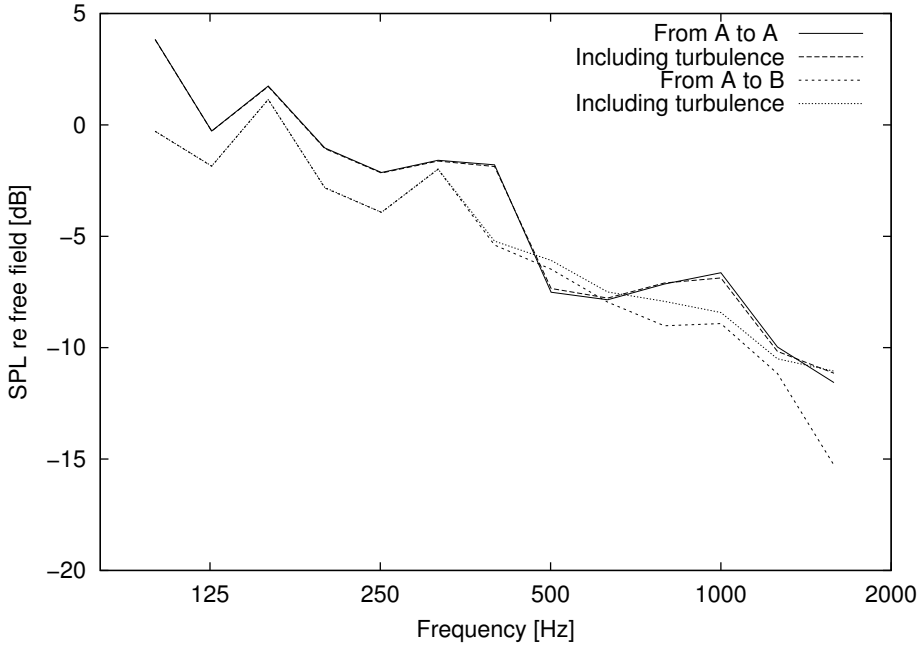

Figure 7: Frequency response in third octave bands relative free field for a double-canyon situation. The effect of turbulence is included for the source canyon only, which is 19 m wide (B).

ture the resonant behaviour of a city canyon than a ray-based model. The original noise sources inside the canyon can be seen as being lifted up to the roof level of the city when replaced by the equivalent sources. The effect of turbulence is modelled on the equivalent sources using a mutual coherence factor, which is thought to be a more successful method than a ray-based one using a scattering cross-section instead.

The level increase due to turbulence is negligible at low frequencies but starts to become important around 500 Hz with the geometries and parameters used here. At the third octave band 1.6 kHz the increase reaches 2–5 dB. Using a traffic noise spectrum (C_{tr} in [16]) to estimate the effect in the A-weighted level gives slightly less than 1 dB increase compared to the homogeneous case. These calculated values do however depend on the geometry and turbulence parameters. For larger geometries and stronger turbulence the effect of turbulence is expected to increase.

For future improvements of predictions in canyon-to-canyon cases it is important to include refraction, at least for canyons that are far from each other. More realistic damping data are also needed, either from measurements on real courtyards or indirectly from measurements on typical façade materials. It is also difficult to

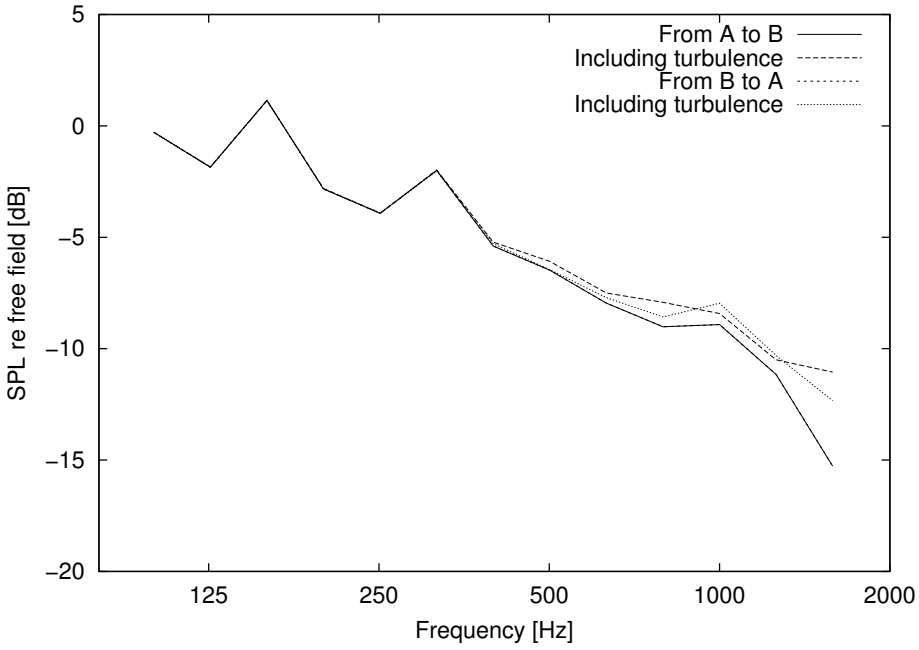

Figure 8: Frequency response in third octave bands relative free field for a double-canyon situation. The effect of turbulence is included for the source canyon only, which is 19 m or 11 m wide (A or B). (Without turbulence the results are identical for A to B and B to A.)

know what values to use for the turbulence parameters. Hopefully more input from research in the field of urban micro climate can help.

5 Acknowledgements

This paper is based on a study performed within the research programme ”Soundscape Support to Health”, sponsored by the Swedish Foundation for Strategic Environmental Research (MISTRA), the Swedish Agency for Innovation Systems (Vinnova) and the Swedish National Road Administration (VV). The work behind this paper has also been funded by Formas (the Swedish Research Council for Environment, Agricultural Sciences and Spatial Planning).

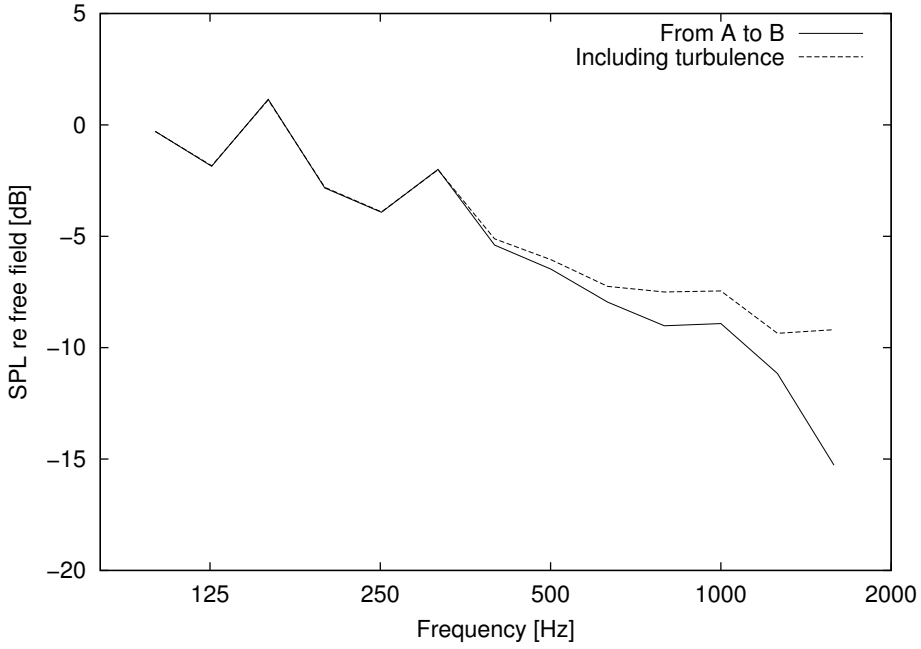

Figure 9: Frequency response in third octave bands relative free field for a double-canyon situation. The effect of turbulence is included for both canyons (A and B).

References

[1] Jonasson H, Nielsen H. Road traffic noise – nordic prediction method. TemaNord 1996:525, Copenhagen, Nordic Council of Ministers, 1996.

[2] Plovsing B, Kragh J. Nord2000. Comprehensive Outdoor Sound Propagation Model. Part 1: Propagation in an Atmosphere without Significant Refraction. Delta report AV 1849/00, Lyngy, Denmark, 2000.

[3] Ögren M, Kropp W. Road traffic noise propagation between two-dimensional city canyons using an equivalent sources approach. Submitted to *Acustica – Acta acustica*, March 2003.

[4] Forssén J. Calculation of noise barrier performance in a turbulent atmosphere by using substitute sources above the barrier. *Acustica – Acta acustica* 2000;86:269-75.

[5] Ögren M, Forssén J. Prediction of noise levels in shielded urban areas. *Proc. Internoise 2001*, The Hague 2001.

[6] Bérillon J, Kropp W. A theoretical model to consider the influence of absorbing surfaces inside the cavity of balconies. *Acustica – Acta acustica* 2000;86:485-494.

[7] Cummings A. The effects of a resonator array on the sound field in a cavity. *Journal of Sound and Vibration* 1992;154(1):25-44.

[8] Kuttruff H. Room acoustics. 2 ed. London, Applied science publishers Ltd., 1979.

[9] Skudrzyk E. The foundations of acoustics. New York - Wien, Springer – Verlag, 1971.

[10] Ostashev VE. Acoustics in moving inhomogeneous media. London, E & FN Spon (an imprint of Thomson Professional), 1997.

[11] Salomons, EM. The fluctuating field of a monopole source in a turbulent atmosphere above a ground surface. Time-averaged sound pressure level and statistical distributions. *Proc. 8th Int. Symp. on Long-Range Sound Propagation*, The Pennsylvania State University 1998:326-351.

[12] L'Espérence A, Herzog P, Daigle GA, and Nicolas, JR. Heuristic model for outdoor sound propagation based on an extension of the geometrical ray theory in the case of a linear sound speed profile. *Applied Acoustics* 1992;37:111-139.

[13] Forssén J, Ögren M. Barrier noise-reduction in the presence of atmospheric turbulence: Measurements and numerical modelling. *Applied Acoustics* 2001;63:173-187.

[14] Wilson KD. A turbulence spectral model for sound propagation in the atmosphere that incorporates shear and buoyancy forcings. *Journal of the Acoustical Society of America* 2000;108:2021-38.

[15] Salomons E. Sound propagation in complex outdoor situations with a non-refracting atmosphere: Model based on analytical solutions for diffraction and reflection. *Acustica – Acta acustica* 1997;83:436-454.

[16] Acoustics – rating of sound insulation in buildings and of building elements – part 1: Airborne sound insulation. ISO 717-1:1996, The International Organization for Standardization, 1996.

Paper IV

Including absorption and diffusion effects in city street canyon calculations using the equivalent sources method

Mikael Ögren and Wolfgang Kropp

Abstract

When predicting urban traffic noise levels at shielded positions, like courtyards, many of the standard methods fail. This is mainly due to the absence of multiple reflections in the modelling, and of the practice to only include the closest road as a source. This work aims at developing a numerical model for urban sound propagation for shielded positions that includes multiple reflections, absorption and diffusion. An equivalent sources approach is used, where the absorption inside the canyon is taken into account. Diffusion effects are included by adding small niches as disturbances. The results show that introducing diffusion and absorption will decrease the sound pressure level in a city street canyon.

1 Introduction

Courtyards are shielded from direct traffic noise exposure by the surrounding buildings, and thereby they represent relatively quiet areas in urban environments. On a directly exposed façade, i.e. toward a street, the noise level can be sufficiently well predicted by standard methods based on ray-tracing (e.g. the Nordic calculation method [1]). Shielded areas seem more difficult to model. The sound paths contain multiple reflections involving diffraction, and the influence of streets further away is increased.

The situation of a depressed road, or a road surrounded by tall buildings, can be seen as a two dimensional (2D) problem, where the traffic will act as a line source and the road together with the buildings' façades will form a "city canyon", the

source canyon. A shielded courtyard forms a second, receiving canyon. A model for this kind of problem using equivalent sources has recently been developed, both for a homogeneous atmosphere [2, 3] and including turbulence effects [4].

The equivalent sources approach to the problem is field-based rather than ray-based, and thereby more easily captures the resonant behavior of a city canyon. The original noise sources inside the sending canyon are exchanged for the equivalent sources at the top of the canyon. This can be seen as changing the position of a noise source from the canyon bottom to a typical roof height of the city, which also changes the strength and directivity of the source.

The reflections between the façades of houses surrounding a street have been studied previously using both ray methods [5, 6], analytical methods [7, 8], numerical methods [9] and scale model measurements [10]. The focus in these papers is on the propagation inside the street canyon itself, or along the length of the street and into side streets. The effect of diffusion due to uneven side walls of the canyon has also been investigated for such situations [11, 12, 13], and it has been concluded that the effect of diffuse reflections can be very strong in many realistic situations.

In this paper a way to include absorption and diffuse reflections into the equivalent sources solution for two dimensional city canyons is proposed. In many calculation models the diffuse reflections are included by transferring energy from the coherent field to a diffuse field using some kind of diffuse reflection coefficient. Here the diffusion is introduced by directly modelling the irregularities instead. This approach has the advantage that no special theory for the propagation of the diffuse part of the sound energy is needed. The diffusion is modeled by the irregular boundary, which means that there is no statistical assumption about the typical size of the irregularities or their distribution. The disadvantage of this approach is that it is valid only for the particular case solved, and that it is relatively computationally heavy.

The first part of the paper briefly introduces the background of the method and how diffusion and absorptions can be included. Then one comparison is given to published scale model results. Finally an example with both diffusion and absorption is given.

2 Theory

2.1 Solving a 2D canyon problem using the equivalent sources method

Consider the two dimensional city canyon shown in Fig. 1. In order to apply the equivalent sources method, the geometry is divided into two parts, the domain inside the canyon and the half-space above $y = l_y$. The intersection between the two

domains is denoted C. In this way the problem is reduced to two subproblems, which can easily be handled; radiation into a half-space by a Rayleigh integral, and a sound field in a rigid cavity by a modal approach. The coupling between the half-space and the cavity is obtained by the set of equivalent sources which correct the field impedance along the intersection. The mathematical derivation of the method has been described elsewhere [14, 3, 2], some details are repeated here for clarity.

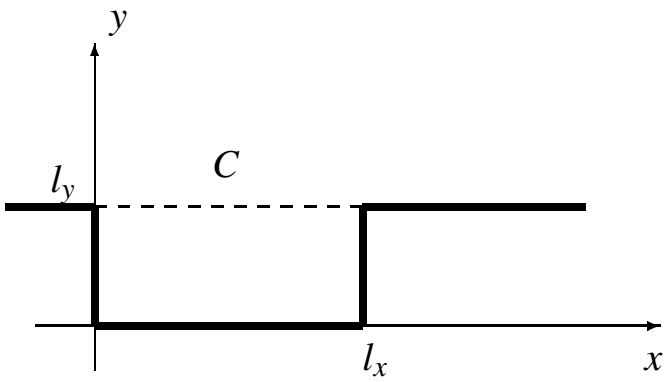

Figure 1: Sketch of the 2D city canyon.

In the following, harmonic time dependence described by $\exp(\mathrm{j}\omega t)$ is assumed, q denotes a distributed source and Q a point source, both in 2D. The Green functions for the two domains can be found for instance in [15] and [16], and they are

$$G_1(x_s, y_s | x_r, y_r) = \frac{c^2}{l_x l_y} \sum_n \sum_m \frac{\Psi_{n,m}(x_s, y_s)\Psi_{n,m}(x_r, y_r)}{\Lambda_{n,m}(\omega_{n,m}^2(1+\mathrm{j}\eta) - \omega^2)}, \tag{1}$$

and

$$G_2(x_s, y_s | x_r, y_r) = \frac{-\mathrm{j}}{2} H_0^{(2)}(kr). \tag{2}$$

The Green function G_1 for the cavity is a modal summation where the eigen frequencies $\omega_{n,m}$, modal shapes $\Psi_{n,m}$, and modal weights $\Lambda_{n,m}$ can be determined using the sound speed c, the loss factor η, and the dimensions of the canyon l_x and l_y. The formulas are omitted here, but can be found in [2].

The modal summation must be truncated somewhere, and here eigen frequencies up to three times as large as the frequency of interest were included in order to ensure convergence. Note that the damping expressed as η applies to the covered canyon only, the effect of power being transferred into the field above the canyon is described by the coupling of the two domains. To avoid problems with singular

values, the damping is set to a small value even if it is assumed to be zero, here $\eta = 10^{-9}$ was used.

The Green function G_2 for the half-space contains the Hankel function of the second kind, and describes a line source in front of a rigid surface. The distance between the source and the receiver is $r = \sqrt{(x_s - x_r)^2 + (y_s - y_r)^2}$, and k is the wave number. This Green function contains no losses, but if necessary the losses due to atmospheric absorption in the propagation from the canyon to an external receiver could be included in the computations.

The coupling between the two domains is introduced by assuming an equivalent sources distribution on the boundary. Using a combination of the primary source of strength Q located inside the canyon at (x_s, y_s), and the boundary source distribution $q_l(x)$ below the boundary and $q_u(x)$ above it, the pressure can be calculated as

$$p_l(x_r, y_r) = QG_1(x_s, y_s|x_r, y_r) + \int_C q_l(x) G_1(x, l_y|x_r, y_r)\,\mathrm{d}x \tag{3}$$

inside the canyon and

$$p_u(x_r, y_r) = \int_C q_u(x) G_2(x, l_y|x_r, y_r)\,\mathrm{d}x \tag{4}$$

above the canyon. The source is assumed to be located inside the canyon for brevity.

At the intersection C between the two domains, the pressure and the velocity fields must be continuous. As a consequence p_l equals p_u and q_l equals $-q_u$ along C, and we can drop the subscripts l and u. The resulting equation system comes from discretizing the boundary C with a piecewise constant complex source strength $[q_1, q_2, \ldots, q_N] = \mathbf{q}^{\mathbf{T}}$ on each element. This gives an equation system $\mathbf{Aq} = \mathbf{b}$. The length of the elements is set to one tenth of the wavelength. The size of the equation system will be $N \times N$, and $\mathbf{A}$ is a symmetric matrix. Solving the equation system one obtains the strengths of the boundary sources $\mathbf{q}$, and can calculate the pressure anywhere inside or above the canyon using Eqs. (3) or (4), respectively.

2.2 Modelling the effect of absorption

The loss factor η can be used to model absorption in the canyon. Note that it does not describe the effect of sound power being transmitted out of (or into) the canyon, this is modeled by the equivalent source strength q. Using the loss factor it is assumed that the absorption is evenly distributed throughout the whole volume of the canyon. In a real case the absorption is of course concentrated on the canyon floor or the side walls. A better model of the absorption in the canyon is to include an impedance boundary condition when solving the problem, as is done for road surfaces in tyre

noise propagation in [17]. This approach assumes that the surface is locally reacting and that it can be described by an impedance. The impedance does not have to be constant, it is allowed to vary along the boundaries.

The boundary condition is included into the solution by placing an equivalent source distribution over the impedance patches, and adjusting the strength of the sources to fulfill the boundary condition

$$p = qZ, \tag{5}$$

where q denotes the source strength and Z the specific acoustic impedance. In fact the the equivalent sources at the canyon opening can be seen to function in an analogous way, adjusting the boundary condition to match the radiation impedance into the domain above the canyon. The source strength is assumed constant over discrete elements and the boundary condition is enforced at the center point of each element.

The equations that describes the boundary condition can be included into the equation system, and the source strengths are obtained when the system is solved. The pressure inside the canyon is then the sum of the contributions from the canyon opening, from the impedance patches and finally from the primary source if it is located inside the canyon.

2.3 Modelling the effect of diffuse reflections

Irregularities can be included when solving a canyon problem with the equivalent sources method by coupling secondary small canyons to the main one. The coupling is achieved with an equivalent source distribution just as for the primary canyon opening. The equations of continuity at the formed boundary can then be solved together with the equations of the main opening, which gives the strengths of all the equivalent sources. By summing up the contributions from all relevant primary and equivalent sources, the pressure can then be determined in positions both inside and outside the canyon.

Trying to give a general formula that describes how the equation system looks when including secondary canyons and absorbing patches gives a long and involved expression. Therefore an example is given here instead. The frequency is assumed to be very low, in order to have few elements. In Fig. 2 one absorbing patch is located on the left sidewall, and one secondary canyon is attached to the right sidewall. The opening, the absorbing patch and the secondary canyon are all discretized using two elements, which gives six elements in total. The matrix equation formed by the six unknown source strengths becomes

$$\mathbf{Aq} = \mathbf{b}. \tag{6}$$

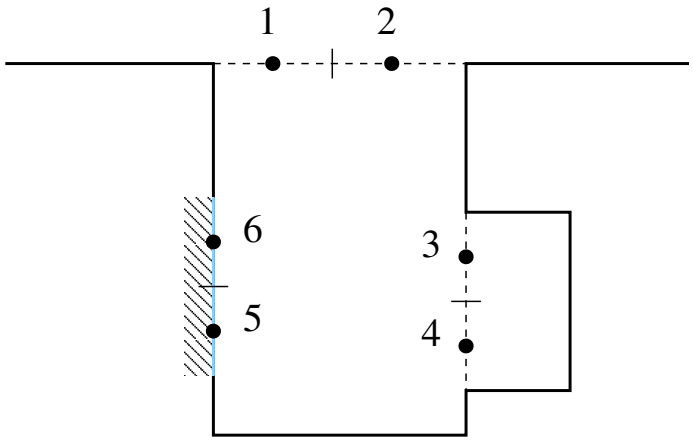

Figure 2: Example of a canyon with one patch with absorption and one irregularity. The opening, the absorbing patch and the secondary canyon boundary are discretized with two elements each.

The matrix **A** is structured as

$$\mathbf{A} = \begin{bmatrix} g_1+g_2 & g_1+g_2 & g_1 & g_1 & g_1 & g_1 \\ g_1+g_2 & g_1+g_2 & g_1 & g_1 & g_1 & g_1 \\ g_1 & g_1 & g_1+g_3 & g_1+g_3 & g_1 & g_1 \\ g_1 & g_1 & g_1+g_3 & g_1+g_3 & g_1 & g_1 \\ g_1 & g_1 & g_1 & g_1 & g_1-Z & g_1 \\ g_1 & g_1 & g_1 & g_1 & g_1 & g_1-Z \end{bmatrix}, \tag{7}$$

where the row index m is the same as the number of the receiving element shown in Fig. 2, and the column index n is the same as the number of the source element. The pressure at the receiving center point of patch m, (x_m, y_m), from a source element n with unit source strength is

$$g_1(n \to m) = \int_{C_n} G_1(x, y|x_m, y_m)\ \mathrm{d}x \tag{8}$$

within the main canyon,

$$g_3(n \to m) = \int_{C_n} G_3(x, y|x_m, y_m)\ \mathrm{d}x \tag{9}$$

within the secondary canyon and

$$g_2(n \to m) = \int_{C_n} G_2(x, y|x_m, y_m)\ \mathrm{d}x \tag{10}$$

in the half-space above the canyon. The element number n is described by C_n and G_3 is the Green function of the covered secondary canyon analogous to Eq. (1) but with other values for the canyon height and width l_x and l_y.

The vectors **q** and **b** are respectively the unknown source strengths and the contributions from the primary source on the center points on each element. This equation system can be solved by for instance Gaussian elimination, which will determine the unknown source strengths.

3 Absorption examples

3.1 Comparison to scale model results

Horoshenkov et al. has published scale model measurements on a canyon treated with absorbers arranged in different ways [10]. The full size of the canyon is 17 m high and 17 m wide, and the length scale factor is 20. Many configurations have absorber patterns that vary along the length of the canyon which is not suitable for comparisons with the equivalent sources method since it assumes that there is no change in that direction. However, the configuration M3 is an absorbing felt mounted on the lowest 3 m (in full scale) of the canyon side walls. The felt can be modeled by the Voronina impedance model [18], as described in [19].

The scale model measurement uses a number of point sources to simulate a line source, and the spectra of the sources are later adjusted to fit that of light traffic. The A-weighted insertion loss is measured compared to the rigid case, which gives a value slightly above 4 dB. A simulation using the ESM with the same geometry and spectrum gives 4.2 dB. The insertion loss varies a lot over frequency though, and a comparison with the scale model results over frequency would give a better validation.

3.2 Optimal placement of absorbers

The efficiency of an absorber in the canyon varies with its position. This can be investigated by making one calculation with an absorbing patch placed at each of the positions given in Fig. 3 and comparing the results to the rigid case without absorption. The geometry chosen for the test was an 11 m wide and 18 m high canyon, and the source was placed 500 m to the left of the canyon on the hard surface (at $(-500, 18)$ in the coordinate system in Fig. 1). This is a simple model of a distant source that will give an approximately plane wave approaching the canyon. The receiver was placed at the ground inside the canyon, slightly off center at $(5, 0)$.

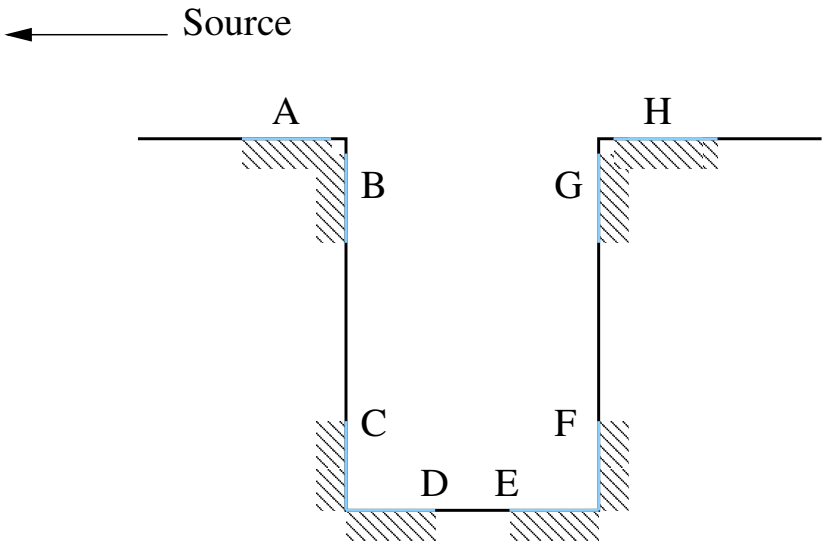

Figure 3: Absorber positions for calculation of insertion loss.

The center line was avoided since all modes in the x-direction will have a nodal line here, and thus the contribution for all those modes would be zero. All patches were 4 m long, A,B,G and H were placed 1 m from the corners, and C–F were placed right next to the corners.

The absorbers represented fibrous absorbers, and were modeled by the single parameter impedance model described in [20] with the effective flow resistivity set to 25 kNs/m^4. They were assumed to represent very thick absorbers, so no correction for finite thickness was applied.

The source spectrum was chosen as C_{tr} from [21], which corresponds to road traffic at low speeds. Each third octave band was evaluated using 20 logarithmically spaced frequencies, and data up to the third octave band 1 kHz was included. The A-weighted insertion loss for the different cases is given in Tab. 1. As visible from the

Table 1: A-weighted insertion loss for the absorber positions A–H described in Fig. 3.

Pos	A	B	C	D	E	F	G	H
IL [dB]	2.6	7.3	8.5	3.5	2.9	6.2	5.6	0.0

table, the most effective position of the absorbers is on the side walls of the canyon. Positioning the absorbers on the canyon floor gives less insertion loss. This can be explained by looking at what modes have a long reverberation time in the undamped canyon. It is the modes that are travelling horizontally between the sidewalls, modes

in the vertical direction are quickly "absorbed" by the canyon opening. An absorber at a side wall will have a stronger influence on the waves that bounce between them than an absorber placed on the canyon floor.

Placing the absorbing patch outside the canyon gives an effect only if it is placed on the source side. If it is placed on the other side of the canyon it will only influence the plane wave from the source as it moves away from the canyon. On the source side the absorber has a greater influence because it makes the main diffracting edge soft, so that less energy is diffracted into the canyon.

Both of the absorber positions on the side wall closest to the source (B and C) gave higher insertion loss than their counterpart on the other side (F and G). However, this insertion loss depends relatively strongly on the receiver position chosen, and the average effect over the whole canyon is expected to be more similar between the positions.

4 Absorption and diffusion

To investigate the effect of diffusion and absorption together, four geometries were used, see Fig. 4. Again the canyon was 11 m wide and 18 m high. The absorption was applied in ten patches, five on each sidewall. Each patch was 1 m long, and the impedance was modeled as above. Furthermore the absorber was modeled as 0.1 m thick with a hard backing, see for instance [22], which means that it has lower absorption at low frequencies compared to an infinite absorber. The irregularities were modeled as 1 m high and 0.3 m deep niches, also ten in total. This means that 28% of the façade surface was covered by absorption, 28% were niches and 44% hard for the case with both absorption and diffusion included.

The sound pressure level was evaluated at ten positions 1.5 m above the canyon floor (at x =1,2,...,10 m), and the result in Fig. 5 is the mean value of the squared pressure at these positions. Again the source was positioned 500 m from the canyon to simulate a distant road. The third octave band levels were determined using 40 logarithmically space frequencies in each band.

The canyon with hard sidewalls gives almost no shielding of the source at all, since the level relative free field is around 0 dB for higher frequencies. At low frequencies the level is high or low depending on if there are any strong resonance effects in the canyon within the band. The strong peak at 80 Hz is due to a very pronounced resonance at 77.4 Hz.

Including diffusive niches lowers the sound pressure level in the canyon. This is due to that energy otherwise trapped in modes with low damping, i.e. the sound waves that bounce between the side walls, is scattered out of the canyon when they

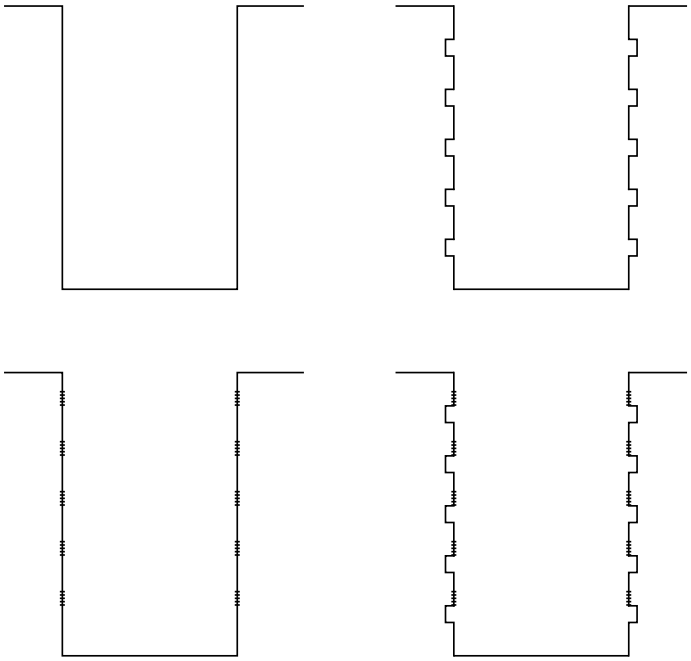

Figure 4: Four calculation cases, a hard canyon, a canyon with hard diffusing niches, a canyon with absorbing patches and finally a canyon including both diffusive niches and absorption.

interact with the irregularities. The same phenomenon is known from room acoustics, where the reverberation time in rooms with an uneven distribution of damping is lowered if diffusion is introduced [23, 24]. The effect of including the diffusive niches is surprisingly high, around 5 dB at the higher frequencies, but absorption is more effective in this case. Including both the absorption and the diffusion generally gives an even stronger effect, but there is also a more complex behaviour around certain frequencies, where the efficiency of the absorbers is reduced by including the diffusive elements.

5 Conclusions

The equivalent source method for two dimensional canyons has been extended to include irregularities (in the form of rectangular niches) and absorption. When only absorption is included the result agrees with those of a scale model measurement. The method can be used to study the effect of different measures for reducing the

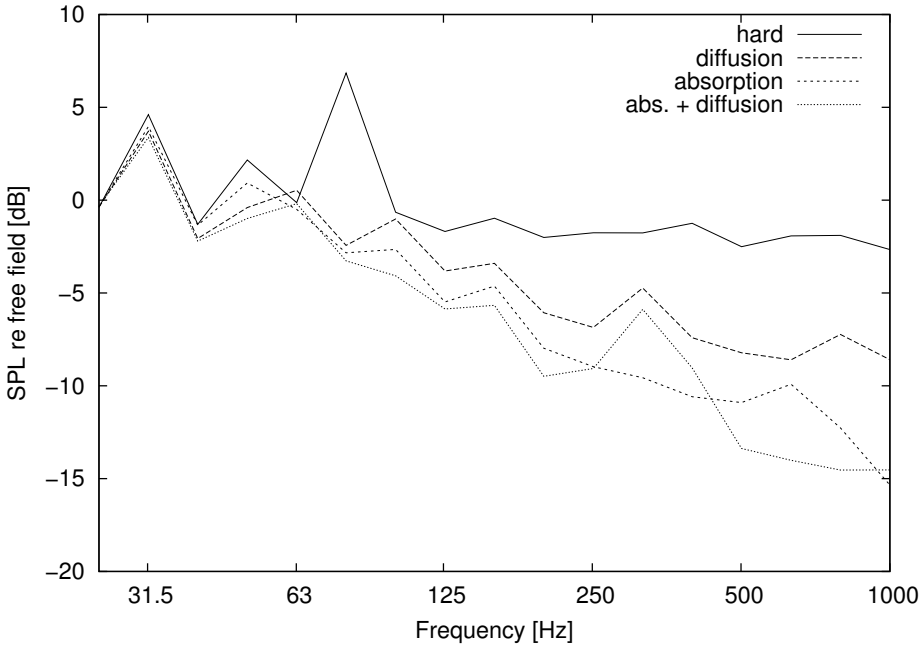

Figure 5: Sound pressure level relative free field in third octave bands for the four cases in Fig. 4.

noise level in courtyards, and to develop simpler models for prediction methods.

The effect of absorption is quite important in the cases studied here. Using a traffic noise spectrum to estimate the effect in the A-weighted level gives an insertion loss of 5–10 dB, and at 1 kHz the effect is as much as 12 dB. However, these results are dependent on the damping included in the rigid case (without extra absorption), which is essentially unknown. Assuming perfectly rigid surfaces overestimates the expected insertion loss obtained by mounting absorbers in a real case. Better estimates of what damping could be expected for a real courtyard without absorbing surfaces can be made directly from measurements, or indirectly from the properties of typical hard façade materials.

Including the diffusive niches gives a relatively strong effect on the noise level in the canyon. This means that the assumption of a simple 2D canyon with perfectly smooth and rigid surfaces gives unrealistic results unless some kind of diffusion is included, since there are always irregularities such as windows or un-smooth façades in real cases. For an engineering approach where only the equivalent level in the canyon is considered, diffusive niches and absorption both act to lower the level, so a complex diffusion model might be replaced by a certain amount of absorption in a simpler absorption model.

An interesting idea for future research is to look at how the well developed tools for prediction of room and concert hall response can be modified to cover the case with an open top such as a courtyard. An obvious idea is to include the open top as a perfect absorber. Investigations on how to include distant sources are still needed, since the source is located outside the room and the energy is diffracted down into it.

6 Acknowledgements

This paper is based on a study performed within the research programme ”Soundscape Support to Health”, sponsored by the Swedish Foundation for Strategic Environmental Research (MISTRA), the Swedish Agency for Innovation Systems (Vinnova) and the Swedish National Road Administration (VV).

References

[1] H. Jonasson and H. Nielsen. Road traffic noise – nordic prediction method. TemaNord 1996:525, Nordic Council of Ministers, Copenhagen, Denmark, 1996. ISBN 92-9120-836-1.

[2] M. Ögren and W. Kropp. Road traffic noise propagation between two dimensional city canyons using an equivalent sources approach. *Acustica – Acta acustica*, 90(2):293–300, 2004.

[3] J. Bérillon and W. Kropp. A theoretical model to consider the influence of absorbing surfaces inside the cavity of balconies. *Acustica – Acta acustica*, 86:485–494, 2000.

[4] M. Ögren and J. Forssén. Modelling of a city canyon problem in a turbulent atmosphere using an equivalent sources approach. *Applied Acoustics*, 65(6):629–642, 2004.

[5] K. Heutschi. A simple method to evaluate the increase of traffic noise emission level due to buildings for a long straight street. *Applied Acoustics*, 44:259–274, 1995.

[6] R. Walerian, R. Janczur, and M. Czechowicz. Sound level forecasting for citycenters. part1: sound level due to a road within an urban canyon. *Applied Acosutics*, 62:359–380, 2001.

[7] K. Horoshenkov, S. Chandler-Wilde, and D. Hothersall. An efficient method for the prediction of sound propagation in a canyon. In *Proceedings of the International Congress on Acoustics*, Rome, 2001.

[8] K. Horoshenkov and S. Chandler-Wilde. Efficient calculation of two-dimensional periodic and waveguide acoustic green's functions. *J. Acoust. Soc. Am*, 111(4):1610–1622, 2002.

[9] P A Morgan, C R Ross, and S N Chandler-Wilde. An efficient boundary element method for noise propagation from cuttings. In *Proceedings of Inter-Noise*, Liverpool, 1996.

[10] K. V. Horoshenkov, D. C. Hothersall, and S. E. Mercy. Scale modelling of sound propagation in a city street canyon. *Journal of Sound and Vibration*, 223(5):795–819, 1999.

[11] R. Bullen and F. Fricke. Sound propagation in a street. *Journal of Sound and Vibration*, 46(1):33–42, 1976.

[12] Huw G. Davies. Multiple-reflection diffuse-scattering model for noise propagation in streets. *J. Acoust. Soc. Am.*, 64(2), 1978.

[13] J. Kang. Numerical modelling of the sound fields in urban streets with diffusely reflecting boundaries. *Journal of Sound and Vibration*, 258(5):793–813, 2002.

[14] A. Cummings. The effects of a resonator array on the sound field in a cavity. *Journal of Sound and Vibration*, 154(1):25–44, 1992.

[15] H. Kuttruff. *Room acoustics*. Applied science publishers Ltd., London, 2 edition, 1979. ISBN 0-85334-813-8.

[16] E. Skudrzyk. *The Foundations of Acoustics*. Springer – Verlag, New York - Wien, 1971.

[17] François-Xavier Bcot, Pontus Thorsson, and Wolfgang Kropp. An efficient application of equivalent sources to noise propagation over inhomogeneous ground. *Acustica – Acta acustica*, 88:853–860, 2002.

[18] N. Voronina. Acoustic properties of fibrous materials. *Applied Acoustics*, 42:165–174, 1994.

[19] K. V. Horoshenkov, D. C. Hothersall, and K. Attenborough. Porus materials for scale model experiments in outdoor sound propagation. *Journal of Sound and Vibration*, 194(5):685–708, 1996.

[20] M. E. Delany and E. N. Bazley. Acoustical properties of fibrous absorbent materials. *Applied Acoustics*, 3:309–322, 1970.

[21] Acoustics – rating of sound insulation in buildings and of building elements – part 1: Airborne sound insulation. ISO 717-1:1996, The International Organization for Standardization, 1996.

[22] K. Attenborough. Acoustical impedance models for outdoor ground surfaces. *Journal of Sound and Vibration*, 99(4):521–544, 1985.

[23] D. Fitzroy. Reverberation formula which seems to be more accurate with nonuniform distribution of absorption. *J. Acoust. Soc. Am.*, 31:893–897, 1959.

[24] Bengt-Inge Dalenbäck, Mendel Kleiner, and Peter Svensson. A macroscopic view of diffuse reflection. *J. Audio Engineering Soc.*, 42:873–907, 1994.

Paper V

Noise level distribution in cities using a flat city model

Pontus J. Thorsson, Mikael Ögren and Wolfgang Kropp

Abstract

The prediction of road traffic noise levels in areas not directly exposed, such as areas behind buildings and courtyards, is difficult using standardised methods. This is mainly due to that traditionally only one or a few sources are included. Here a simple model that assumes a flat city on a rigid ground is used to demonstrate that sources from a large area are important. Calculations are compared to measurements for four cases, and the proposed method predicts levels 6–10 dB too high for the equivalent level at all measurement positions. If a correction is applied for this over-estimation, the results agree well.

1 Introduction

Today many standardised methods exist for the prediction of road traffic noise levels. They typically predict A-weighted equivalent levels, and are reasonably accurate for short ranges and neutral or relatively weak wind and temperature gradients. Recent and ongoing development of prediction methods, such as "Harmonoise" and "Nord 2000" will improve the long range accuracy by including more advanced models for weather and ground effects. For short ranges and large traffic flows the variations over time are small, and the predictions more accurate than at long ranges and small flows.

Calculations at positions not directly exposed to traffic noise are more challenging. Screening from buildings, multiple reflections from building façades and weather effects that affect the sound fields from distant sources make it troublesome. Even more troublesome is that often only one or possibly two sources are taken into account.

Is it important to know the level where it is already low one might ask. Traditionally it is not, since limit values are based on the loudest side of a dwelling. But there is an increased understanding of that decreasing the noise levels at exposed façades requires a huge effort, and that it might be an unrealistic goal for many years to come [1]. It may be more efficient, from an annoyance viewpoint, to ensure that inhabitants have access to a quiet area [2]. In this context a prediction tool for quiet areas is useful.

In the literature there are a few statistical models which can possibly be used for assessing the levels on the quiet side. Three analytical diffusion-type models have been tested in a segment of built-up area [3]. There it was reported that the models, though simple to use, showed considerable differences in calculated results. The models were thus concluded to only be usable for rough field investigations. Bullen has however shown in [4] that sufficiently accurate results, in terms of average levels, can be achieved with little information about the physical environment. Sometimes only the mean length between buildings and the mean absorption is necessary.

Here a simple model is proposed; point source propagation over a hard surface. The simplicity of this approach makes it easy to include a large number of roads as sources. Such a model overestimates the sound level, but an approximate correction factor can be deduced from measurements. A similar approach has been used by Yeow *et al.* [5]. The vehicles were treated as point sources and sound is propagated over a flat plane. The correction factor was there arbitrarily chosen.

The present model is described in the next section, and some application examples are given in the following section. One of the examples compare the model to "traditional" use of the Nordic method for road traffic noise, and to measurements. The final section contains some concluding remarks.

2 Model description

The model is based on the source description part of the Nordic prediction method for road traffic noise [6]. Data on traffic flows and road geometry is input into the model, and finally a prediction of the equivalent level for a 24 h period is obtained.

The starting point for the prediction method is the location of the roads that are close to the area of interest, i. e., the roads that are judged to be of importance. Data on the vehicle flow of both light (up to 3000 kg) and heavy (over 3000 kg) vehicles on those roads are also needed. This includes both the densities and the average vehicle velocities on different road sections. What is needed is essentially a map that shows the road network in the area, and information on the traffic flows.

The information described above is then used to calculate the source strengths of a number of point sources that are evenly distributed over the road network. The Nordic method specifies the sound power level from a line source section, but this can easily be translated into a number of point sources. The model geometry is considered to be flat, and no objects such as buildings are modelled. This corresponds to raising the streets up to the rooftop level, and studying the relatively flat landscape that would be the result of such a transformation.

The distribution of sources can now be used together with a simple propagation model to calculate the pressure at any receiver position within the modelled area. Here a simple approach with only spherical spreading from a point source over hard ground is used. All other effects, such as ground effect, screening and atmospheric absorption are left out. This approach gives an overestimation of the sound level, since all forms of damping have been neglected.

Consider a situation with two parallel roads with surrounding buildings, often referred to as city canyons, see Figure 1. Compared to the flat case with the same distance between the source and receiver the sound level would be somewhat lower. This is due to the interaction of the effects of diffraction around the edges, which reduce the level compared to the flat case, and multiple reflections inside the canyons, which increase it.

From a more advanced calculation model such as [7], or from measurements, one might conclude that the level is 12 dB lower in the canyon case than in the flat case, 5 dB due to the source canyon and 7 dB due to the receiver canyon. By assuming that the same correction applies independently of the distance between the canyons, a simple prediction scheme is obtained. The noise level is estimated by using the correction factor (12 dB in this case) that applies to the area in question. Note that the correction factor contains many different mechanisms that affect the noise level, including screening and ground effect. The area of interest therefore needs to be reasonably homogeneous in terms of building size and density.

3 Application examples

The present model has been used to predict $L_{AEq,24h}$ levels in different types of city environments. Two application examples will be presented in detail:

1. The district Söder in Stockholm, Sweden.

2. The district Björkekärr in Göteborg, Sweden.

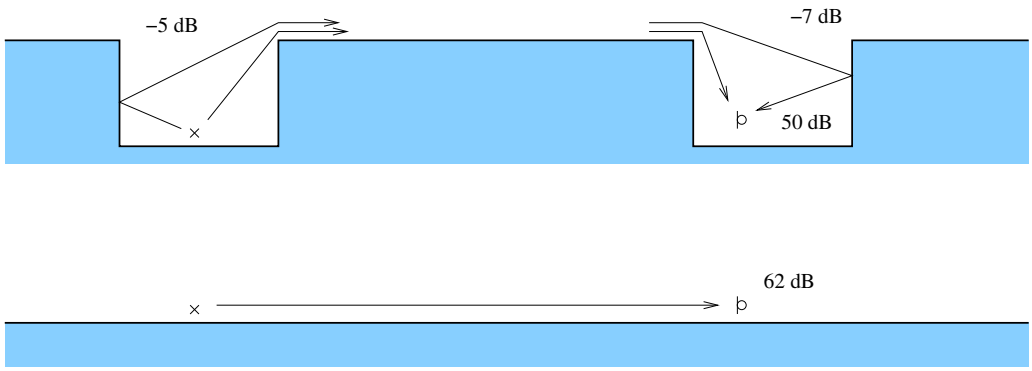

Figure 1: Example of a correction factor for a case with two parallel city canyons.

The first example is a structured grid of street canyons with continuous building façades, which are in general six floors tall. This area is a typical example of a city centre environment which can be found in almost any larger city. The second example is a more loosely built area with less regular building patterns, a type of area which can be found in the city outskirts.

As previously mentioned, a correction factor is used in the model to get correct calculations. In the application examples presented here the correction factor has been determined experimentally using both long-time and short-time measurements.

3.1 Söder, Stockholm

A birds-eye view of the first application area can be seen in Figure 2. The traffic is in this area relatively evenly distributed over the streets, and shielded courtyards can be seen in many blocks. The letters that are given in the figure are measurement positions used to estimate the correction factor for this area. Table 1 presents the measured levels at these positions together with values calculated by the present model without the correction. The measured values are equivalent levels ($L_{AEq,24h}$) measured during periods between 5 and 10 days. The measurement points positioned inside courtyards are located a few meters from the inner façade. Measurements on the directly exposed side are taken on the façade. No corrections have been applied to achieve free field values. The measurement positions that are marked with a star in the table are directly exposed positions. The present model is not intended for calculations on the exposed side and no calculated value is thus given for those positions. Also included in Table 1 are values calculated with the Nordic Prediction for road traffic noise (NPM in the table) [6]. From the results in Table 1 it is clear that the Nordic Prediction Method gives accurate predictions on the directly exposed side. However, inside the courtyards the errors are between 11 and 14 dB.

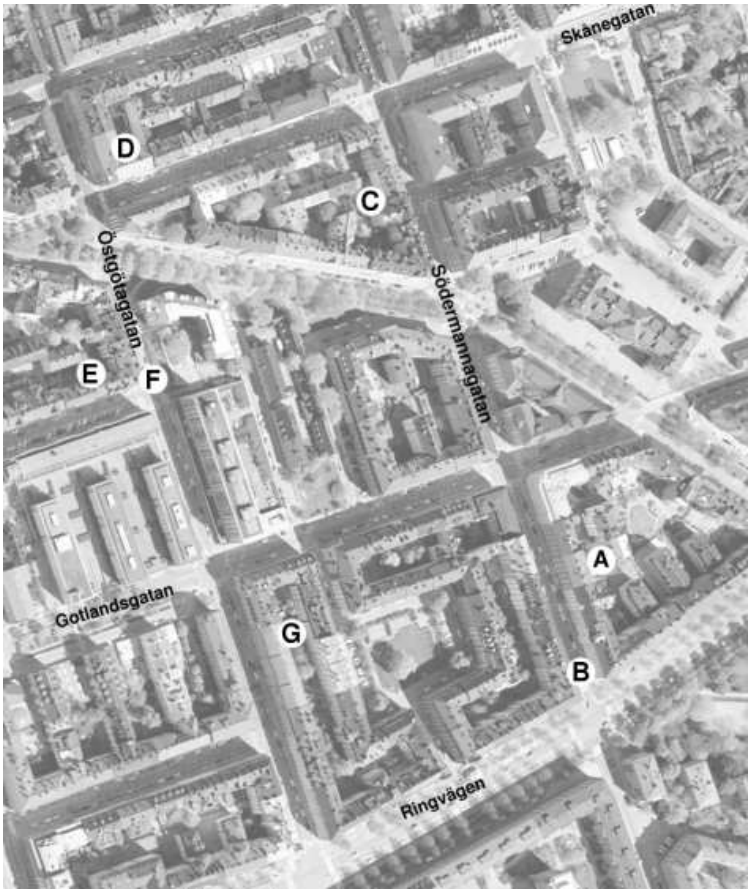

Figure 2: An overview of the application example of Söder, Stockholm. The letters in the figure are measurement positions (see the text for more details).

Position	Meas.	Calc.	NPM	Corr.
A	50	61	39	51
B*	66	-	66	-
C	51	60	39	50
D	50	59	36	49
E	48	59	37	49
F*	59	-	59	-
G	51	61	40	51

Table 1: $L_{AEq,24h}$ in dB for the measurement positions. Also included (from left to right) are calculations with the present model, calculations with the Nordic prediction method, and calculations with the present model when calibrated with the measurements. Measurement positions marked with a star are measurements on the directly exposed side.

The rightmost column in Table 1 are calculations with the present model after calibration with the correction factor which was defined before. The correction factor used in this example was estimated as the arithmetic mean of the differences between the raw calculations and the measurements, giving a value of 10.0 dB. The difference was almost constant for the different positions, and the errors between the measurements and the calibrated results was maximum 1 dB at the measurement points. Therefore it seems probable that the calibrated results from the present model can also be trusted at other points. A calculated contour map (with the correction factor applied) for $L_{AEq,24h}$ in this area can be seen in Figure 3. The highest traffic densities are found on the streets circumferencing the area. From this figure it is clear that the noise levels between streets are almost constant throughout the area. The noise level at a particular position inside a courtyard is not determined by the traffic on one single street. Instead all streets in the area affect it, and many affect the noise level significantly. In the following section it will be shown that a street with strong traffic can influence the noise levels at distant positions. The decrease in noise levels outside the central area of the figure is expected, since no streets outside of the shown area have been included.

3.2 Björkekärr, Göteborg

The second application example is a more loosely built area in Göteborg. The model has also in this case been calibrated to measurements in equal manner as for Söder.

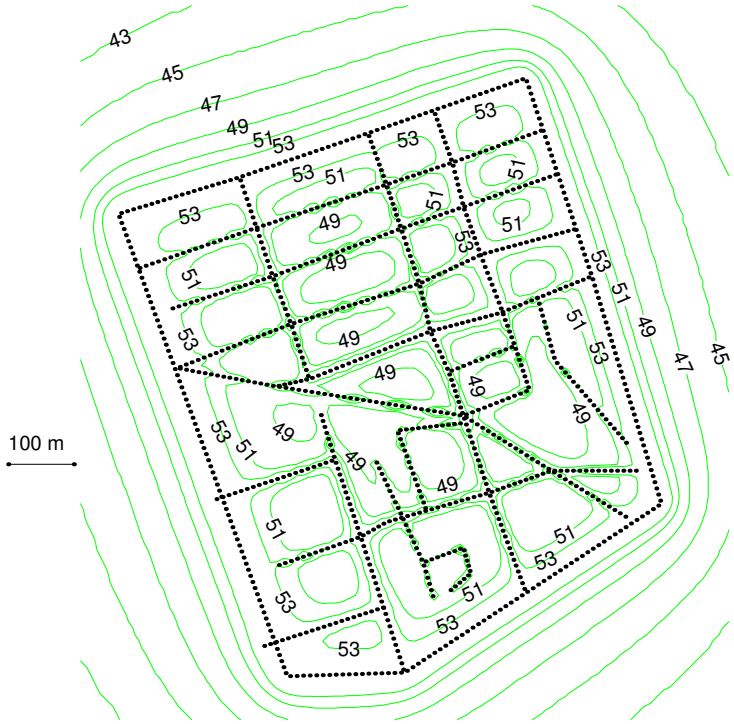

Figure 3: $L_{AEq,24h}$ for the area Söder, Stockholm. The dots in the figure represent the sources used in the calculations.

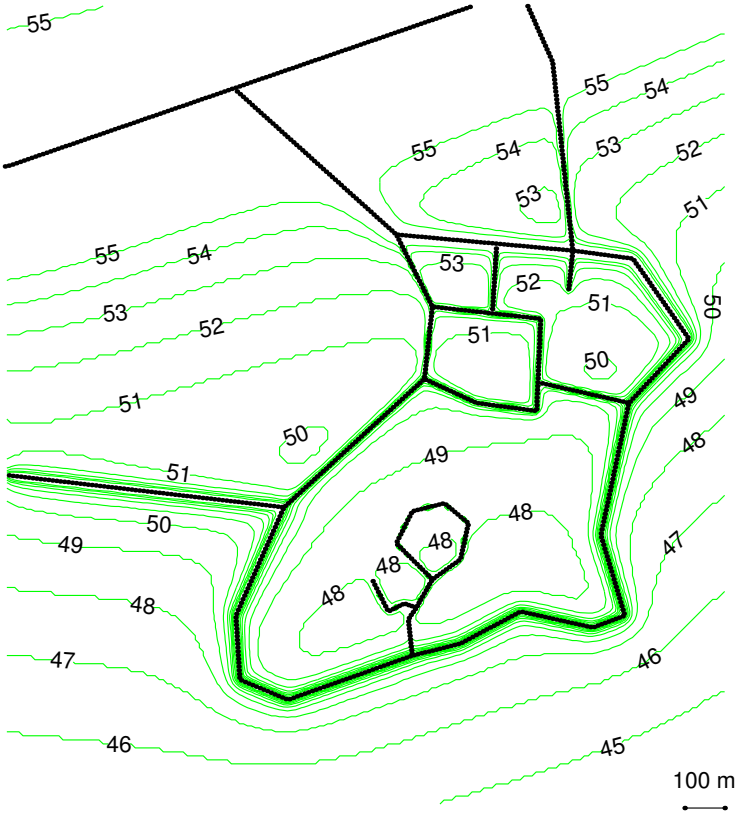

Figure 4: $L_{AEq,24h}$ for the area Björkekärr, Göteborg.

Also in this case the difference between raw calculations and measurements was almost constant (between 9.0 and 10.9 dB with a mean of 10.0 dB) for the different positions, so the model is assumed to be applicable for estimating the noise levels in the area. A $L_{AEq,24h}$ contour map for this area can be seen in Figure 4. The uppermost road in the figure is a motorway with heavy traffic (60,000 vehicles/24 h). It is clear from the contours that the noise levels in this area is dominated by this motorway.

The area of interest in this application example is the area around the small circular street in the lower part of the figure. The street that passes below this area is a street called Rosendalsgatan. The traffic volume on this street is moderate (4,000 vehicles/24 h). Assume now that the traffic volume on Rosendalsgatan is set to zero. This would give a situation as shown in Figure 5 , i. e., a noise level reduction of at most 1 dB in the area of interest. Setting the traffic volume on Rosendalsgatan to half its original value would hardly affect the noise levels in the area of interest at all. However, if the traffic volume on the motorway is set to zero then the reduction in the area of interest would be 7-8 dB giving the results shown in Figure 6, which

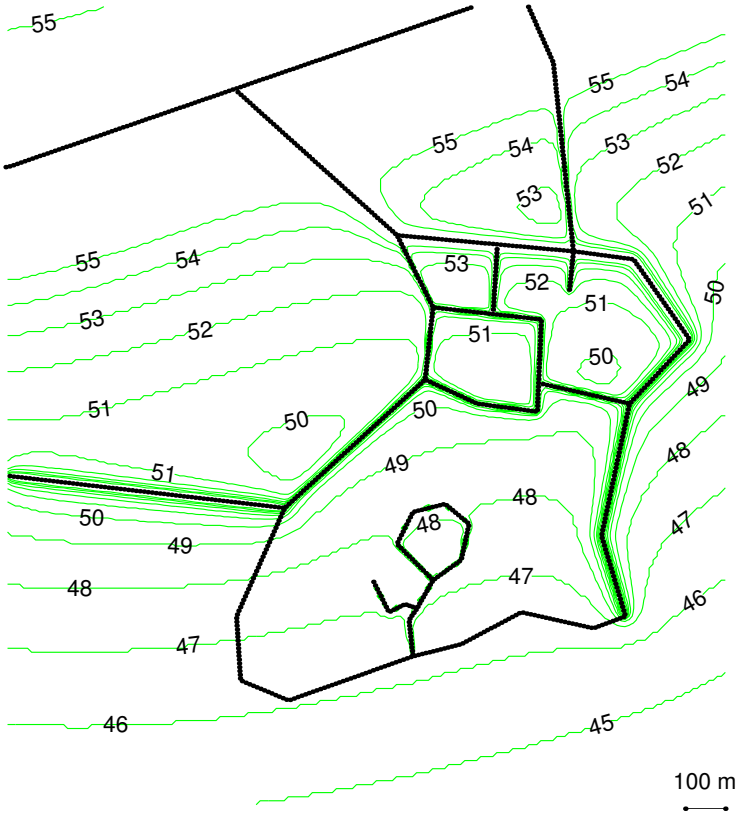

Figure 5: $L_{AEq,24h}$ for the area Björkekärr, Göteborg. The traffic on Rosendalsgatan is set to zero.

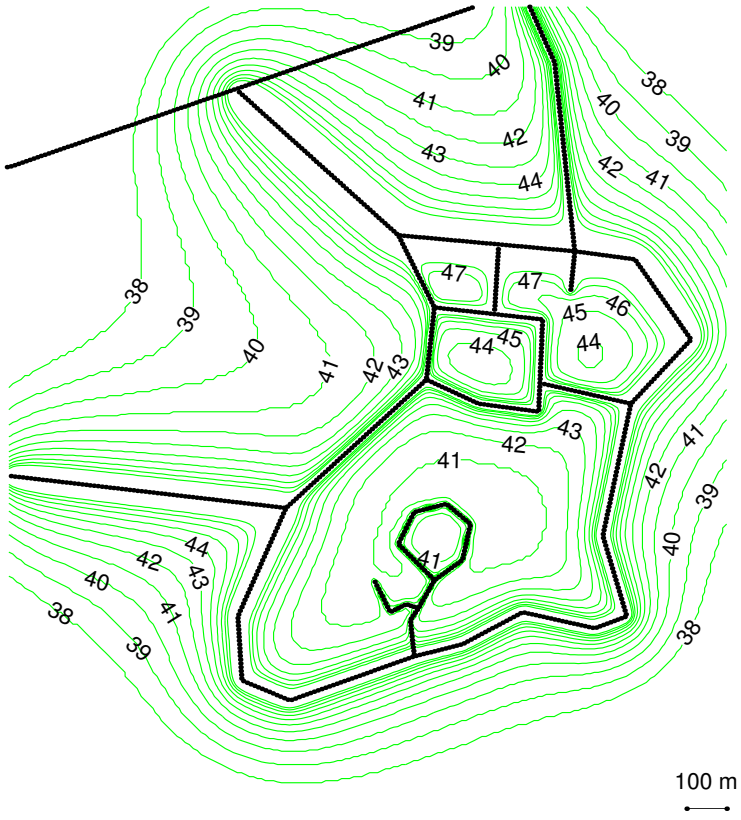

Figure 6: $L_{AEq,24h}$ for the area Björkekärr, Göteborg. The traffic on the freeway is set to zero.

clearly is a completely different noise situation than in Figure 4. The noise levels in the whole area has been reduced drastically. Thus even distant roads can contribute significantly to the noise level, provided that the traffic volume is large.

The present model has also been applied to other city environments in Göteborg and Stockholm with similar results. The buildings in these areas were more detached than in Söder, but more dense than in Björkekärr. The correction factor has also in these environments been estimated from measurements. The correction factor was in one area between 7.0 and 9.5 dB with a mean of 8.3 dB, and in another area between 5.5 and 7.5 dB with a mean of 6.5 dB. Thus the correction factor remains fairly constant also inside these areas.

The correction factor has in the examples presented here been estimated from short- and long-term measurements. However, it would be useful to be able to estimate it for an area directly, without time-consuming measurements. For instance it is not possible to use the Nordic Prediction Method, as shown in Table 1. More advanced models are needed for estimation of the correction factor.

The results from the method can give important guidelines on how traffic volume and velocity on a particular street (or a set of streets) influences the total noise level. It is however important to remember that the predictions from the flat city model are only valid in an area close to the calibration points, i. e. the points from where data has been used to estimate the correction factor. The calibration factor is also only valid over an area which is homogeneous with respect to the size and distribution of buildings. The model presents a possibility to include other kinds of noise sources, like trains or fans, provided that the radiated power from these sources can be estimated.

4 Conclusions

When predicting the noise level at positions not directly exposed to road traffic noise, it is important to include sources from a relatively large area. Using only the closest road as a source will under-predict the sound levels substantially, even if an accurate method is used.

Roads that are distant, but with dense traffic, can also be influential. Even though they are far from the receiver, a higher average speed and a larger vehicle flow can make the noise immission into an area larger than for smaller roads that are closer. For propagation over long distances weather effects are very important, which may further increase the importance of including distant, large roads.

The methods proposed here over-predicts the sound level at shielded positions by 6–10 dB. This can be corrected by using measured results, which of course is a

severe limitation for the applicability of the method. However, if a more accurate propagation model is used for all sources, it is likely that the method would directly yield a usable value. Such a propagation model would have to include the effects of topography, weather influence, multiple reflections and ground effect. These are included in the standardised models currently under development. A drawback of this approach is that more detailed information on the area under study is needed.

5 Acknowledgements

This paper is based on a study performed within the research programme ”Soundscape support to health”, sponsored by the Swedish Foundation for Strategic Environmental Research (MISTRA), the Swedish Agency for Innovation Systems (Vinnova) and the Swedish National Road Administration (VV).

References

[1] T. Kihlman and W. Kropp, City traffic noise – A local or global problem?, Noise Control Engineering Journal, v **49**, n 4, July/August , 2001, p 165-169

[2] T. Kihlman, E. Öhrström and A. Skånberg, Adverse Health Effects of Noise and the Value of Access to Quietness in Residential Areas, *Internoise 2002 - Dearborn*, paper number **484**

[3] E. Walerian and R. Janczur, (1994). Statistical description of noise propagation in a built-up area. *Archives of Acoustics* **19**(2), pp. 201–225

[4] R. Bullen (1979). Statistical evaluation of the accuracy of external sound level predictions arising from models. *Journal of Sound and Vibration* **65**(1), pp. 11–28.

[5] K. W. Yeow, N. Popplewell and J. F. W. MacKay (1977). Method of predicting L_{eq} created by urban traffic. *Journal of Sound and Vibration* **53**(1), pp. 103–109.

[6] Jonasson, H., Nielsen, H. (1996). Road Traffic Noise - Nordic Prediction Method. ISBN 92 9120 836 1, *TemaNord* **1996:525**, Nordic Council of Ministers.

[7] Ögren M, Kropp W. Road traffic noise propagation between two dimensional city canyons using an equivalent sources approach. Submitted to *Acustica – Acta acustica*, March 2003.

Paper VI

Macroscopic modeling of urban traffic noise – influence of absorption and vehicle flow distribution

Pontus J. Thorsson and Mikael Ögren

Abstract

Prediction of noise levels at shielded positions in urban areas is more difficult than on exposed positions. At shielded positions the predictions method must include multiple reflections, and many sources must be taken into account. Using numerical methods that solve the wave equation is possible, but very computationally heavy. Here two methods have been used, a very simplified ray model and a statistical model. The results show that concentrating the traffic and introducing absorption onto building façades will give lower levels at shielded positions.

1 Introduction

When trying to predict the road traffic noise propagation in urban areas, it is important to understand that in positions shielded from direct exposure usually many propagation paths must be included. On an exposed façade close to a strong source it might be sufficient to include the direct path and one or a few reflections, but in a closed courtyard it is important to include multiple reflections and more sources than just the closest road.

In most countries the limits to urban noise exposure is set on the exposed façade only, so that a rather simple prediction tool might be sufficient. But there is an increased understanding of the positive effects that comes from access to a quiet area [1], and substantially reducing the levels on the exposed side can be very difficult and expensive [2]. Therefore the focus in this article is on the prediction of noise levels in areas indirectly exposed to traffic noise.

In these areas there are multiple propagation paths to be considered. The propagation paths involve reflection, diffraction and scattering. To describe this complex process with an exact theory is impractical considering the calculation effort. This is because of the large number of details that need to be taken into account. Models in which the multiple reflections and scatterings are included in a more computationally efficient way is therefore of interest.

An additional property of city environments is that the noise attenuation effects of noise barriers are strongly reduced by the presence of reflecting surfaces around them [3]. In city centers there is a need for alternative methods of noise abatement.

One way of measuring the efficiency of a numerical model is counting the number of elements that are needed to describe a propagation environment properly. Finite element methods need very many elements since all of the propagation domain needs to be discretized. Only the boundary need to be discretized in the boundary element method (BEM) which is more efficient. Even so, the calculation effort is too high for practical calculations if calculations on a city-scale environment is needed.

Ray-tracing methods do not need to discretize the propagation domain. On the other hand ray-tracing methods need to take a large number of rays into account to get reasonable results, especially in environments where reverberation is present, e.g. in closed backyards. Even though the calculation for one ray path is simple, the large number of necessary rays makes these methods computationally heavy. The ray methods are also approximations, they ignore the wave behavoiur of sound. This makes predictions difficult for low frequencies.

A city with homogeneous buildings can be considered as an almost flat plane with canyons containing streets and backyards criss-crossing the landscape. An efficient way to calculate the propagation from one canyon to another is to describe the opening of a canyon which contains a street using equivalent sources in its opening. These sources can then be used to calculate the propagation over the rooftops [4]. The attenuation during propagation from different source canyons into a single receiver canyon can be grouped into a single correction factor. A model built on this assumption has been published [5], but it is also briefly described in section 3.1.

Another possibility is to treat sound propagation in cities as the flow of small packages of sound energy, phonons. Phonons are the sound equivalent of the use of photons for light propagation. The phonons propagate with the speed of sound and are scattered from objects (buildings, cars, trees etc.) present in the propagation domain but not from themselves. This concept has been used before by e.g. Bullen [6] and Kuttruff [7]. By using linear transport a model suitable for city-scale calculation can be formed [8]. This model is presented in section 3.2.

In this paper the flat city model and the transport model described above have

Figure 1: An example of two parallel city canyons.

been used to study sound propagation in cities. The properties of the models are described in sections 2 to 3.2. These models are then used to assess the abatement possibilities of traffic redistribution and absorption in sections 4 and 5.

2 City canyon modeling

2.1 City canyon geometry

The center of a larger city often consists of a network of streets with unbroken façades on both sides. In city noise literature such streets are called “city canyons”, an alternative view is of the rooftop level representing the “ground” and streets consequently as valleys going through the city. An example of two parallel city canyons can be seen in Fig. 1. The propagation from the source canyon to the receiver canyon can be divided into three separate parts: First the propagation from the source to the domain above rooftop level, then the propagation from the opening of the source canyon to the opening of the receiver canyon, and last the propagation from rooftop level to the receiver inside the receiving canyon. The propagation above rooftop level is then a much simplified problem; if the house heights are similar the propagation takes place over an almost flat plane.

2.2 Absorption inside canyons

Inside the canyon the sound waves from either a source within the canyon, or the waves diffracted into it, will be reflected at the side walls and the ground. When the damping in the canyon is low, waves reflected many times will contribute to the total level. Therefore it is essential to include the absorption effects when trying to predict the level, at least if the source is outside the canyon. When the source is inside the canyon the direct field is stronger than the reflections, each order of reflections gets slightly weaker since they travel over longer paths. But when the source is far away on the outside of the canyon each reflected path is approximately of the same length.

On a real courtyard the absorption is due to the finite impedance of building façades and the ground surfaces, and at high frequencies the air itself. Most surfaces are relatively hard, but grass covered surfaces may be soft (absorbing). There is also a possibility to introduce artificial absorbers on the building façades or the ground.

The diffusive properties of the reflecting surfaces are also of importance, at least at higher frequencies. If the canyon is considered as a room with hard walls and a very absorbing roof, increasing the diffusion will lower the reverberation time, since the sound field becomes better mixed, see [14, 15]. This in turn will give lower levels.

Including the absorption in an image source model combined with diffraction theory such as [16] is difficult. If the absorption covers one whole surface it is relatively easy, but if it only covers parts of the canyon, all the edges where the impedance changes will be diffracting. This gives a large number of rays to include, and the accuracy will suffer. On the other hand evenly distributed absorption such as air absorption is easy to include.

An alternative way to model the situation is to use a numerical method based on solving the wave equation. Then patches with absorbers can be included in the boundary conditions as impedances. In order to reach reasonable computation times such models are usually restricted to two dimensions. One possible approach is the boundary element method, another the equivalent sources approach (ES) [4]. BEM is slightly more flexible, but requires that the whole canyon is discretized, and is therefore a bit slower than ES, which only discretize the opening of the canyon and the impedance patches. In both methods it is building the matrices needed that takes most of the computational effort, not the solution of the matrix equations.

3 Macroscopic urban propagation models

3.1 The flat city model

In the previous section propagation between city canyons was divided in three parts: 1) From the source to the rooftop level of the source canyon, 2) From rooftop level of source canyon to the rooftop level of the receiver canyon, and 3) From rooftop level of the receiver canyon to the receiver. The total transmission loss from a source to a receiver, except the geometrical spreading, can be achieved through summing the two transmission losses out of the source canyon and into the receiver canyon. The sound level in a receiver canyon can then be estimated through subtracting the total transmission loss from the total levels with all significant streets in consideration calculated through free-space propagation over rigid ground using a simple ray

model. This way of including the effects of shielding buildings assumes that they are homogeneous in terms of height and absorption characteristics. However, it is possible to estimate the level if the transmission loss between all sources and receiver canyons is known in an inhomogeneous case.

The simplicity of this model makes it possible to use real geometries taken from a map over the city. The source strengths are calculated according to the Nordic prediction model for road traffic noise [9] which uses the vehicle flow density, percentage of heavy vehicles and velocity as input parameters.

An experimental validation of this model can be found in [5], where the difference between the level from all streets on the flat plane and the level inside the canyon was determined from long-term and short-term measurements in a number of receiver locations. The accuracy was found to be very good in a variety of city environments. The correction term, which was subtracted from the free-field values, was in the different city examples between 6 and 10 dB. This can be compared to the value of 15 dB which was found by Shaw and Olson in a similar way [10]. The difference can possibly be explained by different propagation environments, but it is more likely that it is caused by the snow-covered ground which was the case in Shaw and Olsons measurements. All measurements in [5] were performed under dry and snow-free conditions.

3.2 Linear transport modeling

The previous model treat the built environment as buildings with unbroken façades, i.e., the propagation around buildings or through openings is omitted. A statistical model dealing with this type of propagation, based on the assumption that a sound ray experience multiple reflections and diffractions on its way from source to receiver, is presented here. The model is derived using linear transport of phonons and considers the houses as infinitely tall cylinders of constant cross section. The propagation environment is thus considered in a two-dimensional map perspective. Linear transport models are common in particle physics, e. g., in nuclear physics where it is used to study neutron flux inside nuclear reactors [11].

3.2.1 Model description

As shown in [8] it is possible to write the energy density $U(\mathbf{x})$ in a two-dimensional environment with isotropic scattering as an integral equation:

$$U(\mathbf{x}) = \int_{\Omega} \frac{\exp(-\left|\int_{\mathbf{y}}^{\mathbf{x}} \gamma(\mathbf{r})\,\mathrm{d}\mathbf{r}\right|)}{|\mathbf{x}-\mathbf{y}|}[\eta(\mathbf{y})U(\mathbf{y}) + f(\mathbf{y})]\,\mathrm{d}\mathbf{y}. \tag{1}$$

In this equation Ω is the geometrical propagation domain, $\gamma(\mathbf{y})$ is a function proportional to the absorption and scattering strengths and $\eta(\mathbf{y})$ is proportional to the scattering strength (see [8] for details).

$$\begin{aligned}\gamma(\mathbf{y}) &= \alpha(\mathbf{y}) + \lambda^{-1}(\mathbf{y}),\\ \eta(\mathbf{y}) &= [2\pi\lambda(\mathbf{y})]^{-1},\end{aligned}$$

where α is the absorption factor and λ is the mean free path length. The integral equation involves the integral

$$\Lambda = \int_{\mathbf{y}}^{\mathbf{x}} \gamma(\mathbf{r})\, \mathrm{d}\mathbf{r}, \tag{2}$$

which in electromagnetics is called the optical distance [12]. In Eq. (2) $\mathbf{y}$ is the source point, $\mathbf{x}$ is the receiving point and $\mathbf{r}$ is a point on the straight line in between. The optical distance thus differ from the geometrical distance through the parameter γ.

Interestingly, it is possible to derive Eq. (1) starting from the wave equation. As shown in [8], by using Twersky's multiple scattering theory under the assumptions of scattering objects being in the far-field of each other and that the back-scattering is small the same integral equation can be reached.

3.2.2 Propagation over rooftops in the transport model

Since the buildings are considered as infinitely tall in the 2D transport model there can be no propagation over them. From a previous study it was concluded that in many cases this propagation path is dominating [8]. The transport model has therefore been extended to include the transmission over rooftops. The domain over the rooftops is considered as a half-space with flat ground and homogeneous properties. Sound energy is transmitted to the half-space above the houses from the sound field in between the buildings. Since the sound field is already considered as diffuse, and additionally the house sizes are larger than the most important wavelengths, this transmission can be approximated by multiplication of the sound field between the houses with a transmission factor ξ_{up}. Due to reciprocity, a similar factor ξ_{down} can be used for the transmission from the half-space down to the house layer. The contribution from the path over the rooftops is then taken into account in Eq. (1) as an additional source strength:

$$f_{\mathrm{total}} = f_0 + f_{\mathrm{air}},$$

where f_0 is the original source strength (the roads) and f_{air} is the contribution from the air half-space.

Representative values of the transmission factors are not known. In the present model the spaces between buildings can be interpreted as rooms with a perfectly absorbing ceiling. A simple way to estimate ξ_{up} can therefore be to use the quotient between the area of the open ceiling and the total area. Using this approach, the location of the source need not be well-defined, since the field is diffuse.

Another way of estimating the values of the transmission factors is using the solid angle which is covered by the open ceiling, i. e., the solid angle which a source between houses "sees". The validity of this approach have been shown for reverberation time measurements in rooms with inhomogeneous absorption properties [13]. However, in this approach the source location must be known. This can be overcome by using the mean value of the solid angle over all possible source locations inside the canyon. Note that the transmission parameters need not include the ground reflection, again since the field is diffuse. The diffusivity of the field already includes reflections on the ground and on the building walls.

In the examples shown here a single source position in the middle of the space between houses is used, and $\xi_{\text{down}} = \xi_{\text{up}}$. This may be a too rough approximation, and more studies are needed on the transmission factors. For the canyon used in section 2.2, $\xi_{\text{up}} = 0.27$ for the solid angle approximation and $\xi_{\text{up}} = 0.26$ for the area quotient approximation. From measurements in a representative area a value of $\xi_{\text{up}} = 0.32$ can be deduced, which is in fairly good agreement to the two approaches presented above.

In Fig. 2, the 24 h A-weighted equivalent levels for an area in central Stockholm, Sweden is presented, with and without including the effect of propagation over rooftops. In the calculations presented in the figure the values $\xi_{\text{up}} = \xi_{\text{down}} = 0.3$ have been used. The values at marked points are measured levels, and the calculated and the measured levels are in fairly good agreement. It is also clear that in the main part of this area the dominating contribution to the sound levels in the backyards is coming from over the rooftops. The impact of reducing the strength this propagation path is shown in section 5.1 below.

4 Influence of traffic distribution

Changing the traffic density and location is an obvious method to abate noise in urban areas, i.e., to move the noise sources away from the receivers, or to reduce their strengths through reduction of the vehicle flow. The same residential area in Stockholm as in Fig. 2 has been used, due to its homogeneous building structure and regular street geometry. Almost all streets are directed along two directions, one direction is close to north-south (N-S) and one direction is close to east-west

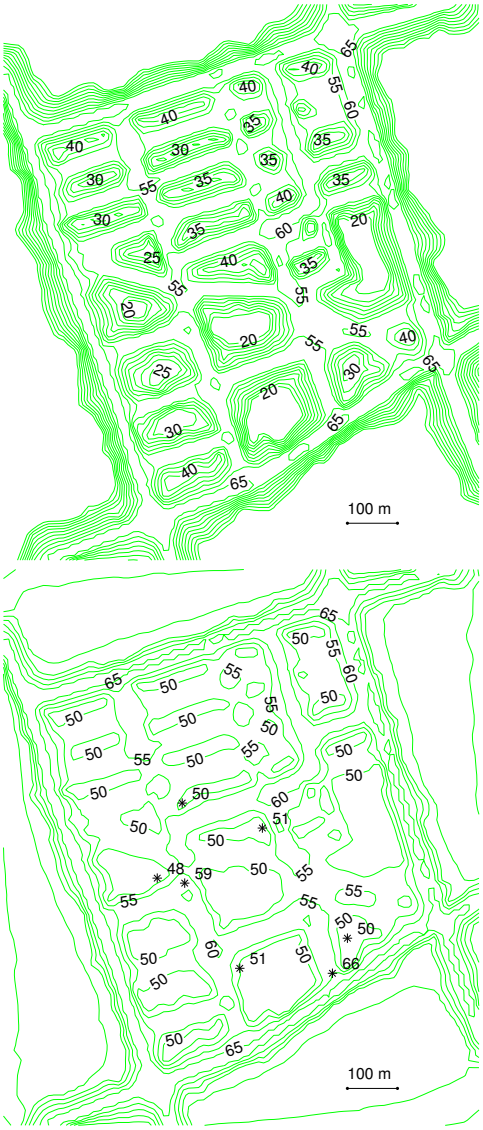

Figure 2: $L_{AEq,24h}$ for an area in central Stockholm, Sweden. Above: no propagation over rooftops, and below: propagation over rooftops included ($\xi_{\text{up}} = \xi_{\text{down}} = 0.3$).

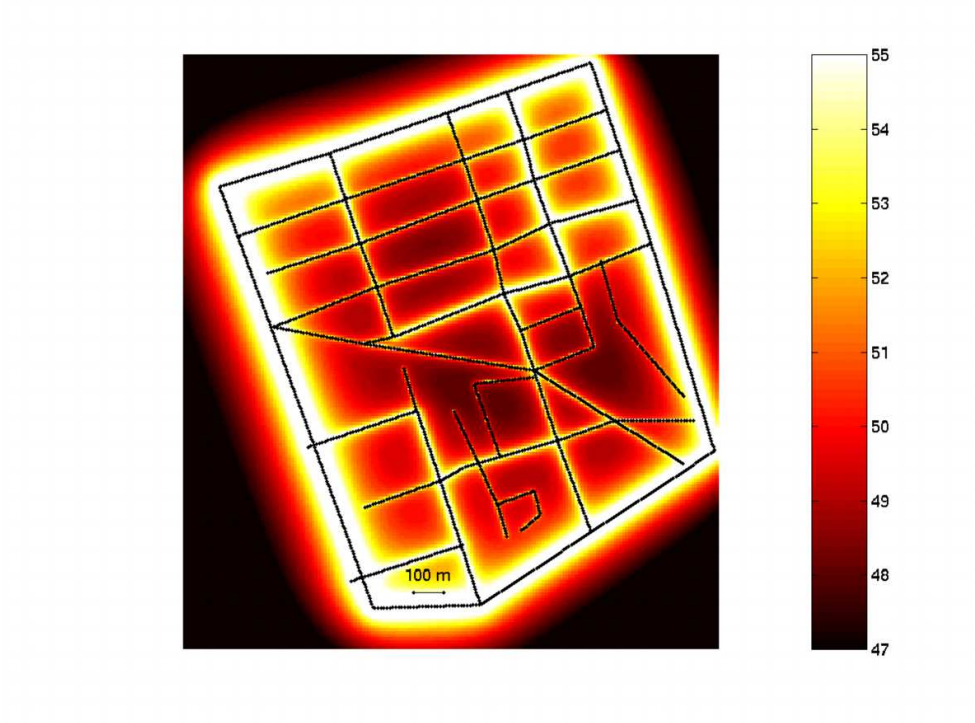

Figure 3: Equivalent levels in the residential area in Stockholm with existing traffic.

(E-W). The traffic distribution in this area has then been modified and its impact on the $L_{AEq,24h}$ noise levels on the shielded side has been studied using the flat city model described above. Screening by houses has been taken into account by using equivalent sources calulations[4].

The starting point was the existing traffic distribution in this area. The equivalent levels in the courtyards can be seen in Fig. 3. The traffic flows were in this area between 500 and 22,000 vehicles/24 h.

The traffic has now been redistributed based on two extreme cases:

- A homogeneous traffic distribution, i. e., equal traffic flows.
- All traffic concentrated on two streets; one in each main direction of the street grid.

Two examples of even distributions have been studied: 1) Equal traffic on the streets in N-S direction and equal traffic on the streets in E-W direction, and 2) Equal traffic on all streets. The results for one of these examples can be seen in Figure 4. Only one figure is shown, since the differences between the examples were negligible. In the case of equal traffic the flow was 7,300 vehicles /24 h. When comparing Fig. 4 with Fig. 3 it is clear that the original traffic distribution gives lower levels in a large

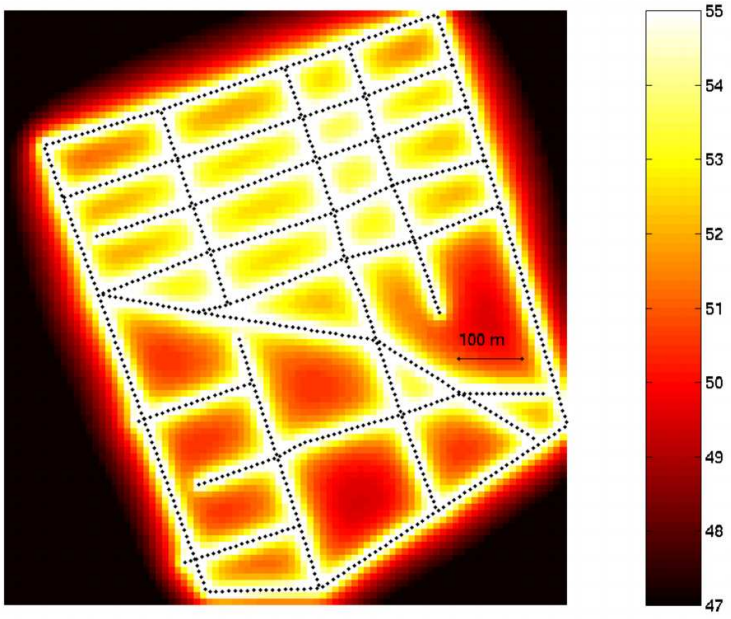

Figure 4: Equivalent levels in the area with equal traffic on all streets.

part of the area. Very close to the surrounding roads with strong traffic the levels are however lower in the case of equal traffic. Thus, an even traffic distribution is not desirable when considering the noise levels in the whole area.

In the second case all traffic was concentrated to two streets: one in N-S direction and one in E-W direction. The traffic on these streets was then 46,000 and 48,900 vehicles/24 h respectively. The equivalent level distribution for this case is shown in Fig. 5. In this case a larger area has a shielded side with lower levels than in either the even case or the original case. By concentrating the traffic to a few streets noise reducing measures, such as barriers or absorption, can also be more cost-effective since they need only to be applied to a small range of locations.

Figure 5 represents an ideal case with no traffic on any other street. Some traffic will always be needed on the streets inside the silent area, and the importance of the size of the vehicle flow on the inner streets has therefore been studied. Inner streets are here defined as all other streets but the two streets with strong traffic above. By counting how much of the area which is exposed to equivalent levels lower than a chosen value, e.g. 50 dBA, it is possible to estimate how much traffic can be allowed on the inner streets for a determined maximum level. Here it is implicitly assumed that the number of inhabitants per unit area is constant. In a homogeneous urban area, such as the area under study here, this assumption is probably fulfilled. Fig.

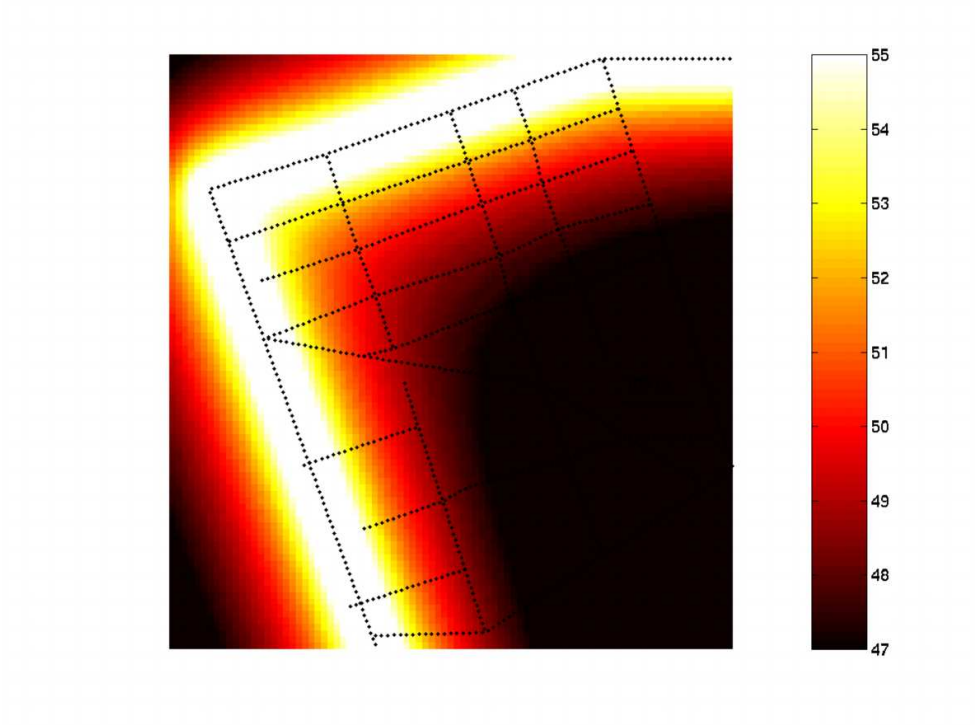

Figure 5: Equivalent levels if all traffic in the area is concentrated to two streets.

6 shows results for the area with equal traffic on all inner streets. In this figure evenness is a measure of how evenly distributed the traffic is. An evenness of 0 % means that all traffic flows on the same two streets as before, and an evenness of 100 % means that the traffic is equal on all streets. For example, an evenness of 10 % corresponds to a flow of 730 vehicles/24 h which is a small flow.

From the results in Fig. 6 it is clear that if low levels are desirable, virtually no traffic can be allowed inside the area. Furthermore, in this area it is not sufficient to redistribute the traffic if equivalent levels below 45 dBA are wanted. To achieve such low levels the total traffic volume in the area must be reduced. The results in the figure have been calculated with equal traffic on all inner streets. Local enhancements of the equivalent levels can probably be achieved by more detailed modifications, but the requirement that very small vehicle flows are needed to get low levels of course remains. The velocity of the vehicle flow has been 50 km/h for all streets, and has been constant in the results presented here. Velocity modifications also present possibilities for improvements.

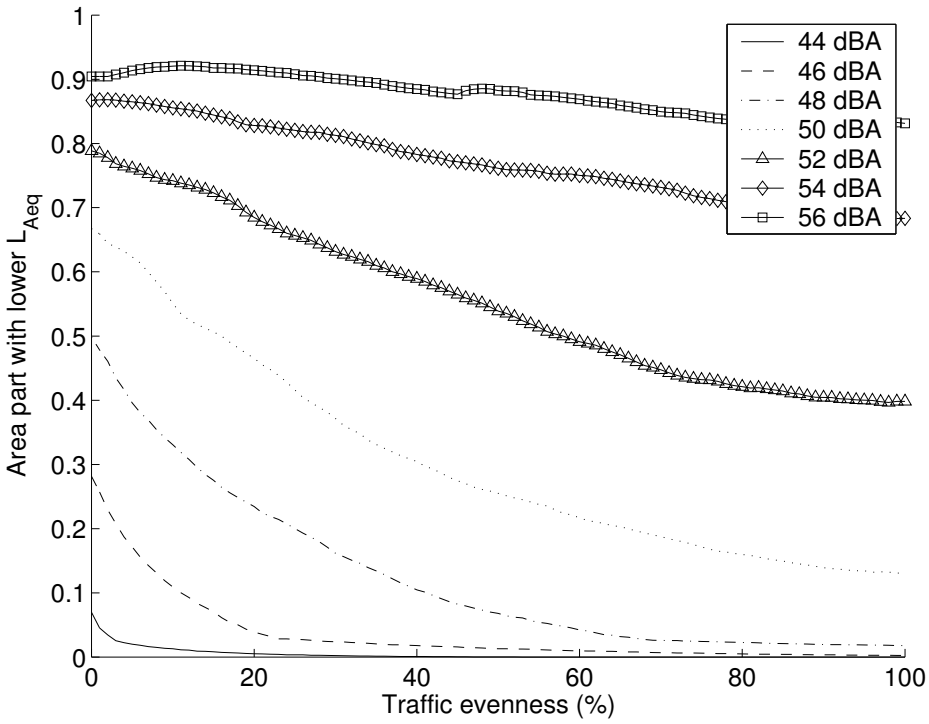

Figure 6: Area part with levels lower than example levels as a function of traffic flow evenness.

5 Influence of absorption

5.1 Absorption along the propagation path

A second option to abate noise is to reduce the transmission through absorption. Noise barriers generally do not absorb energy, they redistribute it, which means that in a mean value sense over a large area around the barrier the levels are probably not reduced to a significant degree.

The impact of absorption along the propagation path over the rooftops, which has been shown earlier to be the dominant propagation path, has been studied here by using an attenuation model similar to the common model of air absorption, i. e., exponential decay with distance:

$$U(r) = U_0 \frac{\mathrm{e}^{-\alpha_{tr} r}}{r^2}. \tag{3}$$

The parameter α_{tr} describes the equivalent absorption of the propagation. It is of course possible to use a more exact model for this propagation, but the aim here is to study the influence of absorption on city noise propagation and not to find the optimum absorption material. Additionally, the lack of knowledge of how noise propagates from one canyon into a parallel one (as described in Fig. 1 of [8] and the corresponding text) makes the use of an exact model for the propagation questionable. In this context the simple model in Eq. (3) is sufficient.

The same residential area as before has been used in this numerical survey. In the area, three representative locations have been chosen as observation points. One point is located in a street, one point in a small backyard (streets are close), and one point is in a large backyard (streets are more distant). The resulting noise levels are shown in 7 for α_{tr} values between 10^{-3} and 10^{-1}, which corresponds to a damping of $4.3 \cdot 10^{-3}$ dB/m and 0.43 dB/m respectively. In the results in Fig. 7 it can be seen that the potential of noise reduction on the silent side by reducing the propagation path over rooftops is high, both for the small and the large backyard. To achieve 10 dB reduction on the silent side $\alpha_{tr} = 0.04$ or a damping of between 0.15 and 0.20 dB/m is needed.

It can also be seen in Fig. 7 that increasing the absorption on the house façades (α) reduces the noise levels significantly. A reduction of around 5 dB in the backyards can be achieved if α is increased from 0 to 0.15. This value agrees reasonably well with the values achieved with the canyon model [17]. An increased façade absorption also reduces the levels in the streets; in this example with about 3 dB.

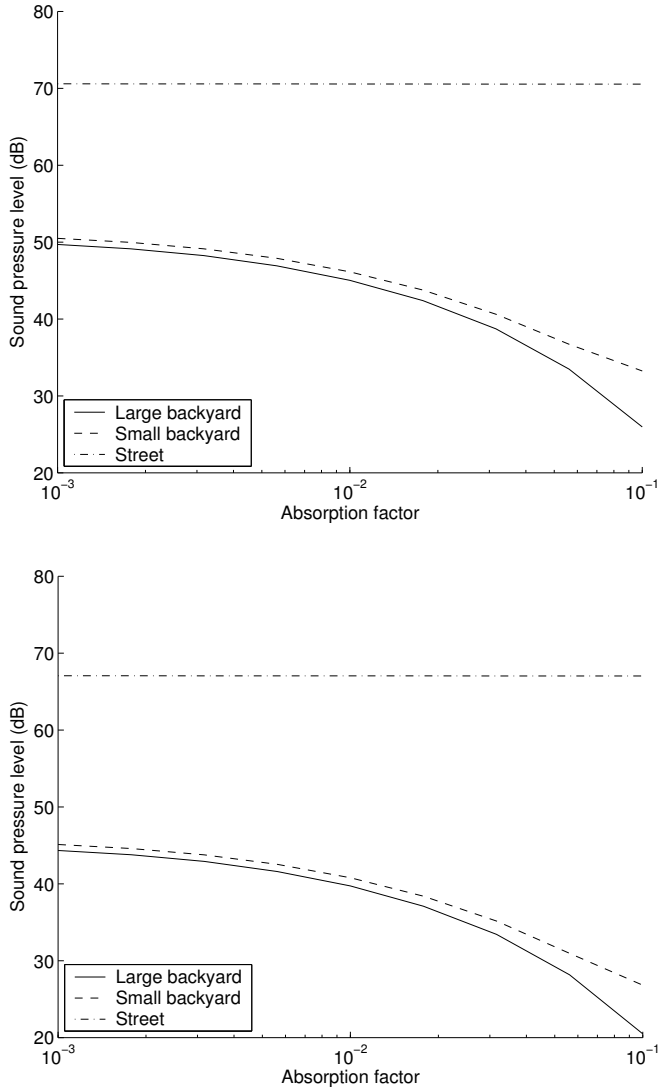

Figure 7: $L_{AEq,24h}$ noise levels calculated with the linear transport model for locations in the residential area used above as a function of the equivalent absorption along the path above the rooftops α_{tr}. Above: hard façade surfaces ($\alpha = 0$), below: soft façade surfaces ($\alpha = 0.15$).

6 Conclusions

Specialized models for noise calculations at shielded positions in city environments are needed. Three examples of such models are presented in this paper.

By combining the attenuation from all significant streets into a single correction factor compared to the free field levels, a simple and efficient model for noise propagation into backyards can be formed. This model has been shown elsewhere to agree well with measurements [5].

The linear transport model has here been extended to include propagation over rooftops. When this propagation path has been included calculated levels and measured levels are in fairly good agreement, both for receiver locations in the streets and in closed backyards.

Noise levels can be reduced through redistributing the traffic flows. From the examples presented here it is advantageous to concentrate the traffic to a few streets and to locate these as far from receivers as possible. Virtually no traffic can be allowed inside areas where low noise levels are needed.

Absorptive materials can be used to reduce the noise levels. As has been shown using the linear transport model, absorptive material can reduce the noise levels with at least 5 dB when located inside the canyons. Results in the same order have been obtained using the equivalent sources model in [17].

It has furthermore been shown here that a reduction of the strength of the propagation path over the rooftops has a large noise reduction potential. More studies on how such a reduction can be practically realized are however needed.

7 Acknowledgements

This paper is based on a study performed within the research programme ”Soundscape support to health”, sponsored by the Swedish Foundation for Strategic Environmental Research (MISTRA), the Swedish Agency for Innovation Systems (Vinnova) and the Swedish National Road Administration (VV).

References

[1] T. Kihlman, E. Öhrström and A. Skånberg (2002). Adverse Health Effects of Noise and the Value of Access to Quietness in Residential Areas. *Internoise 2002 - Dearborn*, paper number 484

[2] T. Kihlman and W. Kropp. City traffic noise – A local or global problem ? *Noise Control Engineering Journal* 2001;49:165–169.

[3] L. Godinho, J. António and A. Tadeu. Sound propagation around rigid barriers laterally confined by tall buildings, *Applied Acoustics* 2002;63:595–609.

[4] M. Ögren and W. Kropp. Road traffic noise propagation between two dimensional city canyons using an equivalent sources approach. Accepted for publication in *Acustica – Acta acustica* 2003.

[5] P. J. Thorsson, M. Ögren and W. Kropp. Noise levels on the shielded side in cities using a flat city model. Submitted for publication in *Applied Acoustics* 2003.

[6] R. Bullen. Statistical evaluation of the accuracy of external sound level predictions arising from models. *Journal of Sound and Vibration* 1979;65:11–28.

[7] H. Kuttruff. A mathematical model for noise propagation between buildings. *Journal of Sound and Vibration* 1982;85:115–128.

[8] P. J. Thorsson. Application of linear transport to noise propagation in cities. Submitted for publication in *Acustica – Acta Acustica* 2003.

[9] H. Jonasson and H. Nielsen. Road Traffic Noise - Nordic Prediction Method. ISBN 92 9120 836 1, *TemaNord* 1996:525, Nordic Council of Ministers.

[10] E. A. G. Shaw and N. Olson. Theory of steady-state urban noise for an ideal homogeneous city. *J. Acoust. Soc. Am* 1972;51:1781–1793.

[11] M. Asadzadeh. Analysis of a fully discrete scheme for neutron transport in a two-dimensional geometry. *SIAM Journal of Numerical Analysis* 1986;23:543–561.

[12] A. Ishimaru. Wave propagation and scattering in random media. New York, IEEE Press and Oxford University Press, 1997.

[13] J. Ducourneau and V. Planeau. The average absorption coefficient for enclosed spaces with non uniformly distributed absorption. *Applied Acoustics* 2003;64:845–862.

[14] D. Fitzroy. Reverberation formula which seems to be more accurate with nonuniform distribution of absorption. *J. Acoust. Soc. Am.* 1959;31:893–897.

[15] B.-I. Dalenbäck, M. Kleiner, P. Svensson. A Macroscopic View of Diffuse Reflection. *J. Audio Eng. Soc.* 1994;42:973–807.

[16] E. Salomons. Sound Propagation in Complex Outdoor Situations with a Non-Refracting Atmosphere: Model Based on Analytical Solutions for Diffraction and Reflection. *Acustica – Acta acustica* 1997;83:436–454.

[17] M. Ögren, J. Forssén and W. Kropp. Turbulence and absorption effects in city canyon calculations. *Int. Congress on Sound and Vib. 2003 - Stockholm*